Novel roles of human desmoglein 3 in the regulation of E-cadherin-mediated adherens junctions and the reorganisation of actin cytoskeleton

A thesis submitted to Queen Mary, University of London for the Degree of Doctor of Philosophy

By Mandy Siu Man Tsang

Institute of Dentistry
Barts and The London School of Medicine and Dentistry
Queen Mary, University of London

April, 2013

DEDICATION

This thesis is dedicated to the Tsang & Lam family.
Thank you for supporting all my choices, even the ones that scared you.
Thank you for letting me do it my way.

I, Mandy Siu Man Tsang, confirm that the work presented here in this thesis is my own.

Where information has been derived from other sources, I confirm that it has been indicated clearly in the thesis.

ABSTRACT

Desmosomes and adherens junctions are intercellular junctions crucial for epithelial cell-cell adhesion and maintenance of normal tissue architecture. Desmoglein 3 (Dsg3), a member of the desmoglein sub-family, serves as an adhesion molecule in desmosomes. Its importance in cell-cell adhesion has been highlighted by the autoimmune blistering disease *pemphigus vulgaris*, where autoimmune antibodies directed against Dsg3 trigger a cascade of intracellular events, resulting in structural defects and blister formation in the skin and oral mucosa. In addition to its adhesive function, Dsg3 is also acknowledged to have other important roles in the regulation of cell proliferation and differentiation. Our group suggested that Dsg3 is involved in the regulation of keratinocyte stem cell differentiation, but the underlying mechanism(s) were unclear (Wan et al, 2003; Wan et al, 2007). We hypothesise that Dsg3 may be involved in the regulation of the E-cadherin-mediated cell adhesion and the reorganisation of actin cytoskeleton, which in turn contributes to differentiation programs and tissue morphogenesis. Thus, the aim of this study was to examine the interactions between Dsg3, E-cadherin and actin and to explore the underlying signalling pathways that are associated with these intercellular junctions. Using both a gain and loss of Dsg3 functional approaches, I demonstrate that Dsg3 is capable of interacting with E-cadherin and involved in the regulation of calcium-induced E-cadherin junction assembly and the activation of Src signalling pathway. Overexpression of Dsg3 increased E-cadherin/Src signalling with enhanced levels of Src and pSrc co-purified with E-cadherin. Knockdown of Dsg3 inhibited this pathway with reversed effect, suggesting that Dsg3 acts as an upstream regulator of Src signalling in the regulation of E-cadherin-mediated adherens junction formation. In addition, I show another novel function of Dsg3 in promoting actin dynamics through regulating Rac1 and Cdc42-GTPase activities, resulting in pronounced membrane protrusions and enhanced rate of actin turnover. Taken together, my work suggests that Dsg3 play an important signalling role in the assembly of E-cadherin-mediated cell adhesion and the dynamic of actin cytoskeleton.

ACKNOWLEDGEMENTS

I would like to thank my supervisor Dr Hong Wan for the wonderful opportunity to work in her group and her selfless guidance. There were many happy and bad days. Thank you for believing in me from the very beginning, and helping me throughout these few years. Without her support, this thesis would have not been written.

Secondly, I would like to acknowledge my second supervisor Professer Farida Fortune for her encouragement and guidance. I am also very grateful to the following people who have contributed, in one way or another to the successful completion of this work- Dr Ann Wheeler, Professor Ken Parkinson, Dr Ahmad Waseem, Dr Alan Cruchley and Steven Cannon (the best manager in CDOS).

Thank you to Ryan Salucideen, Bilal Fazil, Biancastella Cereser and Cecilia Gonzales-Marin for being a source of inspiration and encouragement. Thank you for listening to my many non-problems, and always be there.

Thank you everyone in Blizzard for your invaluable guidance, support and friendship especially Louise Brown (a wonderful buffer), Amrita Bose, Paul Ryan, Tanya Novak, Miguel Vargas, Lisa Nanty, Zacharoula Nikolakopoulou, Mojgan Hamedi and Alice de Castro. This PhD would be a boring journey without a good dose of friendship and gossip to colour my world.

Thank you to Francesca Chiara and James Wang for putting up with my occasional moments of panic and insanity, and for keeping me in touch with reality. Thank you to Kevin Purseglove for reading this thesis countless times even though you didn't understand it at all.

Thank you to Kevin Teng, Javier Low, Joseph Oh and Efi Papaev. I wouldn't have contemplated this road if not for your encouragement. Thank you to my undergraduate and postgraduate tutors: Professor Helen Hurst, Dr Chiara Berlato, Dr Mike Wheeler and Dr Gary Khoo. I wouldn't have come this far without your teaching and guidance. Thank you to Putt Chwee Rong, Lin Lili, Tan Tiong Peng and Jennifer Kwan for your long distance support, through all the good and bad times.

This project would not have been carried out without the generous support provided by the Medical Research Council-funded studentship to Barts and The London School of Medicine and Dentistry. I had neither been starved or homeless for the past three years.

PUBLICATIONS AND AWARDS

Manuscripts:

Tsang SM, Brown L, Gammon L, Fortune F, Wheeler A, Wan H. **A novel role for human desmoglein 3 acting as an upstream regulator of Rho GTPases in the regulation of actin organisation and dynamics.** Exp Cell Res. July 2012.

Tsang SM, Brown L, Lin K, Liu L, Piper K, O'Toole EA, Grose R, Hart IR, Garrod DR, Fortune F, Wan H. **Non-junctional human desmoglein 3 acts as an upstream regulator of Src in E-cadherin adhesion, a pathway possibly involved in the pathogenesis of Pemphigus vulgaris.** J Pathol. May 2012.

Tsang SM, Liu L, Teh MT, Wheeler A, Grose R, Hart IR, Garrod DR, Fortune F, Wan H. **Desmoglein 3, via an interaction with E-cadherin, is associated with activation of Src**. PLoS One. Dec 2010.

Awards:

2011-Runner up for oral presentation: PhD day, Institute of Dentistry, QMUL**.**

2010-Best Poster prize: Wellcome Trust Centre for Cell-Matrix Research Conference & 22nd UK Adhesion Society Meeting 2010.

2010-The Italian Associazione di Biologia Cellulare e del Differenziamento Travel Fellowship: Travel grant to Wellcome Trust Centre for Cell-Matrix Research Conference & 22nd UK Adhesion Society Meeting 2010.

2008-Medical Research Council Studentship: Doctoral funding.

TABLE OF CONTENTS

TABLE OF FIGURES

INDEX OF TABLES

CONTRIBUTIONS

*The Western blot in Figure 19 and confocal images in Figure 12, 23, 29 and 31 were carried out/ acquired by Wan H; the confocal images in Figure 35 were acquired together with Wheeler A. All image processing and data analysis were carried by Tsang SM.

ABBREVIATIONS

4',6-diamidino-2-phenylindole (DAPI)

Activator protein-1 (AP-1)
Adherens junctions (AJs)
Anti-urokinase plasminogen activator (Anti-uPA)
Arrhythmogenic right ventricular cardiomyopathy (ARVC)

Caveolin 1-3 (Cav 1-3)
Caveolin-scaffolding domain (CSD)
Cell adhesion recognition (CAR)
Co-immunoprecipitation (Co-IP)
Cytoskeletal buffer (CSK)

Desmocollin 1-3 (Dsc 1-3)
Desmoglein 1-4 (Dsg 1-4)
Desmoglein terminal domain (DTD)
Desmoplakin (Dsp)
Desmosomes (DSMs)
Dimethyl sulfoxide (DMSO)

E-cadherin (E-cad)
Epidermal growth factor receptor (EGFR)
Escherichia coli *(E coli*)
Ethylene glycol tetraacetic acid (EGTA)
Ethylenediaminetetraacetic acid (EDTA)
Extracellular anchor (EA)

Fetal calf serum (FSC)
Fogo selvage (PF)

GTPase activating proteins (GAPs)
Guanine nucleotide exchange factors (GEFs)

IC cadherin segment (ICS)
Inner dense plaque (IDP)
Intercellular adhesion molecule 1(ICAM-1)
Interleukin-6 (IL-6)
Intracellular anchor (IA)
Intracellular C-terminal domain (IC)
Intracellular proline-rich linker domain (IPL)

Keratin intermediate filaments (KIF)

Lysogeny broth (LB)

Madin Darby canine kidney (MDCK)
Metalloproteinases (MMP)
Myosin light chain (MLK)

Myosin light chain kinase (MLCK)
Myristoylation (M)

Nuclear factor-kappa B (NF-κB)

Outer dense plaque (ODP)

P38 mitogen-activated protein kinases (p38 MAPK)
P-cadherin (P-cad)
Pemphigus foliaceus (PF)
Pemphigus vulgaris (PV)
Phosphate buffered saline (PBS)
Phosphatidylinositol 3-kinases (PI3K)
Phosphorylation (P)
Plakoglobin (Pg)
Plakophilins (Pkps)
Plasma membrane (PM)
Protein kinase C (PKC)
Proximity ligation assay (PLA)

Radio-Immunoprecipitation Assay buffer (RIPA Buffer)
Repeat unit domain (RUD)
Room temperature (RT)

Signal transducer and activator of transcription 3 (STAT3)
Sodium chloride (NaCl)
Sodium dodecyl sulfate (SDS)
Squamous cell carcinoma (SCC)
Standard deviation (SD)
Super optimal broth (SOC)

Tight junctions (TJs)
Transmembrane domain (TM)
Tris-Buffered Saline and Tween 20 (TTBS)
Tumor necrosis factors (TNF-α)

Life is best lived by being bold and daring. People tend to grow fearful when they taste failure, face a daunting challenge or fall ill. Yet that is precisely the time to become even bolder. Those who are victors at heart are the greatest of all champions.

Daisaku Ikeda

CHAPTER 1

INTRODUCTION

1.1 Epidermis

The epidermis, the outermost layer of the skin, serves as the body's primary barrier against water loss and provides essential protective functions. It is a multi-layered stratified squamous epithelium composed of four sub-layers: the basal layer, spinous layer, granular layer and the stratum corneum (Figure 1) (Eckert & Rorke, 1989; Morasso & Tomic-Canic, 2005). To allow for constant renewal of the skin, epidermis is replenished through mitosis of the proliferating cells at the basal layer and maintained by continual stratification and differentiation throughout one's lifetime. When this balanced regulation is disturbed, a range of human diseases characterised by varying degrees of epidermal fragility and blistering may ensue.

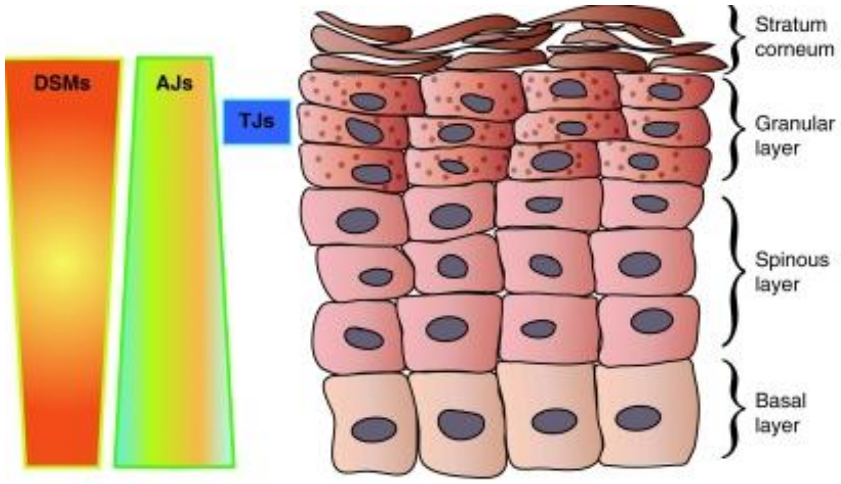

Figure 1: The composition of the epidermis and the distribution of intercellular junctions.

The epidermis is composed of the basal layer, spinous layer, granular layer and the stratum corneum. Desmosomes (DSMs) and adherens junctions (AJs) are found throughout the epidermis, while the tight junctions (TJs) are found only in the granular layers (Green et al, 2010).

Keratinocytes of the basal layers are attached to the basement membrane through hemidesmosomes and other integrin-mediated cell adhesion junctions. When terminal differentiation begins, some of their daughter keratinocytes lose their attachment from the basement membrane and migrate upward toward the upper stratum corneum. During this process, they undergo a continuous remodelling of adhesive junctions and reorganisation of the cytoskeletal networks, in which the expression levels of many structural proteins including intercellular junction components change, as does the expression of transcription factors. Once they reach the stratum corneum of the skin, these terminally differentiated keratinocytes begin to shed from the skin surface and are replaced by cells arising from the basal proliferative compartment. In normal skin, the whole process of cell renewal is over a period of 30 days (Kerr, 1999).

1.2 Intercellular junctions

Intercellular junctions are specialised attachment structures that mediate firm cellular adhesion between adjacent cells. They are abundantly expressed in epithelial tissues that experience extensive mechanical stress. In vertebrates, there are three major groups of intercellular junctions: tight junctions (also known as occluding junctions), adhering junctions (including adherens junctions and desmosomes) and gap junctions (also known as channel-forming junctions) (Simpson et al, 2011) (Figure 1 and 2). Besides imparting structural integrity, these dynamic structures are also involved in various functions such as the maintenance of tissue polarity, regulation of cell shape, exchange of selected small ions and molecules and signalling events. Studies are beginning to suggest a broader role for these intercellular junctions and hence, there is no doubt that the formation, maturation and homeostasis of epidermis require dynamic coordination between assembly and disassembly of these junctions. Dysfunction of any aspect not only disrupts their intercellular adhesive functions, but also affects the signalling pathways associated with de-differentiation and malignance. It is therefore believed that the precisely controlled mechanisms of

cell adhesion can in addition serve as crucial regulators for other downstream processes such as proliferation, differentiation, cell migration and wound healing. Here I am focusing on the adhering junctions and their associated signalling pathways and explore how these mechanisms are associated to desmoglein related disease-*pemphigus vulgaris*.

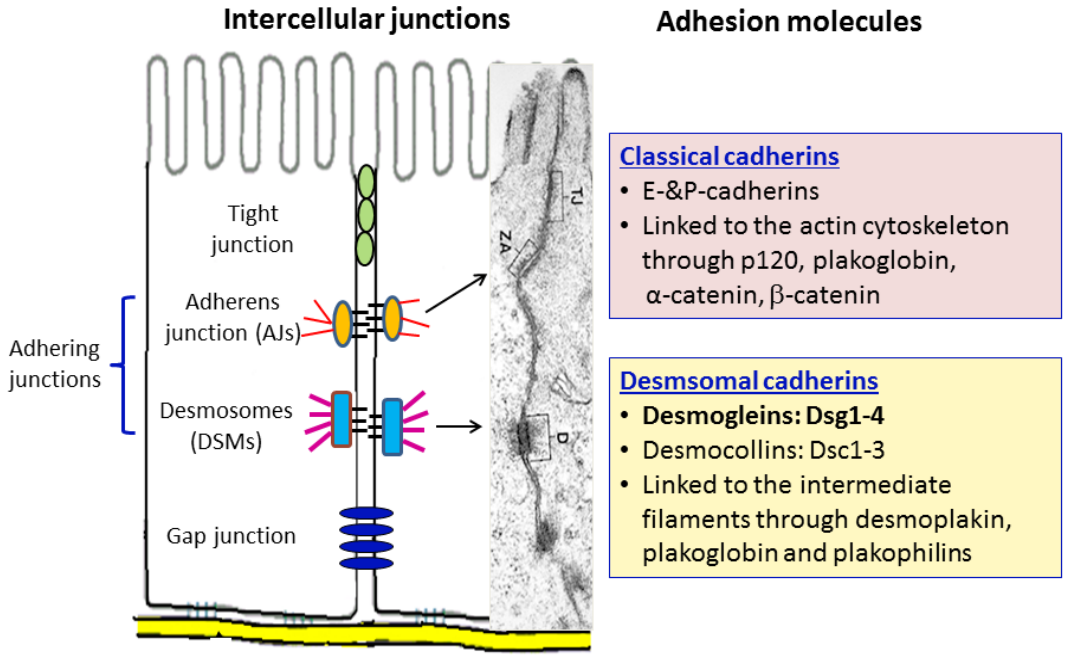

Figure 2: A schematic diagram of intercellular junctions in epithelial cells.

Intercellular junctions consist of tight junctions, adhering junctions (adherens junctions and desmosomes) and gap junctions. In adherens junctions, classical E- and P-cadherins are linked to the actin cytoskeleton via β- and α-catenins, while in desmosomes, desmogleins and desmocollins are linked to the intermediate filaments through plakoglobin, plakophilins and plakin family members such as desmoplakin (Green & Simpson, 2007).

Adherens junctions and desmosomes, are composed of members of the cadherin superfamily of transmembrane proteins. Their extracellular domains mediate calcium-dependent homophilic and/or heterophilic adhesion, while the cytoplasmic domains form a stable attachment with the underlying cytoskeletal filaments through armadillo and cytoskeletal adaptor proteins. In adherens junctions, the classical E- and P-cadherins are linked to the actin cytoskeleton via

catenins, while in desmosomes the desmosomal cadherins: desmogleins and desmocollins are linked to the intermediate filaments through armadillos and plakin family proteins (Simpson et al, 2011). Together desmosomes and adherens junctions work cooperatively with the underlying actin and intermediate filaments, which serve as a mechanical link between adjacent cells in epithelial layer, and thereby providing mechanical stability and the maintenance of the overall tissue integrity of the epidermis. The function of intermediate filaments will not be discussed in this thesis.

1.3 Desmosomes and the desmosomal components

1.3.1 Desmosomal cadherins

Desmosomes are calcium-dependent, cadherin-based cell adhesion structures. They are mainly composed of three sub-families and these include the desmosomal cadherins: desmogleins (Dsgs) and desmocollins (Dscs), the armadillo family proteins: plakoglobin (Pg) and plakophilins (PKPs) and the plakins: desmoplakin (DSP), plectin, envoplakin and periplakin (Bazzi et al, 2007; Green & Gaudry, 2000; Ishii et al, 2001). As illustrated in Figure 3, the transmembrane core of desmosomes is composed of desmosomal cadherins. Desmogleins (Dsgs) cooperate with desmocollins (Dscs) to form the initial adhesive interface via their EC1 extracellular domains. Their cytoplasmic tails then interact with the armadillo family members, including plakoglobin and plakophilins (Garrod et al, 2002; Getsios et al, 2004; Green & Gaudry, 2000; Hatzfeld, 2007), which in turn links the plakin family member desmoplakin to the intermediate filaments (Green & Simpson, 2007).

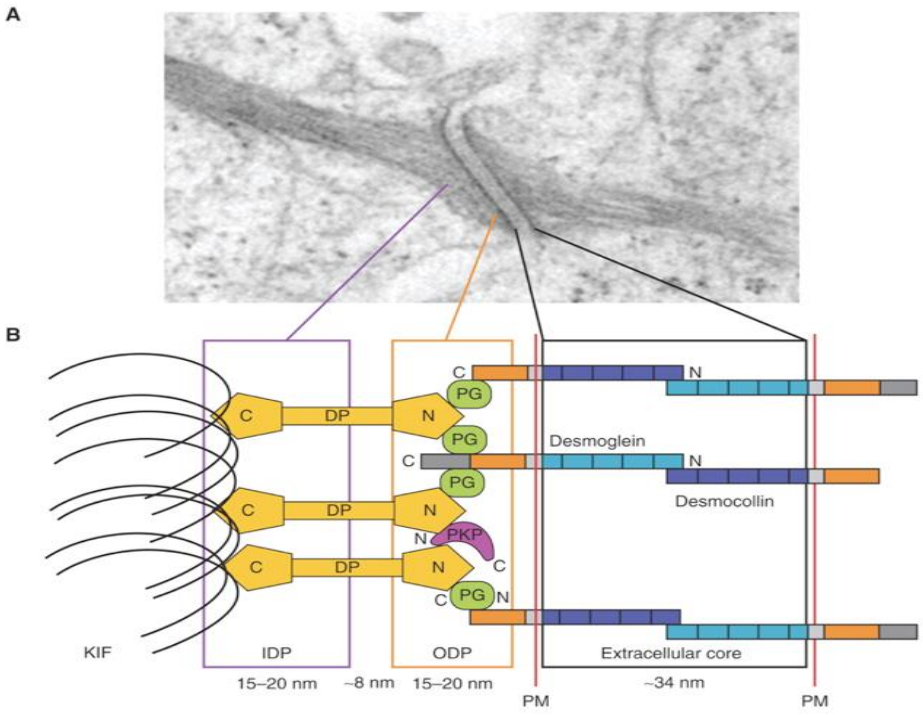

Figure 3: A model for the structure of desmosomes.

A) Electron micrograph of a desmosome. B) Schematic diagram of desmosomal proteins and relative distance from the plasma membrane (PM); Plakoglobin (PG); Plakophilins (PKPs); Desmoplakin (DP); Keratin intermediate filaments (KIF); Inner dense plaque (IDP); Outer dense plaque (ODP) (Kottke et al, 2006).

1.3.1.1 The structure of desmosomal cadherins

In terms of molecular structure, the extracellular N-terminal domains of desmosomal cadherins are highly homologous to those of the classical E-cadherin. As shown in Figure 4, the N-terminal consists of five sub-domains: EC 1-4 and the extracellular anchor (EA) domain. These domains are approximately 110 amino acids long (Pokutta & Weis, 2007) and are separated by calcium-dependent binding sites essential for cell-cell adhesion (Gloushankova, 2008). The precise molecular mechanisms of cadherin adhesion are still unclear. It has been reported that the EC1 domain contains a highly conserved cell adhesion recognition sequence (CAR) primarily responsible for mediating adhesive interaction between cadherins (Heupel et al, 2008).

Next to the extracellular anchor (EA) domain is a single pass transmembrane domain (TM), which is followed by an intracellular C-terminal domain (IC) containing variable numbers of sub-domains. In particular, desmoglein has a much longer IC domain, which consists of an intracellular anchor (IA), an IC cadherin segment (ICS), an intracellular proline-rich linker domain (IPL), a repeat unit domain (RUD) and a glycine rich desmoglein terminal domain (DTD) (Huber, 2003). It is known that the ICS and IA domains bind to the armadillo family members such as plakoglobin and p120, respectively (Kanno et al, 2008b; Mathur et al, 1994). The functions of the remaining C-terminal domains are currently not clear.

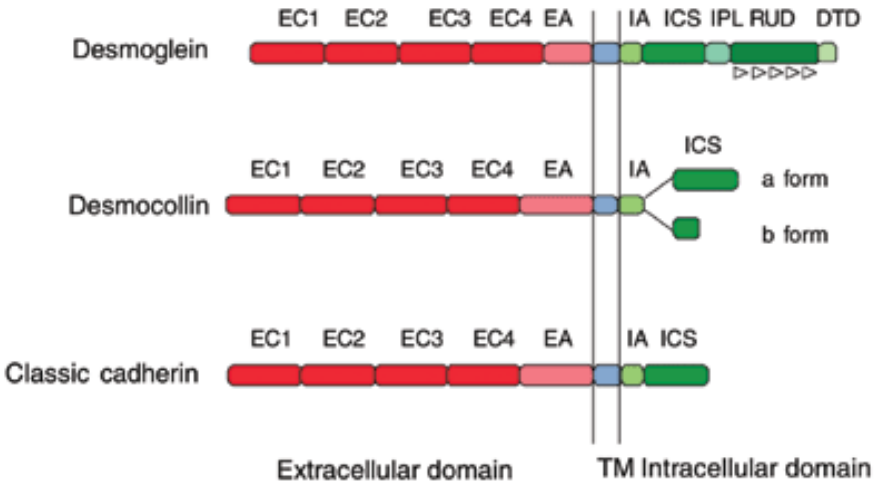

Figure 4: The structure of desmosomal and classical cadherins.

The extracellular N-terminal domains consist of five sub-domains: EC1-4 and the extracellular anchor (EA) domain. Next to the extracellular anchor domain is a single pass transmembrane domain (TM), which is followed by an intracellular C-terminal domain (IC) containing variable numbers of sub-domains. IA, intracellular anchor domain; ICS, intracellular cadherin specific domain; IPL, proline-rich linker domain; RUD, repeating unit domain; DTD, desmoglein-specific terminal domain (Amagai, 1999; Ishii et al, 2001).

As for desmocollin, each isoform comes in splice variant 'a' and a shortened 'b' isoform due to alternative splicing. Splice variant 'a' interacts with plakophillin 3 (Bonne et al, 2003), plakoglobin and desmoplakin (Troyanovsky et al, 1994), while splice variant 'b' which lacks the catenin-binding domain only interacts with plakophillin 3 (Choi et al, 2009). The function of the Dsc 'b' form is currently unknown. It was hypothesised that the cytoplasmic tail of 'b' is involved in Dsc signalling activity. However, Hardman and colleagues demonstrated that the expression of both Dsc3 splice variant 'a' and 'b' driven by the keratin 1 promoter have similar β-catenin-inducing activities in culture, suggesting that the cytoplasmic tail of 'b' may not solely play a key role in signalling function (Hardman et al, 2005). The authors instead suggest that Dsc3 'b' might be involved in Dsc signalling via plakophillin 3, since it is the only known Dsc3 'b'-protein interaction to date (Bonne et al, 2003).

1.3.1.2 Homophilic and heterophilic binding of desmosomal cadherins

It is known that both desmocollin and desmoglein are required to confer strong cell-cell adhesion between keratinocytes. Studies based on the cadherin-null L-cell system demonstrated that co-expression of both types of desmosomal cadherins Dsc2a and Dsg1 together with plakoglobin greatly increased cell aggregation (Andl & Stanley, 2001; Marcozzi et al, 1998; Tselepis et al, 1998). At present, it is unclear how desmosomal cadherins interact with each other *in vivo* since data supporting both homophilic and heterophilic trans-interaction have been reported. For instance, heterophilic interactions between Dsg2 and Dsc1a or Dsc2 have been observed on the molecular level (Chitaev et al 1997; Syed et al 2002), while homophilic interactions mediated by desmosomal cadherins such as Dsg2 or Dsc2 have also been observed in *in vitro* studies (Waschke et al 2005; Heupel et al 2008). More recently, Nie and colleagues suggested that homophilic, isoform-specific binding is a much preferred pairing as compared with heterophilic binding in HaCaT cells that contains abundant desmosomes (Nie et

al, 2011). Further studies are required to understand how these interactions may contribute to epidermal cohesion *in vivo.*

1.3.1.3 Calcium-dependent desmosomal cadherin adhesion

Calcium is a necessary prerequisite for a variety of cellular processes such as the assembly of intercellular junctions, differentiation and stratification (Brooke et al, 2012). The dynamic assembly of adherens junctions and desmosomes can be monitored experimentally in culture by the calcium switch assay (Hennings et al, 1980; Watt et al, 1984). In low calcium medium (below 0.1 mM), keratinocytes grow as a monolayer and do not form desmosomes or adherens junctions. Under such conditions, the junctional proteins continue to be synthesised, but they are unstable and do not assemble into intercellular junctions. The junctional proteins become quickly degraded, resulting in a diffuse cytoplasmic staining of the junctional proteins including E-cadherin (Hodivala & Watt, 1994; Lewis et al, 1994; O'Keefe et al, 1987; Wheelock & Jensen, 1992). Upon raising the extracellular calcium concentration of the growth medium from μM range to 0.2 mM and above (Yin et al, 2005a), E-cadherin begins to bind to its counterpart on the surface of neighbouring cells, and in turn provides a structural framework or signalling cues to guide the formation of other intercellular junctions such as desmosomes. It has been reported that the assembly of desmosome begins with the binding of desmocollin to β-catenin, a component of the adherens junctions (Hanakawa et al, 2000).

Following the calcium switch assay, the Triton solubility assay (Green & Simpson, 2007) is commonly used to distinctly extract the non-ionic detergent soluble fraction of cells, while leaving the cytoskeletal associated proteins as the insoluble fraction (Patton et al, 1989). The soluble fraction of Dsg3 is referred to as the “free” non-junctional Dsg3 found outside of desmosomes, whereas the insoluble fraction is found in desmosomes, which is associated with the intermediate filaments (Aoyama et al, 1999). The titration of the desmosomal components from the soluble to insoluble fractions upon the addition of calcium

reflects the recruitment of desmosomal components from the cytoplasm to the plasma membrane where they form stable interactions with the intermediate filaments (Kowalczyk et al, 1994). In accordance with this, the stability of the desmosomal proteins especially the detergent insoluble fraction increases over the course of junction assembly. It is important to note that the calcium concentration of tissue fluid is maintained at around 1 mM and hence, variations of the extracellular calcium concentrations may not truly represent the regulation of cell-cell adhesion. However with careful interpretation, these methods are still useful in studying junction assembly *in vivo* (Garrod, 2010).

Another characteristic feature of desmosomes is the acquisition of hyper-adhesion, which does not appear to occur in adherens or tight junctions (Wallis et al, 2000). It was demonstarted that desmosomes in early stages of junction assembly or during wound healing exhibit a weaker calcium-dependent adhesion, in which the protein stability and assembly process could easily be disrupted by depletion or chelation of extracellular calcium. Continued culture of cells over several days (2-6 days) increases the levels of adhesion between neighbouring cells and desmosomes gradually mature to become functionally calcium-independent, a concept known as hyper-adhesion (Garrod & Kimura, 2008; Kimura et al, 2007). In general, it is believed that hyper-adhesion in desmosomes is associated with tissue strength. Wallis and colleagues suggested that desmosomes in tissues are calcium-independent unless wounded or diseased and such condition cannot be replicated in sub-confluent or early confluent epithelial cells in culture (Wallis et al, 2000). The authors went on to hypothesise that epidermal wounding causes desmosomes to lose their hyper-adhesiveness at the wound edge, which in turn facilitate cell migration and re-epithelialisation (Garrod & Kimura, 2008).

To date, the underlying mechanisms and signalling pathways governing the acquisition of hyper-adhesion remain unclear. Garrod and colleagues suggested that cells in their hyper-adhesion state undergo structural reorganisation that resists calcium-induced uncoupling (Garrod & Kimura, 2008). Other independent studies demonstrated that the activation of protein kinase C (PKC), a family of

serine/threonine protein kinases (Cosentino-Gomes et al, 2012), is involved in converting desmosomes from a calcium-independent to a calcium-dependent state in both Madin-Darby canine kidney (MDCK) and HaCaT cell lines (Cirillo et al, 2010; Wallis et al, 2000). This finding is further supported by a study of Cirillo and colleagues, who showed that inhibition of protein kinase C induces hyper-adhesion, which in turn prevents epithelial sheets from PV IgG-mediated loss of cell-cell adhesion and cadherins depletion (Cirillo et al, 2010).

1.3.2 Armadillo family Proteins

Armadillo family proteins are characterised by a central domain containing variable numbers of amino acid repeats. They include plakoglobin, plakophilins, p0071 (also known as plakophilin 4), α- and β-catenin, p120 and ARVC (Hatzfeld, 2007). Mutations of armadillo proteins are associated with defects in the heart such as arrhythmogenic right ventricular cardiomyopathy (ARVC) and skin such as ectodermal dysplasia or skin fragility syndrome.

Plakoglobin (Pg), also known as γ-catenin, is a major regulatory component in both desmosomes and adherens junctions. It exhibits a higher affinity for desmosomal cadherins (Garrod & Chidgey, 2008) and found predominately in desmosomes. Plakoglobin links desmosomal cadherins to desmoplakin and anchors it to the intermediate filaments (Troyanovsky et al, 1994). Its binding to Dsg3 was reported to be essential for desmosome assembly (Andl & Stanley, 2001). As for the adherens junctions, plakoglobin links E-cadherin to the α- and β-catenin complex. It shares more than 76% in homology with β-catenin (Peifer & Wieschaus, 1990) and is known to compensate the function of β-catenin and modulates the Wnt/β-catenin signaling pathway (Miravet et al, 2002; Yin & Green, 2004). Like other junctional proteins, plakoglobin is subjected to modulation by tyrosine kinases and its downstream effect could affect the cadherin-mediated adhesion in both adherens junctions and desmosomes (Getsios et al, 2004). It was shown that EGF-induced tyrosine phosphorylation of plakoglobin results in a loss of desmoplakin from desmosomes with the consequent weakening of cell adhesion strength (Yin et al, 2005b). Taken

together, it is believed that plakoglobin is vital for cross-talk between desmosomes and adherens junctions (Lewis et al, 1997).

The plakophilin family consists of four members: PKP 1 to 3 and p0071 (Bonne et al, 1999; Hatzfeld et al, 2000). They are found predominantly at desmosomes and involved in reinforcing junction stability through lateral interactions between desmosomal proteins and the intermediate filaments (Hatzfeld, 2007). Plakophilins also share a high functional conservation with p120 and play a regulatory role in adherens junctions (Getsios et al, 2004; Kowalczyk et al, 1997).

Both plakophilin 1 and 2 come in two isoforms 'a' and 'b' due to alternative splicing (Hatzfeld, 2007). Plakophilin 1, the major component of desmosomes, interacts with Dsg1, desmoplakin and the intermediate filaments (Hatzfeld et al. 2000). Its functions include recruitment of desmoplakin to the cell borders (Getsios et al, 2004), ensuring proper attachment of intermediate filaments to the desmosomes (Kottke et al, 2006; McGrath et al, 1997) as well as influencing the transition of desmosomes from a calcium-dependent to a calcium-independent state (Garrod & Kimura, 2008). Plakophilin 2 and 3 are also known to be involved in mediating distinct effects on desmosomal adhesion such as the formation of functional desmosomes (Bass-Zubek et al, 2009; Godsel et al, 2010). Emerging evidence suggests that plakophilins might have an additional role in nuclear function. PKP1 are sometimes present in the nucleus (Green & Simpson, 2007), while PKP2 and PKP3 are associated with RNA polymerase III and cytoplasmic particles containing RNA-binding proteins, respectively (Mertens et al, 2001). It is currently unclear what role these proteins may play in nuclear function (Hatzfeld et al, 2000).

1.3.3 Plakin family proteins

Like plakophilins, desmoplakins come in two isoforms: DPI and DPII due to alternative splicing. They are found in all desmosome-containing tissues (Getsios et al, 2004) and mutation of this gene is associated with a wide range of inherited disorders affecting the heart and the skin (Awad et al, 2006; Kljuic et al,

2003; Pilichou et al, 2006; Rickman et al, 1999). Desmoplakins are primarily involved in linking desmosomal plaque to the intermediate filament networks and disruption of such attachment has been shown to impair cell-cell adhesive strength *in vitro* (Bornslaeger et al, 1996; Huen et al, 2002).

The desmoplakin N-terminal globular plakin domain is essential for protein-protein interactions, where it binds to plakoglobin, plakophilin, Dsc1a (Kowalczyk et al, 1997; Smith & Fuchs, 1998; Troyanovsky et al, 1994) and possibly Dsg1 (Getsios et al, 2004). The function of the N-terminal domain is involved in recruiting the desmoplakin to the desmosomal plaque (Stappenbeck et al, 1993), while the C-terminal tail is thought to facilitate the binding of desmoplakin to intermediate filaments of epithelial cells (Kouklis et al, 1994; Stappenbeck et al, 1993). Other important functions of desmoplakins include the proper assembly of functional desmosomes (Vasioukhin et al, 2001b), regulation of desmosome hyper-adhesion (Hobbs & Green, 2012)(Refer to Introduction Chapter 1.3.1.3) and reorganisation of the microtubule and actin cytoskeleton (Lechler & Fuchs, 2007).

1.3.4 Expression patterns of desmosomal cadherins

Considerable variations in the expression patterns and molecular composition of desmosomes are observed along different epithelial layers of a given tissue or cell types. Four desmoglein (Dsg1-4) and three desmocollin (Dsc1-3) isoforms have been identified in human tissues and each isoform is encoded by different genes (Green & Simpson, 2007). The schematic diagram in Figure 5 shows the isoform-specific expression pattern of the desmosomal cadherins in normal human epidermis. Dsg1 and Dsc1 are expressed predominately in the upper layers and decrease gradually toward the lower layers. Dsg2 is expressed in the basal cell layer. Dsg3 and Dsc2/3 are expressed more to the basal and immediate suprabasal layers and decrease gradually toward the upper layers (Brennan et al, 2007; Delva & Kowalczyk, 2009). Distinctively, Dsg4 is only expressed in the

highly differentiated granular layer of the epidermis (Getsios et al, 2009; Ishii et al, 2001).

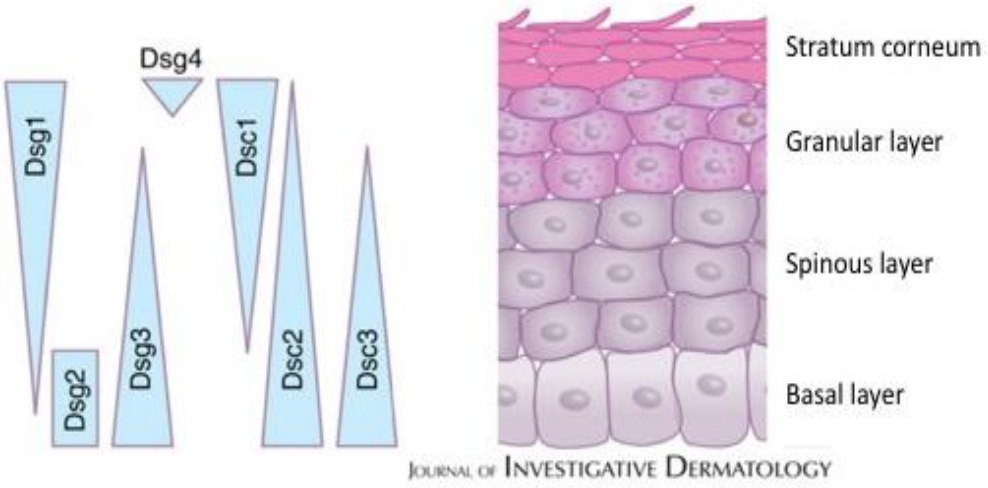

Figure 5: **Isoform-specific expression pattern of the desmosomal cadherins in normal human epidermis.**

The epidermis is a stratified epithelium comprised of four distinct layers: the basal layer, spinous layer, granular layer, and the stratum corneum. Variations in the expression patterns of desmosomal cadherins were observed along distinctive epithelial layers. The relative expression profiles are depicted on the left (Green & Simpson, 2007).

The precise role for such distinct expression patterns of desmosomal cadherins is still a matter of discussion and not fully understood. Early evidence demonstrated that desmosomes at different epithelial layers are involved in transducing signalling events associated with epidermal differentiation (Fuchs & Byrne, 1994). A followup study suggested that reciprocally graded distributions of desmosomal isoforms are required at different levels of the stratified epithelia to suit specialised mechanical needs during morphogenesis of multi-layered tissues (Thomason et al, 2010). In general, it is believed that the correct stoichiometry ratios of these desmoglein isoforms in the epidermis are crucial to the normal tissue homeostasis. Nonetheless, there is some evidence of functional redundancy between different desmosomal components or isoforms since overlapping expression patterns of plakophilins and other desmosomal

components are detected in mammalian tissues (Neuber et al, 2010). The expression pattern of desmosomal components and associated diseases in human and mouse models are depicted in Table 1 (Page 29).

Table 1: The expression patterns of desmosomal proteins, desmosome associated human diseases and transgenic mouse models (H, human; M, mouse; KO, knockout).

Desmosomal components	Expression patterns in the skin	Desmosome-associated human diseases (H)/Transgenic mouse models (M)
Dsg1	Only in stratified squamous epithelia, predominately in the upper layers of the epidermis (Evangelista et al, 2008)	**H: mutation**-> Striate palmplantar keratoderma (Getsios et al, 2004); **PV-IgG**->*Pemphigus* foliaceus, **ETA**->staphylococcus scalded skin syndrome (Waschke, 2008)
Dsg2	Ubiquitously in most desmosome containing tissues, basal layer of the epidermis (Evangelista et al, 2008)	**H:mutation**-> Arrhymogenic right ventricular cardiomyopathy (Awad et al, 2006) **M:KO**->Embryonic lethality (Getsios et al, 2004)
Dsg3	Basal and lower spinous layers of the epidermis, decreases gradually toward the upper layers (Evangelista et al, 2008)	**H: PV-IgG**->*Pemphigus* vuglaris (Amagai et al, 1991) **M:KO**->Supra-basal acantholysis (Saito et al, 2009)
Dsg4	Hair follicles, granular layer (Delva et al, 2009)	**H:mutation**-> Hypotrichosis (Kljuic et al, 2003) **M:KO**->Defective hair follicle differentiation in mice (Getsios et al, 2004)
Dsc1	Throughout the epidermis, highly in the upper layers (Evangelista et al, 2008)	**M:KO**->Hyperproliferation, hair follicles degeneration, increased expressions of keratin 6 and 16 (Chidgey et al, 2001)
Dsc2	Ubiquitously in most desmosome containing tissues, (Evangelista et al, 2008), basal and lower spinous layers (Delva et al, 2009)	**H:mutation**-> Arrhymogenic right ventricular cardiomyopathy (Awad et al, 2006)

Dsc3	Lower epidermis, decreases gradually toward the upper layers (Evangelista et al, 2008)	**M:KO**->Epidermal fragility, hair loss, preimplantation embryonic lethality (Chen et al, 2008)
PKP1	Highly in suprabasal layers of stratified epithelia (Delva et al, 2009)	**H:mutation**-> Ectodermal dysplasia, skin fragility syndrome (McGrath et al, 1997)
PKP2	Simple epithelia, the heart, a variety of mesenchymal cell types, lower stratified epithelia (Lahtinen et al, 2008)	**H:mutation**-> Arrhymogenic right ventricular cardiomyopathy (Gerull et al, 2004) **M:KO**->Heart Defects (Grossmann et al, 2004)
PKP3	Simple, stratified epithelia (Mertens et al, 2001), uniform expression throughout the epidermis (Bonne et al, 1999)	
plakoglobin	Throughout the epidermis (Waschke, 2008)	**H:mutation**-> Naxos disease (McKoy et al, 2000) **M:KO**->Fragility of the myocardium (Bierkamp et al, 1996)
Desmoplakin	In all desmosomes containing tissues (Getsios et al, 2004).	**H:mutation**-> Arrhymogenic right ventricular cardiomyopathy, striate palmplantar keratoderma (Armstrong et al, 1999; Rampazzo et al, 2002) **M:KO**->Embryonic lethality (Gallicano et al, 1998)

1.3.5 Desmosome function

Desmosomes have long been recognised as an adhesive core that anchors the intermediate filaments to the plasma membrane. Their primary role is to provide strong cell-cell adhesion to maintain the structural and functional integrity of tissues. They are crucial for tissues that are subjected to continuous mechanical stress and are particularly abundant in stratified epithelia such as skin, mucous membranes (Farquhar & Palade, 1963), myocardial and Purkinje fibre cells of the heart (Green & Gaudry, 2000). Besides serving as an adhesion structure, desmosomes are also involved in the regulation of epithelial morphology, tissue homeostasis (Getsios et al, 2004), cell positioning (Runswick et al, 2001), proliferation and differentiation (Allen et al, 1996; Hardman et al, 2005; Merritt et al, 2002; Morasso & Tomic-Canic, 2005).

The importance of desmosomes in development can be observed from gene ablation studies (Table 1). Mice with ablation of Dsg3 are normal at birth but exhibit epidermal adhesion and differentiation defects at 6 months of age (Koch et al, 1997). Mice with ablation of Dsg2 exhibit an embryonic lethal phenotype and die shortly after implantation (Eshkind et al, 2002). Even more remarkably, ablation of Dsc3 is lethal before implantation suggesting an additional non-desmosomal role prior to the formation of desmosomes during development (Den et al, 2006).

Other misexpression experiments also revealed that a tight regulation of desmosomal cadherin expression is critical to the normal tissue homeostasis. It was demonstrated that redirecting the expression of desmosomal cadherins to suprabasal layers of the skin has a dramatic effect on cell proliferation and differentiation. For instance, misexpression of desmosomal cadherins Dsc3a and Dsc3b to suprabasal differentiating keratinocytes is strongly associated with altered stability of β-catenin, impaired keratinocyte proliferation and differentiation in transgenic mice (Hardman et al, 2005). The expression of

NH2-terminally truncated Dsg3 mutant driven by the K14 promoter, resulted in the widening of the intercellular spaces, accumulation of truncated Dsg3 proteins and disruption of the ultrastructural organisation of desmosomes. These phenotypes are also accompanied with hyper-proliferation, altered epidermal differentiation and inflammatory response in some skin regions of the transgenic animal (Allen et al, 1996). Similarly, it was demonstrated that overexpression of Dsg3 by the K1 promoter in the suprabasal epidermis of transgenic mice was associated with hyper-proliferation and altered differentiation (Elias et al, 2001; Hardman et al, 2005; Merritt et al, 2002). However, this finding is in contrast with another study, in which overexpression of Dsg3 by the involucrin promoter resulted in altered differentiation and severe barrier defects. It converts the stratum corneum to a mucous like phenotype leading to early postnatal lethality due to dehydration or water loss, but fails to induce hyper-proliferation at the granular layer (Elias et al, 2001). The underlying cause of the discrepancy is still unclear. The role of desmosomal cadherins in the regulation of keratinocyte proliferation can also be demonstrated clinically in the autoimmune skin blistering disease *pemphigus vulgaris* (PV). It was shown that PV autoantibodies impair Dsg3/plakoglobin signalling and in turn leads to c-Myc overexpression and enhanced keratinocyte proliferation in PV patients (Muller et al, 2008; Williamson et al, 2006) (Refer to Introduction Chapter 1.5.2).

It is also known that desmosomal cadherins are mediators of diverse signalling pathways that could influence the regulation of epidermal morphogenesis. Getsios and colleagues showed that the expression of Dsg1 without its N-terminal domain, which is responsible for cell-cell adhesion, is capable of promoting keratinocyte differentiation. The authors suggested that such response is mediated through the inhibition of the epidermal growth factor receptor-extracellular signal-regulated kinase 1/2 (EGFR-Erk1/2) signalling pathway, an adhesion-independent pathway that does not rely on its adhesive capability with other desmosomal cadherins (Getsios et al, 2009). Similarly,

Brennan and colleagues showed that overexpression of Dsg2 under the control of the involucrin promoter enhances the activation of multiple signalling pathways such as phosphatidylinositol-3-kinase (PI3-kinase), MEK-MAPK and STAT3, contributing to enhanced growth rate, anchorage-independent cell survival and malignant phenotype in the epidermis of transgenic mice (Brennan & Mahoney, 2009). Taken together, these studies suggest that desmosomal cadherins are capable of activating signalling events that are independent of their adhesive function (Refer to Introducton Chapter 1.5.2.4).

1.4 Molecular crosstalk between desmosomes and other junctional components

It has long been an area of interest in understanding the cross-talk between desmosomes, adherens junctions and the actin cytoskeleton. It was demonstrated that these intercellular junctions are mutually dependent and emerging evidence suggests that adherens junctions and the actin cytoskeleton are also involved in the pathogenesis of skin blistering disease *pemphigus vulgaris*. Thus, it will be interesting to identify how desmosomes couple to other intercellular junctions and signalling pathways to drive the differentiation programs and tissue morphogenesis.

1.4.1 Adherens junctions

Adherens junctions (AJs) are another type of cell adhesion structure, which differs from desmosomes both in terms of morphological structure and molecular composition (Haftek et al, 1996). They are expressed throughout the epidermis and participate in various important cellular functions such as embryonic development, maintenance of tissue integrity, epithelial polarity and differentiation (Tu et al, 2008). Adherens junctions are primarily composed of the classical E- and P-cadherins and the cytoplasmic catenins such as p120, β- and α-catenins (Figure 6). The classical cadherins mediate

homophilic cell-cell adhesion through their extracellular domains, while the cytoplasmic tails link the cadherin complex to β-catenin or plakoglobin and α-catenin. α-catenin in turn binds directly to actin filaments or indirectly through association with vinculin and VASP (Green & Simpson, 2007). This cadherin–catenin complex further interacts with other proteins such as the nectin–afadin complex (Niessen, 2007) and signalling molecules such as phosphatidylinositol 3-kinases, Rho family GTPases and Src family tyrosine kinases (Braga et al, 1997; Calautti et al, 1995; Tu et al, 2008), rendering the adherens junctions into a highly dynamic supramolecular complex. The presence of these signalling molecules has been well associated with both positive and negative regulatory roles on the cadherin function (Behrens et al, 1993; Calautti et al, 1998; Matsuyoshi et al, 1992; Tsukita et al, 1991).

The conventional view of adherens junctions is that E-cadherin links through α-/β-catenin complex to the actin cytoskeleton (Skoudy et al, 1996; Tsukita et al, 1992). However, recent biochemical and protein dynamics analysis have shown that such a direct physical linkage between α-catenin to actin filaments might not exist (Yamada et al, 2005). On the contrary, a more transient interaction between α-catenin and actin filaments is proposed (Kobielak & Fuchs, 2004) and such linkage may involve other actin-related proteins such as vinculin, α-actinin, formin, ZO-1, afadin and a recently discovered protein: EPLIN (Gumbiner, 1996; Harris & Tepass, 2010).

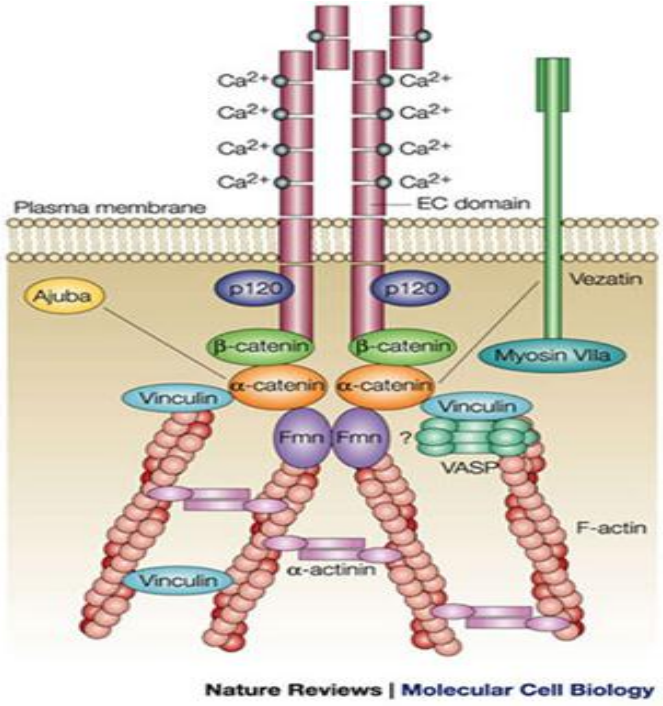

Figure 6: A model for the structure of adherens junctions.

The extracellular domains of the classical cadherin interact with the opposing cells, while the cytoplasmic tails link the cadherin complex to p120 and β-catenin or plakoglobin at different regions, the latter of which binds to α-catenin and the actin filaments (Kobielak & Fuchs, 2004).

1.4.1.1 Classical cadherins

The classical E-cadherin, the principal component of adherens junctions, is found in all layers of the epidermis (Hirai et al, 1989), while P-cadherin is restricted only to the basal cell layer (Delva et al, 2009). E-cadherin interacts with other catenins and the actin cytoskeleton to mediate strong cell-cell adhesion. Loss or mutation of E-cadherin not only disrupts intercellular adhesion, but also contribute to the epithelial-mesenchymal transition. A common hallmark of cancer progression where epithelial cells become less polarised in apical-to-basal axis and acquire a more migratory and invasive phenotype (Furukawa et al, 1997). Studies have confirmed that aberrant expression of E-cadherin is associated with invasiveness and metastasis potential for many cancer types including lung, prostate, gastric, breast and colon cancers (Shinmura et al, 1999). Thus, it is believed that E-cadherin

expression can serve as a significant prognostic marker for tumour progression and behaviour (Wijnhoven et al, 2000).

1.4.1.2 Catenins

β-catenin and p120 are members of the armadillo-repeat-containing family of proteins and they share a high sequence similarity. β-catenin binds to the distal part of the E-cadherin cytoplasmic tail and connects it to the actin cytoskeleton via α-catenin (Figure 7). Besides bridging E-cadherin with the actin-binding proteins, β-catenin has a second function as a transcriptional co-activator in the Wnt signalling pathway. Abnormal Wnt signalling caused by mutation of β-catenin is frequently detected in cancer (Austinat et al, 2008).

p120 catenin is originally described as a substrate of Src. It binds to the juxtamembrane region of E-cadherin and does not bind to α-catenin (Figure 7). At present, four isoforms derived from alternative splicing have been identified. p120 is known to participate in a wide range of biological processes such as influencing cell motility (Shen et al, 2008), cadherin clustering (Yap et al, 1998) and modulating the activities of Rho family GTPases in cell adhesion and the reorganisation of actin cytoskeleton (Michael & Yap, 2013; Noren et al, 2000). There is a substantial body of literature suggesting that p120 catenin is involved in stabilising the E-cadherin catenin complex. It was shown that p120 protects E-cadherin at the cell surface from endocytosis and in turn strengthens the adhesiveness of the adherens junctions (Yap et al, 2007). This finding is in line with a study by Reynolds and colleagues, which showed that down-regulation of p120 is associated with the concomitant loss of E-cadherin in some cases of metastatic cancer (Reynolds, 2007).

α-catenin is an actin-binding protein that lacks the armadillo domain and differs from other catenins in terms of sequence and structural organisation. Its N-terminal domain interacts with β-catenin, while the C terminal tail binds to α-actinin, vinculin (Yamada et al, 2005) and links the E-cadherin-catenin

complex to the actin cytoskeleton (Kobielak & Fuchs, 2004). It was suggested that α-catenin could not simultaneously bind to both E-cadherin-β-catenin and actin filaments *in vitro*, suggesting a more complex molecular events between α-catenin and actin complex (Yamada et al, 2005). Besides serving as an essential component of adherens junctions, α-catenin can integrate adhesion with other essential cellular events. It was demonstrated that ablation of α-catenin enhances the Ras-MAPK signalling pathway resulting in hyper-proliferation and defective cell polarisation of keratinocytes (Vasioukhin et al, 2001a). Taken together, catenins play a crucial role in linking cadherins to the actin cytoskeleton and control the overall adhesive function of adherens junctions.

1.4.2 Actin cytoskeleton

The actin cytoskeleton provides mechanical stability and strong cell adhesion based on their anchorage to adherens junctions and focal contacts (Brieher & Yap, 2012; Perez-Moreno et al, 2003), a prerequisite for epithelial polarisation and stratification (Zhang, 2005). However, in response to environmental cues, rapid and localised disassembly of adhesive interactions and reorganisation of the underlying actin cytoskeleton allow remodelling of epithelial cells into an alternate morphology state more favourable to cell migration and wound healing. These spatial and temporal regulations of intercellular adhesions and the actin cytoskeleton are often associated with a wide range of cell signalling molecules including Rho GTPases (Blanchoin & Michelot, 2012; Fukata & Kaibuchi, 2001; Michael & Yap, 2013).

During early phases of calcium-induced intercellular junction formation, cells project membrane protrusions such as lamellipodia and filopodia at the leading edge of cells (Kovacs & Yap, 2008). This forward translocation mechanism helps to initiate cell-cell contacts and allows a series of transient weak adhesion zipper to form (Borisy & Svitkina, 2000; Mack et al, 2011; Zhang et al, 2005). The adhesion zipper attaches the extending membrane to

the extracellular matrix, which is followed by the clustering of adherens junctional proteins such as E-cadherin, β-/α-catenins along the developing cell-cell contacts (Hansen et al, 2002; Perez et al, 2008). Concomitantly, these cadherin-catenin complexes trigger the reorganisation of actin cytoskeleton and other regulators such as Rho GTPases to form a productive and stable adhesion (Zhang, 2005).

As shown in Figure 9, Braga and her group have identified two spatial populations of actin at the cell-cell contacts during the process of calcium-induced junction formation. One of the populations is referred as the junctional actin, which is associated with wavy, thin punctate staining pattern at junctions. The second population is referred as the peripheral thin bundles, which are associated with an array of thin bundles of actin filaments prior to the formation of cell-cell contacts. During the assembly of adherens junctions, progressive reorganisation of these two populations merges at the cell-cell contacts, resulting in a continuous line of mature junctional actin around the cell periphery (Zhang, 2005).

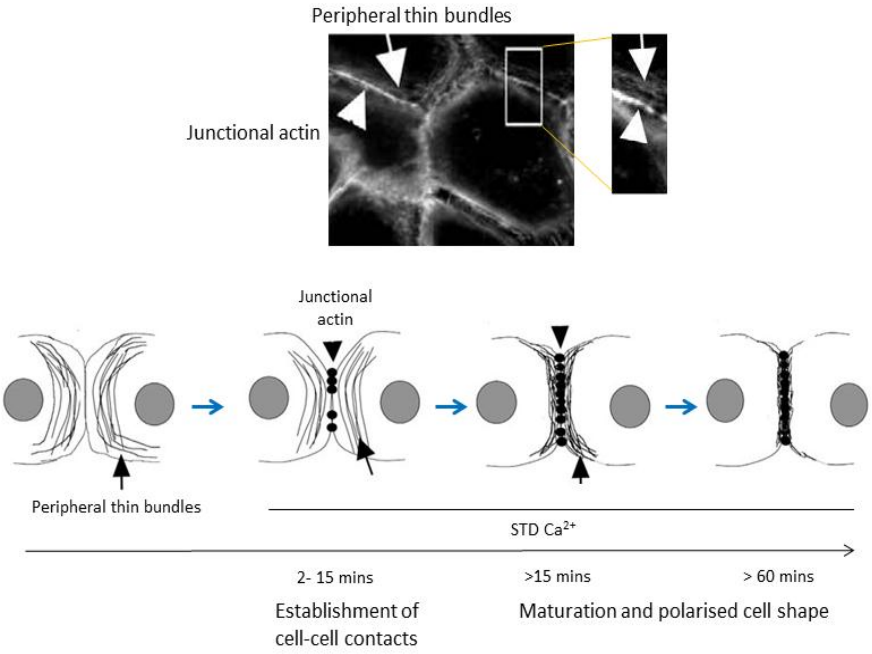

Figure 7: Two spatial actin populations.

As adherens junctions assemble, peripheral thin bundles and junctional actin merge at the cell-cell contacts to form mature junctional actin. Arrows indicate bundles; arrowheads indicate junctional actin (Zhang, 2005).

1.4.3 Molecular dialogue between desmosomes, adherens junctions and the actin cytoskeleton.

It is well established that adherens junctions assemble first during development and play a master regulatory role in the initiation, organisation and formation of other adhesive junctions such as desmosomes and gap junctions. Studies have shown that inhibition of E-cadherin or P-cadherin *in vivo* not only impairs the adherens junctions, but also affects the desmosomes, tight junctions and the cortical actin cytoskeleton (Hodivala & Watt, 1994; Lewis et al, 1994; Tinkle et al, 2008). More recently, emerging evidence suggests that reduced function of desmosomes may also interfere with the formation and/or maintenance of adherens junctions and the actin cytoskeleton.

Studies have shown that loss of plakoglobin resulted in the intermingling of desmosomal and adherens junctional components in the intercalated discs of heart tissue (Bornslaeger et al, 1996; Ruiz et al, 1996; Vasioukhin et al, 2001b). Similarly, keratinocytes derived from desmoplakin-null skin have very few desmosomes or adherens junctions *in vitro*. They also lack the intermediate filaments to connect desmosomes at sites of cell–cell contact, which in turn compromise the actin reorganisation and membrane sealing during epithelial sheet formation (Vasioukhin and Fuchs, 2001). Others reported that plakophilin (PKP), a p120-related desmosomal plaque protein, is involved in the regulation actin-dependent regulation of desmosome assembly. Godsel and colleagues showed that a pool of PKP2 localises to cell–cell borders is essential for proper localisation of RhoA at cell–cell interfaces and facilitates the translocation of desmoplakin into newly forming desmosomes (Godsel et al, 2010; Godsel et al, 2005).

1.4.4 Signalling pathways associated with these junctions

Intracellular signalling pathways play an essential role in the interplay between different adhesion systems. Their downstream effects have been associated with both positive and negative changes in the stability and function of intercellular adhesion. Thus, understanding the spatiotemporal and bidirectional intracellular signalling events between these systems are important in addressing the molecular mechanisms involved. Here I focus on the signalling pathways that are associated with desmosomes, adherens junctions and the underlying actin cytoskeleton, in particularly the activation of small GTPases and Src family tyrosine kinases.

1.4.4.1 Rho family GTPases

The Rho GTPases family consists of three subfamilies: Rho, Rac and Cdc42 (Noren et al, 2001). They belong to a group of low molecular weight GTP binding proteins, which can be activated by a variety of growth factors and

adhesion molecules. The Rho family GTPases cycle between the inactive GDP-bound and active GTP-bound states, which are catalysed by three key classes of regulators (Braga & Yap, 2005; Menke & Giehl, 2012). Guanine nucleotide exchange factors (GEFs) regulate the exchange of GDP for GTP; GTPase-activating proteins (GAPs) enhance the GTPase activity and reconvert it back to the inactive GDP-bound form; Rho GDP dissociation inhibitors (Rho GDIs) prevent the exchange of GDP for GTP. Upon activation, the GTP-bound GTPases are translocated to specific membrane sites, where they interact with other effector proteins to regulate a wide range of biological processes such as the organisation of actin cytoskeleton, morphogenesis, apoptosis and tumourigenesis (Ridley, 2012).

The Rac subfamily consists of three members namely: Rac1, -2 and -3 (Ridley, 2006). Rac co-localises with E-cadherin at sites of cell–cell contact and its activation is primarily associated with the formation of lamellipodia and membrane ruffles via Arp2/3 and WAVE complex (Menke & Giehl, 2012). The Cdc42 subfamily consists of G25k and Cdc42Hs (Johnson, 1999; Kodama et al, 1999) and are found at sites of cell–cell contacts as well as the Golgi apparatus (Friesland et al, 2013). The activation of Cdc42 GTPases is primarily involved in the formation of filopodia and establishment of cell polarity through the reorientation of the microtubule organising center (MTOC) and Golgi apparatus (Desai et al, 2009; Palazzo et al, 2001). The Rho subfamily consists of primarily three members namely: RhoA, -B and -C. In contrast to Rac and Cdc42, the localisation of Rho varies depending on cell type (Yonemura et al, 2004). For instance, RhoA and -C are localised in both cytoplasm and at the cell membrane, while RhoB is localised primarily on endosomes (Dietrich et al, 2009; Takaishi et al, 1997; Wheeler & Ridley, 2004). The activation of Rho GTPase is mainly associated with the formation of stress fibers and maturation of focal adhesion (Ridley, 2006). Its downstream effect influences the myosin light chain kinase (MLCK), cell contractility (Renaudin et al, 1999) as well as maintenance of cell-cell adhesion (Spindler & Waschke, 2011). It has been demonstrated that signalling downstream of Rho through ROCK

destabilises adherens junctions, whereas signalling through Diaphanous is required for maintenance of adherens junctions (Sahai & Marshall, 2002).

1.4.4.2 Rho GTPases in cadherin-mediated adhesion

The Rho family GTPases have emerged as key players in the regulation of cadherin-mediated cell-cell adhesion. The inside-out signalling activated by GTPases can either act directly on the cadherin-catenin complex or indirectly through influencing other junctional components or the cadherin recycling and degradation pathways. Braga and colleagues reported that blocking the function of Rac1 and RhoA inhibits the accumulation of cadherin at sites of cell–cell contact following calcium-induced intercellular adhesion in keratinocytes (Braga et al, 1997). Takaishi and colleagues showed that overexpression of dominant positive Rac (Rac1V12) induces the accumulation of E-cadherin, β-catenin and actin filaments at sites of cell–cell contact in MDCKII cells, while overexpression of dominant negative Rac (Rac1N17) reverses this effect with reduced accumulation of these components (Takaishi et al, 1997). These studies suggest that the activation of Rho proteins especially Rac1 is required for the cadherin-directed actin assembly (Braga et al, 1997; Noren et al, 2001; Yap & Kovacs, 2003a).

It was reported that Cdc42 and Rac1 could indirectly regulate the E-cadherin activity via IQGAP1 (Fukata et al, 1999). For instance, the binding of active GTP-bound Cdc42/Rac1 to IQGAP1 inhibits the interaction of IQGAP1 with β-catenin. This in turn positively regulates cadherin function by enhancing the association of cadherin/catenin complex with the actin cytoskeleton (Fukata et al, 2001). However, Hage and colleagues showed that the binding of active Rac1 to IQGAP1 decreases the E-cadherin-mediated adherens junctions in pancreatic carcinoma cells, suggesting a cell type-specific Rac1-E-cadherin-IQGAP mechanism (Hage et al, 2009). Alternatively, Rac1 and Cdc42 were reported to regulate the activity of matrix metalloproteinases (MMP-2), thereby indirectly modifying E-cadherin-mediated cell–cell adhesion (Fukata et al, 2001).

The signals triggered by these newly formed adherens junctions can in turn generate a feedback loop influencing the organisation of the established adhesions. Homophilic binding of E-cadherin at cell-cell contacts can trigger the activation of outside-in signal, resulting in local activation of Rac1 and Cdc42 essential for the junction stability. It was demonstrated that homophilic binding of E-cadherin activates Rac1 through PI3K-dependent pathway in MDCKII cells to control adhesive contacts (Jeanes et al, 2009) and induces rapid activation of Cdc42 in MCF-7 epithelial cells (Kim et al, 2000). However, the requirement of Cdc42 in new junction assembly or maintenance is still unclear. Erasmus and colleagues assessed the activation of Cdc42 specifically using only confluent keratinocytes cultures and induced cell–cell contacts by the addition of calcium ions to avoid cell migration or growth factor-related Cdc42 activation. It was found that cell-cell contacts do not induce filopodia or require Cdc42 to initate stable cadherin adhesion in keratinocytes (Erasmus et al, 2010).

With respect to desmosomes, it was shown that activation of Rho GTPases RhoA, Rac1 and Cdc42 using an array of bacterial toxins resulted in an enhanced Dsg3 cell membrane staining and increased Dsg1-mediated adhesion (Spindler & Waschke, 2011). In reverse, inhibition of these GTPases showed fragmented Dsg3 membrane staining, enlarged intercellular gap formation and reduced Dsg1 and Dsg3-mediated adhesion, suggesting that these GTPases regulate keratinocyte adhesion, at least in part, on the level of desmosomal cadherins (Spindler & Waschke, 2011). The clinical relevance of Rho GTPase signalling in modulation of desmosomal adhesion will be discussed in Chapter 1.5.2.4 Signal transduction pathways.

Taken together, the functions of cadherins and small GTPases correlate in many different levels and one could not exclude the possibility that they cooperate/ overlap with one another to regulate specific targets such as cell-cell adhesion. It is believed that cooperation of these downstream signalling

events is required during establishment and maintenance of the epithelial phenotype (Braga et al, 1997; Takaishi et al, 1997) and the precise regulation of these GTPases is dependent upon the degree of junction maturation, cellular context and the cell system used (Braga, 2002).

1.4.4.3 Tyrosine kinases

Non-receptor Src family consists of a large number of structurally related-tyrosine kinases. They are known to play essential role in signalling transduction pathways that regulate cell proliferation, migration, cell-cell/cell-matrix adhesions and differentiation (Calautti et al, 1998; Nagathihalli & Merchant, 2012; Serrels et al, 2011). Among the nine known family members, Src, Fyn and Yes are expressed in the keratinocytes. c-Src, the cellular form of protein tyrosine kinase, is composed of six functional domains such as SH4, a unique domain, SH3, SH2, SH1 and a C-terminal tail, which varies among family members (Brown & Cooper, 1996). The oncogenic v-Src, which lacks the C-terminal inhibitory phosphorylation site (Tyr530) differs from the cellular form primarily in enzymatic activity and is constitutively active as opposed to normal c-src.

External stimuli such as growth factor or cell-cell adhesion can trigger transient activation of Src through a number of different mechanisms such as phosphorylation of Tyr416/de-phosphorylation Tyr530 (*in vivo*), protein-protein interactions via its SH domains or other kinase independent pathways. Among these mechanisms, regulation of Src by phosphorylation of Tyr416 seems to play a key role in the formation of E-cadherin-mediated adherens junctions (McLachlan et al, 2007). Structural analysis demonstrated that Src kinase can switch between active and inactive states in response to intra- or extracellular signals. As shown in Figure 8, auto-phosphorylation of Tyr416 activates Src through a conformational change in SH domains, which “opening” up the molecule for intermolecular interactions with other Src binding partners. Conversely, phosphorylation of Tyr530 inactivates Src through blocking its active site with the SH and kinase domains, resulting in a

"closed" auto-inhibited conformation (Brown & Cooper, 1996; Xu et al, 1997). This "closed" conformation can also be reversed by dephosphorylation of Tyr530, which relieves the intramolecular inhibition of c-Src kinase activity and leads to Src activation.

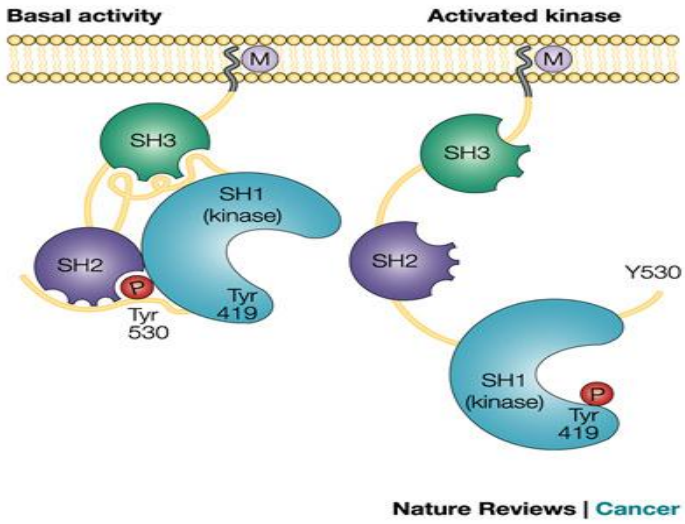

Figure 8: Activation of Src proteins.

Phosphorylation of Tyr530 results in a "closed" conformation, which prevents access of other Src binding partners to the kinase domain. Conversely, auto-phosphorylation of Tyr416 mediates a conformational change in the SH domains, which "opening" up the molecule for intermolecular interactions with other substrates. M, myristoylation; P, phosphorylation (Yeatman, 2004).

1.4.4.4 Src family kinases in cadherin-mediated adhesion

The functional interplay between Src kinases and cadherin-mediated cell adhesion has been well reported. It has been shown that the E-cadherin mediated cell–cell contacts trigger the activation of c-Src and/or other Src family kinases (SFKs) at the site of cell–cell contacts. Once activated, these kinases are recruited to specific membrane sites such as adherens junctions (Baumgartner et al, 2008), where they phosphorylate multiple effector proteins and transduce signals from the extracellular cues to the cell interior. Junctional proteins including E-cadherin, β-catenin, plakoglobin and p120

catenins have been identified as the major targets for Src-induced tyrosine phosphorylation in the adherens junctions (Abram & Courtneidge, 2000; McLachlan & Yap, 2011; Parsons & Parsons, 1997; Tsukamoto & Nigam, 1999).

Calautti and colleagues found that β-catenin, plakoglobin and p120 are all tyrosine phosphorylated at the onset of calcium-induced keratinocyte differentiation in primary mouse keratinocytes. Such changes were also accompanied by increased association between α-catenin and p120 with E-cadherin, suggesting tyrosine phosphorylation of the cadherin-catenin complex plays a positive role in the strengthening of cell-cell adhesion. Consistently, it was demonstrated that cells treated with tyrosine kinase inhibitors or keratinocytes of Src/fyn double-knockout mice have similar effect with reduced adhesive strength of differentiating keratinocytes (Calautti et al, 1998; Calautti et al, 2002). These studies suggested that tyrosine phosphorylation of Src kinases is essential in the keratinocyte junction formation and differentiation (Calautti et al, 1998; Calautti et al, 2002).

Unlike what has been proposed for differentiating keratinocytes, tyrosine phosphorylation of adherens junctional components is also associated with the increased invasiveness in human cancer (Behrens et al, 1993; Hamaguchi et al, 1993; Irby & Yeatman, 2000). The expression of v-Src or constitutively active Src has been shown to enhance the tyrosine phosphorylation of the cadherin/catenin complex components and thereby perturbing the cadherin adhesion and cell–cell integrity (Behrens et al, 1993; Matsuyoshi et al, 1992). For instance, overexpression of Src and Fyn enhance the tyrosine phosphorylation of β-catenin with a concomitant downregulation of E-cadherin-mediated adhesion (Irby & Yeatman, 2000). Similarly, Fyn was shown to induce phosphorylation of β-catenin at Tyr-142, resulting in a loss of the β-catenin/α-catenin interaction and disruption of cell-cell adhesion (Piedra et al, 2003). Additionally, modulation of cadherin-mediated adhesion by Src kinase can arise indirectly through other processes such as E-cadherin turnover/degradation. It was showed that the expression of v-Src alters the E-

cadherin trafficking from a recycling pathway to a lysosomal targeting pathway, thus further weakening of cell-cell adhesion (Palacios et al, 2005).

Based on these studies, it was concluded that increased tyrosine phosphorylation of the cadherin–catenin complex is a negative regulator of cadherin function in oncogene-transformed or mitogenically stimulated cells and thus implicated as a key promoter of cell migration. Some studies suggest that targeting Src signalling pathways could potentially restore E-cadherin-mediated cell adhesion with a concomitant suppression of migratory capacity. For instance, Src-specific inhibitor PP2 was reported to restore the E-cadherin/catenin adhesion system, possibility through up-regulation of E-cadherin/catenin gene expression or other mechanisms involving downstream effector, Rho (Nam et al, 2002).

One possible explanation regarding this discrepancy is that Src has both positive and negative regulatory role in cell-cell adhesion depending on the signalling events and cell system used (McLachlan et al, 2007). McLachlan and colleagues pointed out that the loss of function approach may reduce the enhanced levels of tyrosine phosphorylation in adherens junctions and hence contributes to its positive regulatory role on cadherin function (Calautti et al, 1998). On the other hand, the gain of function approach may give excessive tyrosine phosphorylation that is far beyond the physiological levels and thus perturbs the cadherin adhesion and cell–cell integrity (Amagai et al, 2000; Behrens et al, 1993; Matsuyoshi et al, 1992; McLachlan et al, 2007).

Unlike the adherens junctions, the effects of tyrosine phosphorylation on desmosomes are less studied. Gaudry and colleagues demonstrated EGFR-induced tyrosine phosphorylation of plakoglobin compromises the linkage between the desmosomal plaque protein desmoplakin and the intermediate filaments and thus destabilises the desmosomal adhesion (Gaudry et al, 2001). Conversely, Kowalczyk and colleagues showed that Src-induced phosphorylation of plakoglobin Tyr643 increases its association with desmoplakin (Green & Gaudry, 2000; Kowalczyk et al, 1997), suggesting a

positive function in desmosomes. This finding is in line with another study, which showed that MDCK cells treated with tyrosine phosphatase inhibitor sodium pervanadate increase the tyrosine phosphorylation of Dsg2 and plakoglobin, which in turn stabilise the desmosomal adhesion with enhanced hyper-adhesiveness (Garrod et al, 2008). The reason for such discrepancy is still not clear. The underlying molecular mechanism could be dependant on the signalling strength and cellular context similarly to adherens junctions.

1.4.4.5 Caveolin

Caveolae are small indentations of the plasma membrane that function in a number of cellular processes such as cholesterol homeostasis, membrane trafficking, lipid recycling and signalling transduction (Echarri et al, 2007). They have a characteristic flask shape and are enriched with a variety of signalling molecules such as G proteins subunits, receptor and non-receptor tyrosine kinases and mitogen-activated protein kinases (Hernandez-Deviez et al, 2008).

Caveolins (Cav), the 21 to 24k Da integral membrane proteins, are the principal structural component of caveolae. Among its three family members, Cav-1 and Cav-2 are expressed in adipocytes, endothelial, epithelial and fibroblastic-cells, whereas Cav-3 is predominately found in muscle tissue types (Tang et al, 1996). Cav-1 is essential for the structural and regulatory role of caveolae formation and involved in other functions such as cell migration, apoptosis, cellular proliferation and differentiation (Williams & Lisanti, 2005). In human cancers, both up- and down-regulation of this gene are associated with cell transformation and metastasis**.**

In Chapter 6.1.4, it was shown that Dsg3 is involved in the regulation of Src activation. However, the underlying mechanism is still unknown. Since Dsg3 does not possess a tyrosine kinase domain, another protein that associates with both Src and Dsg3 is likely involved in the Dsg3-induced Src activation.

We hypothesised that Dsg3 might activate Src through its association with caveolin-1, which has been reported to interact with desmosomal cadherin Dsg2 and Src kinases. Lisanti and colleagues proposed a popular caveolin signalling mechanism. It was showed that caveolin-1 might regulate the activation state of caveolae-associated signalling molecules through holding the signalling molecules in their inactive state via its 'caveolin-scaffolding domain' (CSD) (Lisanti et al, 1995). Similarly, a follow-up study by Li and colleagues also demonstrated that binding of caveolin residues 82-101 to Src inhibits the auto-activation of c-Src (Li et al, 1996). Brennan and colleagues suggested that Cav-1 is associated with Dsg2 through a putative Cav-1 binding motif and involved in the Dsg2-induced signalling and malignant transformation. It was shown that the enhanced expression and proteolytic processing of Dsg2, possibly through its interaction with Cav-1, interferes with the assembly and maintenance of desmosome junctions and homeostasis (Brennan et al, 2007; Brennan & Mahoney, 2009; Brennan et al, 2012).

1.5 Desmosome-associated diseases

1.5.1 Genetic and infectious diseases

A wide range of studies revealed that disruption of desmosomal cadherins and cytoplasmic plaque proteins could have significant clinical consequences, particularly affecting the heart and the skin. These human diseases highlight the important functions for desmosomes in cell–cell adhesion and tissue intergrity. Firstly, inherited disorders can be found in three of the desmoglein isoforms. Mutations in Dsg1 lead to skin disorder such as striate palmoplantar keratoderma (Getsios et al, 2004), while mutations in Dsg2 are associated with heart disorder isoarrhythmogenic right ventricular cardiomyopathy (ARVC) (Awad et al, 2006). There is no example for the inherited disorder induced by mutation of the Dsg3 gene was identified (Delva et al, 2009). Loss of Dsg4 is associated with defective hair-follicle differentiation (Kljuic et al,

2003). Other desmosomal components and associated diseases in human and mouse models are depicted in Table 1 (Page 28).

In addition to genetic defects, desmosomal cadherins can be inactivated by infectious bacteria toxins. Staphylococcal scalded-skin syndrome and bullous impetigo (Amagai et al, 2000) are caused by infectious bacteria toxins produced by some strains of staphylococcus aureus bacteria resulting in widespread or localised superficial blistering. The histopathologies of these diseases are similar to patients with *pemphigus foliaceus*, where bacterial proteases specifically cleave the extracellular domain of Dsg1 and lead to the disruption of cell–cell adhesion and blister formation in the superficial layer of the epidermis (Amagai et al, 2000; Hanakawa et al, 2000).

1.5.2 Desmoglein-related disease: *Pemphigus*

Pemphigus is an autoimmune, life threatening blistering skin disease. It is characterised by autoantibody binding to Dsg1 and Dsg3, resulting in the loss of cell-cell adhesion and blister formation in skin and mucous membranes. This process is also known as *pemphigus* acantholysis, which referred to the disruption of the intercellular connections between the stratum spinosum of the epidermis or mucosa, resulting in the separation and atrophy of the prickle cells layer (Amagai, 2009; Mascaro et al, 1997). There are two major types of *pemphigus*: *pemphigus foliaceus* (PF) and *pemphigus vulgaris* (PV). In *pemphigus foliaceus* (PF), patients with autoantibodies targeting Dsg1 are characterised by blistering lesions in the upper granular cell layer of the epidermis (Beutner et al, 1965), without affecting the mucosal epithelia (Rivitti et al, 1994). *Pemphigus vulgaris* (PV), the more severe form, is further divided into two subtypes. Patients with mucosal dominant PV produce autoantibodies against Dsg3, resulting in blistering lesions in the basal/spinous epidermal layers (Figure 9). Patients with mucocutaneous dominant PV experience additional skin lesions involving autoantibodies against both Dsg3 and Dsg1 (Amagai, 1999; Culton et al, 2008).

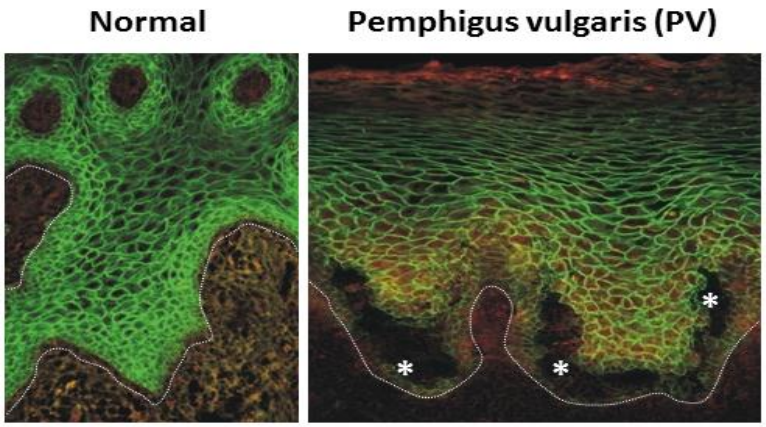

Figure 9: Normal and PV oral mucosal sections.

Normal and *pemphigus vulgaris* (PV) oral mucosal sections show characteristic blister formation (*) between basal and suprabasal layers. The dotted line denotes the basal membranes. Confocal images co-stained for E-cadherin (Green) and phospho-Src (pSrc) (Red) (courtesy of Wan H).

Unlike other autoimmune diseases, PV-IgG are sufficient to induce blistering even in the absence of complement system or cellular factors such as leukocytes *in vivo* (Anhalt et al, 1982; Schiltz & Michel, 1976). To date, it remains unclear how exactly the *pemphigus* autoantibodies cause loss of cell cohesion. Several mechanisms of blister formation including proteinase activation, steric hindrance, desmoglein isoform compensation and signal transduction have been proposed in the literature, and will be discussed below.

1.5.2.1 Proteolytic cleavage of desmosomal cadherins

It was first proposed that proteolytic cleavage of desmosomal cadherins is a potential mechanism for the disruption of cell-cell adhesion in *pemphigus* acantholysis (Hashimoto et al, 1983; Morioka et al, 1987). For instance, a number of studies have shown that inflammatory mediators such as ICAM-1, TNF-α and IL-6 (Narbutt et al, 2008) and a series of metalloproteinases (MMP) increase following treatment with PV/PF-IgG in skin samples of PV patients (Feliciani et al, 2003; Lo Muzio et al, 2002; Schaefer et al, 1996). These

findings are in line with other independent studies, which demonstrated that the proteinase inhibitors such as anti-uPA (urokinase plasminogen activator) are sufficient to inhibit PV/PF-IgG-induced acantholysis in skin cultures (Feliciani et al, 2003; Morioka et al, 1987).

The significance of these findings is still unclear since no direct evidence has yet demonstrated that these inflammatory mediators or metalloproteinases are able to cleave members of the desmosomal proteins. It is possible that the proteolytic cleavage of demosomal cadherins is a secondary event to keratinocyte detachment, which aggravates the phenotype of the disease. This view is in line with a study by Mahoney and colleagues, who showed that the plasminogen activator system is not required for gross blistering in the mouse disease model (Mahoney et al, 1999). Recent work on cellular responses such as proteolytic cleavage of Dsg3 has been demonstrated in *in vitro* PV model (Cirillo et al, 2009), prompting investigators to reconcile the "specific proteolysis theory" in PV pathogenesis.

1.5.2.2 Direct inhibition of desmoglein binding

Amagai and colleagues proposed the direct inhibition theory based on the discovery that PV-IgG bind to Dsg3 in *pemphigus vulgaris* (Amagai et al, 1991). Subsequent insights from the protein structural analysis suggested that pathogenic PV-IgG are primarily targeting the aminoterminal part of the EC1 domain (1-162 amino acids), a region responsible for trans-interaction of desmoglein cadherins. This view is further supported by a number of functional studies, which demonstrated that blocking the EC1 domain with peptides or pathogenic monoclonal anti-Dsg3 antibody-AK23 contributes to loss of cell-cell adhesion in PV pathogenesis *in vitro* (Al-Amoudi et al, 2007; Amagai et al, 1991; Ishii et al, 2008; Muller et al, 2008; Sharma et al, 2007). These and other studies have led to a concept that direct inhibition is most likely caused by steric hindrance, where pathogenic PV antibodies induce loss of keratinocyte cell adhesion by directly interfering with the desmosomal

transinteraction (Sekiguchi et al, 2001). Similarly, other studies using atomic force microscopy experiments revealed that PV-IgG and AK23 are capable of interfering with homophilic Dsg3 binding under cell-free condition, providing direct evidence that inhibition of Dsg3 binding is important for PV pathogenesis (Heupel et al, 2008). However using the same technique, PF-IgG were unable to directly interfere with Dsg1 transinteraction (Heupel et al, 2008) and hence, this theory is unable to fully explain the mechanism of PF acantholysis. Conversely, other study using the laser trapping technique showed that PF-IgG cause significant release of Dsg1-coated microbeads and cellular dissociation in cultured human keratinocytes, suggesting that the loss of cell-cell adhesion in PF is likely mediated by signalling events (Heupel et al, 2008; Waschke et al, 2005).

1.5.2.3 Desmoglein compensation hypothesis

Stanley and colleagues proposed the desmoglein compensation hypothesis to explain the autoantibody profiles and clinical phenotypes of PV and PF patients (Payne et al, 2004; Sharma et al, 2007; Stanley & Amagai, 2006; Udey & Stanley, 1999). This hypothesis is also used to support the "steric hindrance" theory where autoantibodies are assumed to reduce Dsg binding via direct inhibition (Amagai, 1999). According to this concept (Figure 10), Dsg3 in the lower layers of the epidermis is able to compensate for the functional loss of Dsg1 induced by PF-IgG, resulting in superficial blistering in the region where Dsg3 is absent. Blistering would not occur in the mucous membrane since Dsg3 is expressed uniformly throughout the membrane to compensate for the functional loss of Dsg1 induced by PF-IgG. In mucosal-dominant PV, Dsg1 is present in the upper layers of the mucous membrane to compensate the functional loss of Dsg3 induced by PV-IgG, resulting in more suprabasal blistering in the mucous membranes. In the same way, Dsg1 is expressed throughout the epidermis to compensate for any functional loss of Dsg3. Therefore, in mucocutaneous-dominant PV, epidermal blistering would only occur when PV-IgGs are targeting both Dsg1 and Dsg3.

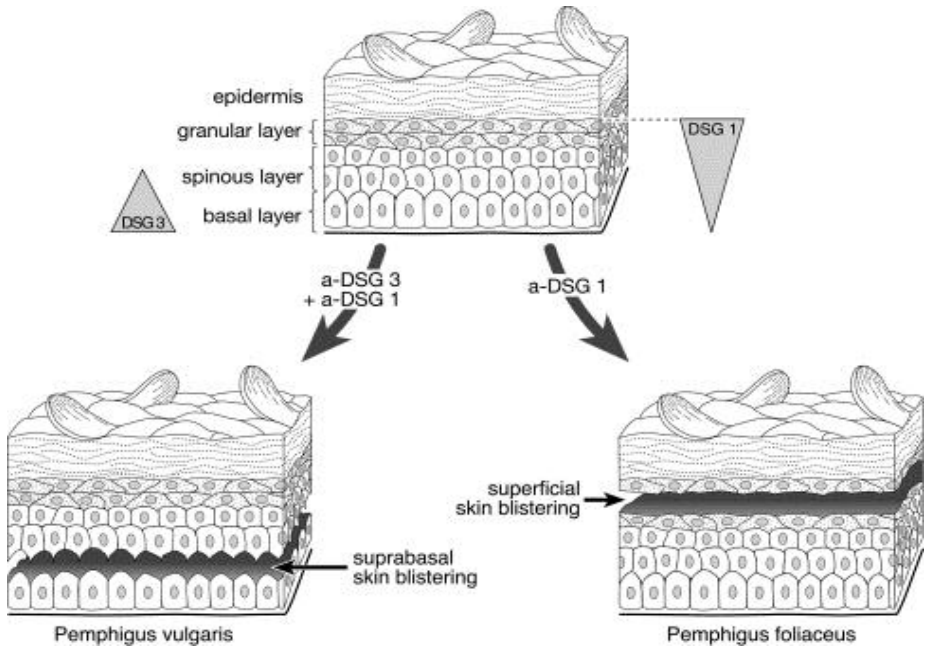

Figure 10: **The desmoglein compensation hypothesis.**

In PF, Dsg3 compensates the functional loss of Dsg1 induced by PF-IgG, resulting in superficial blistering. In mucocutaneous-dominant PV, PV-IgG target both Dsg1 and Dsg3 resulting in suprabasal blistering (Amagai, 2009).

Unfortunately, the clinical spectrum of *pemphigus* is more complex and this theory cannot fully explain the blister formation. For instance, it is unclear why autoantibodies of mucocutaneous-dominant PV, which target to both Dsg1 and 3, induce blistering only between the basal and first suprabasal cell layer and not throughout the epidermis. Similarly, it has been reported in certain cases that the autoantibody profiles do not correlate to the clinical phenotypes of the patients (Amagai, 2009; Bystryn & Rudolph, 2005; Muller et al, 2002; Spindler et al, 2007).

These conflicting findings may be explained by the fact that this theory is based on two assumptions obtained from the mouse model. Firstly, the hypothesis is that the expression patterns of Dsg1 and 3 do not overlap with

each other in epidermal and mucosal layers. However, recent studies indicated that the expression patterns of Dsg1 and 3 in humans are different from those in mice with broadly overlapping expression in the epidermis (Mahoney et al, 2006). The second assumption is made on the basis that autoantibodies against Dsg1 and Dsg3 only lead to inactivation of their respective desmoglein subtype (Mahoney et al, 2006). However, Spindler and colleagues demonstrated that PF/PV-IgG containing Dsg1/Dsg3-specific antibodies from patients are equally effective in reducing the binding between Dsg1/3-coated beads and the surface of cultured keratinocytes and hence, fail to support the second assumption of the compensation hypothesis (Spindler et al, 2007).

1.5.2.4 Signal transduction pathways

In disease model, cellular signalling responses triggered by PV autoantibodies were first reported by Yasuo Kitajima (Amagai, 1999; Seishima et al, 1995). Since then, it has been convincingly demonstrated that binding of PV-IgG to keratinocytes evokes an array of intracellular signalling cascades resulting in acantholysis. Indeed, passive transfer of PV-IgG into neonatal mice together with chemical inhibitor have confirmed that binding of PV-IgG to Dsg3 activates signalling effectors such as p38 MAPK, protein kinase C, Src and EGFR, further defining the role of Dsg3 as a mediator of diverging extracellular information into intracellular responses (Muller et al, 2002).

Waschke and colleagues observed that PV and PF IgG-induced keratinocyte dissociation resulted in loss of Dsg1 and Dsg3 binding in cultured keratinocytes. Such effect is mediated by the p38 mitogen-activated protein kinase pathway (p38MAPK) with concomitant inactivation of RhoA GTPase and reorganisation of the actin cytoskeleton, which could be abolished by the bacterial toxin cytotoxic necrotizing factor y (CNFy). This finding suggests that p38MARK-mediated RhoA inhibition is one of the main events responsible for the loss of cell-cell adhesion in *pemphigus* pathogenesis (Spindler et al, 2007; Waschke et al, 2006). The important of RhoA in the regulation of desmoglein

cytoskeletal anchorage is further supported by other experiment, which showed that RhoA activation could prevent PV-IgG-induced intermediate filaments and actin cytoskeleton rearrangement (Waschke et al, 2006). Gliem and colleagues found that the protective effect of Rho GTPase activation on cell-cell adhesion is prevented by inhibition of actin polymerisation and hence suggests that the actin cytoskeleton is likely involved (Gliem et al, 2010).

These studies are in line to the work of Berkowitz and colleagues, who demonstrated the activation of p38MARK is involved in epithelial blistering pathophysiology. They showed that pharmacologic inhibition of p38MARK activation could abolish blister formation in PV and PF-IgG-treated keratinocytes and found that phosphorylation of the heat shock protein (HSP27) is the main downstream effector of activated p38MAPK (Berkowitz et al, 2008; Berkowitz et al, 2006). However, it is known that p38MAPK is also associated with the apoptotic cascade, which can be triggered by the cell injury or downstream after the loss of intercellular adhesion (Mao et al, 2011; Marchenko et al, 2010). Hence, one cannot completely rule out that p38MAPK is activated secondary to keratinocyte detachment.

Limited studies were carried out focusing on the role of Src in PV-IgG induced blistering formation. Chernyavsky and colleagues reported that the tyrosine kinase Src is involved in PV acantholysis. It was showed that PV-IgG are capable of inducing Src tyrosine kinase activation within 30 minutes and such activation is correlated with the subsequent enhancement of EGFR and p38MAPK activities. This finding is supported by inhibition of Src, which reduced both the pathogenic effects of PV-IgG as well as the phosphorylation of EGFR and p38MAPK (Chernyavsky et al, 2007). Alternatively, Src-induced loss of cell-cell adhesion could be mediated via other mechanism such as phosphorylation of adherens junctional proteins. It was demonstrated that PV-IgG-induced phosphorylation of p120 is associated with keratinocyte dissociation in *pemphigus* (Chernyavsky et al, 2007). However, these results are in contrast to the work by Heupel and colleagues, who showed that

inhibition of c-Src signalling does not prevent the loss of Dsg3 transinteraction in response to PV-IgG (Heupel et al, 2009).

Among the desmosomal proteins, plakoglobin is being viewed as the prime candidate to have signalling capacity. Plakoglobin can influence the Wnt/β-catenin signalling pathway in the absence of β-catenin. Its signaling capacity is believed to be critical to govern outside-in signalling in PV pathophysiology (Muller et al, 2008). It was shown that keratinocytes of plakoglobin-deficient mice resists the PV IgG-induced loss of cell-cell adhesion and retraction of intermediate filaments from cell-cell junctions (de Bruin et al, 2007). A follow-up study by Williamson and colleagues suggested the mechanism underlying the plakoglobin-dependent disruption of cell-cell adhesion in *pemphigus* is in part mediated by continuing keratinocyte proliferation. It was found that PV-IgG depletion of plakoglobin triggers downstream up-regulation of c-Myc, which in turn triggers hyper-proliferation and disrupts the desmosomal plaque at the plasma membrane. The clinical relevance of this pathway was confirmed using c-Myc inhibitors, which prevent skin blistering in newborn pups injected with PV-IgG (Williamson et al, 2006; Williamson et al, 2007).

Currently, inhibition of the specific signalling pathways targeted in PV is viewed as a new therapeutic approach to treat this blistering skin disease (Berkowitz et al, 2005; Sanchez-Carpintero et al, 2004). However, it is noted that direct manipulation of a single signalling pathway without desmoglein-specific autoantibodies could not fully reproduce the distinct clinical and immunopathologic features of *pemphigus* (Amagai, 2009). This indicates that a single signalling pathway alone is not sufficient to induce loss of cell-cell adhesion and blister formation.

1.5.3 Desmosomal cadherins and cancer

Studies on the desmosomal proteins, genes and expression patterns during cancer development have yielded conflicting results. There is a substantial

amount of evidence supporting that both up- and down-regulation of desmosomal components are associated with epithelial cancer progression (Brennan et al, 2007; Teh et al, 2011; Yashiro et al, 2006). It has been reported that down-regulation of desmoglein isoforms 1–3 is associated with poor prognosis in human squamous cell carcinomas (SCC) of the oral, head and neck, stomach and lungs (Teh et al, 2011; Wang et al, 2007; Yashiro et al, 2006). Up-regulation of Dsg2 and Dsg3 was also reported in squamous cell carcinoma of the head, neck and lung cancers (Chen et al, 2007; Savci-Heijink et al, 2009).

The mechanism(s) by which these cadherins particularly Dsg3 are involved in tumourgenesis have not been fully elucidated. Various models have been proposed to explain how de-regulation of desmosome could promote cancer. The most straightforward explanation is that dysfunction or loss of desmosomal cadherins compromises cell-cell adhesion and encourages metastasis of cancer cells during malignant transformation. It is also possible that modulation of cell-cell adhesion releases a desmosomal constituent with oncogenic potential, leading to hyper-proliferation, enhanced inflammation and augmented survival. For instance, the release of plakoglobin can substitute for β-catenin and regulate the transcription of LEF/TCF-target genes (Miravet et al, 2002; Yin & Green, 2004). Similarly, the redistribution of plakophilins (PKPs) from desmosomes to cytoplasm or nucleus, which plays an essential role in cell adhesion and differentiation, could stimulate abnormal gene expression. PKP2 has been reported to interact with β-catenin and induces the endogenous β-catenin–TCF transcriptional activity. Lastly, as the role of desmosomal cadherins in signalling becomes more apparent, dysfunction or modulation of desmosomal cadherins could activate signalling pathways associated with cellular proliferation and survival during cancer development.

1.6 Desmoglein 3 (Dsg3)

Dsg3, a member of the desmoglein subfamily, serves as an adhesion molecule in desmosomes. It is expressed in the basal and immediate suprabasal layers of the skin and uniformly in oral mucosa. The importance of Dsg3 in the maintenance of normal desmosomal adhesion has been well demonstrated. It now appears clear that Dsg3 have an important role in regulating important aspects of cell behaviour such as cell proliferation and differentiation.

Previously, Wan and colleagues showed an inverse correlation between the protein levels of Dsg3 and cell proliferative capacity in various keratinocyte populations. Cells with low levels of Dsg3 protein (Dsg3-dim) exhibit increased colony forming efficiency and enhanced skin regeneration capability as compared with cells with high levels of Dsg3 protein (Dsg3-bright) (Wan et al, 2003). These findings have led to the hypothesis that Dsg3 may play a potential role in cell differentiation process through mechanism(s) involving the regulation of E-cadherin-mediated cell adhesion and the actin cytoskeleton. Additionally, intracellular signalling pathways also play an essential role in the interplay between different adhesion systems. Hence, the aim of this study was to examine the interactions between Dsg3, E-cadherin and actin and to explore the underlying signalling pathways associated with these intercellular junctions.

The mechanisms underlying PV-induced loss of cell-cell adhesion are the subject of intense debate in the field of *pemphigus* research for a long time. It seems that impaired desmosome functions are more complex than previously thought. PV-IgG is known to activate a number of signalling pathways and changes in these signalling transduction pathways are almost certainly involved in *pemphigus* pathogenesis. However, a direct mechanism that adequately explains how Dsg3 triggers these signalling events in response to PV-IgG has yet been proposed. Other evidences suggested that PV-induced loss of cell-cell adhesion is accompanied by alterations of adherens junctions with profound cytoskeletal reorganisation including increased formation of stress fibres and fragmentation of actin filament bundles (Berkowitz et al,

2005; Gliem et al, 2010; Waschke et al, 2006). At present, it is unclear if the alterations of adherens junctions and the actin cytoskeleton contribute directly to acantholysis or are triggered consequently by keratinocyte dissociation.

Identifying the 1) signalling capacity of Dsg3 and its downstream targets and 2) the mechanism(s) that adequately explain how PV-IgG trigger the disruption of adherens junctions and the reorganisation of actin cytoskeleton will help to elucidate the early events responsible for PV-induced acantholysis. Taken together, further analysis of desmosome function and signalling pathways are warranted to shed new light on both the basic developmental processes such as wound healing and pathological processes underlying desmosomal diseases such as *pemphigus* and cancer.

CHAPTER 2

RESEARCH AIMS

Previous studies suggested that Dsg3 is involved in the regulation of keratinocyte stem cell differentiation through an unknown mechanism (Wan et al, 2003; Wan et al, 2007). Here, we speculate that Dsg3 may be involved in the regulation of E-cadherin-mediated cell adhesion and the reorganisation of actin cytoskeleton, which in turn contribute to differentiation programs and tissue morphogenesis.

The hypothesis is that Dsg3 is capable of interacting with E-cadherin and actin and regulates the associated intracellular signalling pathways involving Rho family GTPases and Fyn/Src tyrosine kinases. Therefore, the first aim of this investigation was to confirm the association between Dsg3 and E-cadherin or actin, while the second aim was to identify the roles and signalling capacity of Dsg3 in the regulation of E-cadherin-mediated adherens junctions and the reorganisation of the actin cytoskeleton.

The specific objectives of this study are as follows:

- In Chapter 4 and 7, to examine in detail the association between Dsg3 and E-cadherin or actin in a number of cell lines and human skin tissue.

- In Chapter 5, to determine whether manipulation of Dsg3 affects the protein levels of other junctional cadherins and the assembly of E-cadherin-mediated adherens junctions.

- In Chapter 6, to study if Dsg3 is an upstream regulator of Src-mediated signalling pathway.

- In Chapter 7, to study whether Dsg3 is involved in the Rho GTPase-mediated actin reorganisation and dynamics.

This study will broaden our knowledge of Dsg3 in cell biology and enhances our understanding of its roles in the pathogenesis of *pemphigus*.

CHAPTER 3

MATERIALS AND METHODS

3.1 Cell culture methods

3.1.1 Cell lines and culture conditions

A431 cell line

A431 cell line is derived from squamous cell carcinoma of the vulva. It is morphologic and phenotypic similar to the normal differentiated squamous epithelium but with reduced expression of junctional proteins (Atsumi et al, 2008). A431 also expresses high levels of the epidermal growth factor receptor (EGFR) and contains no functional p53. This is often used as a model to study desmosome function and EGFR downstream signalling cascades such as Src family tyrosine kinases. These cells were cultured routinely in Dulbecco's Modified Eagle Medium (DMEM) (Gibco, Invitrogen) supplemented with 10% Fetal Calf Serum (FCS) (Biosera, UK).

HaCaT cell line

HaCaT is a spontaneously immortalised keratinocyte line derived from normal human skin. It retains all the functional differentiation properties of normal keratinocytes and serves as an ideal *in vitro* model to study normal cellular processes such as cell-cell adhesion, proliferation and differentiation (Boukamp et al, 1988). These cells were cultured routinely in Dulbecco's Modified Eagle Medium (DMEM) (Gibco, Invitrogen) supplemented with 10% Fetal Calf Serum (FCS) (Biosera, UK).

All cells were maintained in an appropriate tissue culture flask and incubated at 37^0C in a 10% CO^2 humidified incubator. Upon 80-90% confluence, cells were trypsinised with 2-5ml of trypsin/EDTA (Lonza) for 5-20 minutes at 37^oC to dissociate cell attachment. Subsequently, the trypsin activity was

neutralised by adding equal volume of culture medium containing serum and recovered by centrifugation at 800-1200 rpm for 3-5 minutes. The resulting pellet was re-suspended with 5-10ml of culture medium and seeded into an appropriate tissue culture flask depending on the density required. Culture medium was changed every 2-3 days.

NHEK cell line

Primary cultures of normal human epidermal keratinocytes (NHEK) were obtained from neonatal foreskin. Primary cultures give comparable result to *in vivo* studies and therefore used to valid the results obtained from HaCaT keratinocyte cell line (Tsang et al, 2012b). NHEK cells were routinely cultured in EpiLife (Invitrogen) and were passaged upon reaching 60–70% confluence as described above. The medium was replaced every 2 days and cells were discarded after 5 passages.

3.1.2 Cryopreservation and recovery of cells

For cryopreservation, cells were trypsinised to dissociate adherent cells and recovered by centrifugation. The resulting pellet was re-suspended with freezing medium containing 90% FCS and 10% DMSO. Subsequently, 1ml of cell suspension was transferred to each plastic cryovial and stored in cryobox in a -80°C freezer for 2 days before transferring to liquid nitrogen for long term storage. For recovery, the cryovial was thawed in water bath at 37°C for 1 minute or so and disinfected with 70% ethanol. The cell suspension was washed with 3-5ml of culture medium and recovered by centrifugation. The resulting pellet was re-suspended in culture medium and allowed to grow for a week prior to use.

3.2 The experimental models

3.2.1 Gain of Dsg3 function

A431 cells, which express low levels of endogenous Dsg3, were used for my gain-of-function study. Stable cell lines with Dsg3 overexpression were generated as follows: Full-length human Dsg3 cDNA tagged with a myc epitope was cloned into the pBABE.puro retroviral vector (pBABE-hDsg3.myc). This and two other matched controls: an empty vector control (pBABE-V) and a vector containing GFP transgene (pBABE-GFP) were transduced individually into A431 cells. All stable lines were subjected to 2µg/ml puromycin selection for 2 weeks and were further cultured in normal growth medium (DMEM with 10% FCS) for a week prior to use or storage. Drug selection is repeated every 3-4 months to ensure all growing cells express the puromycin resistance gene. It was tested that the levels of Dsg3 protein in hDsg3.myc cells remained below the endogenous levels found in HaCaT and primary oral keratinocytes, indicating that the increased levels of Dsg3 protein is not supra-physiological. Both the retroviral transfection and transduction were carried out in this laboratory by Wan H.

3.2.2 Generation of hDsg3.myc clones

Limiting dilution and clonal expansion were used to select clones with high levels of Dsg3 protein. A431-pBABE-hDsg3.myc mixed clone was first diluted with normal growth medium (DMEM+10% FCS) and the resulting cell suspension was aliquoted into each well of 96-well plates to give a cell density of approximately 1 cell/well. Three days after cell seeding, those wells with a single cell were marked and allowed to grow for a couple of weeks to form a larger colony. Each of these clones was transferred to larger dishes for clonal expansion, while an aliquot of the cell suspension was taken for Western blot analysis. The clones with the lowest/highest levels of Dsg3 protein such as C11/C7 were used in the subsequent experiments.

3.2.3 Loss of Dsg3 function by siRNA

HaCaT cells, which express high levels of endogenous Dsg3, were used for my loss-of-function study. Two siRNA sequences specifically targeting the human Dsg3 gene were used. **RNAi-1:** A siRNA sequence (AAATGCCACAGATGCAGATGA) specific for human Dsg3 mRNA (Accession: NM_001944), which corresponds to nucleotides 620–640 of the respective coding region, was designed by Wan H and synthesised by Dharmacon Research (USA). **RNAi-2:** An On-TARGETplus SMARTpool of siRNAs targeting human Dsg3 was purchased from Dharmacon Research (USA) (Table 2). **Control siRNA:** A randomised control sequence based on RNAi-1, which does not target to any genes (AACGATGATACATGACACGAG), was designed by Wan H and synthesised by Dharmacon Research (USA). RNAi-1, the more potent duplex, was used in most experiments, while the results obtained from RNAi-2 were comparable to those obtained from RNAi-1.

To transiently knockdown Dsg3 using RNAi-1, $2x10^5$ cells were plated in a 6-well plate for 24 hours before transfection. Five to ten microliters (µl) of Dsg3 RNAi-1 and 5µl of oligofectamine (Invitrogen) were diluted with 175-180µl and 10µl of OPTI-MEM (Invitrogen), respectively and incubated at room temperature for 5 minutes. Contents of the tubes were mixed gently and incubated for another 20 minutes at room temperature. The culture medium in the 6-well plate was replaced with 800µl of OPTI-MEM without serum. Two hundred microliters (µl) of RNAi-oligo mixture were subsequently added to each well to give a final concentration of 50-200nM of RNAi-1. Four hours post-transfection, 500µl of OPTI-MEM containing 30% FCS was added and incubated for at least 24 hours prior to other analysis. Silencing efficiency was optimised using PT-PCR by Dr Muy-Teck Teh (Institute of Dentistry) and the result showed no off-target effects, particularly on Dsg2 and other desmosomal cadherins. For negative control, cells were transfected with control siRNA at the same concentration following the same protocol.

To transiently knockdown Dsg3 using RNAi-2, $2x10^5$ cells were plated in a 6-well plate for 24 hours before transfection. Three to five microliters (µl) of

Dsg3 RNAi-2 and 3µl of Dharmfect transfection reagent were diluted with 95-97µl and 97µl of OPTI-MEM (Invitrogen), respectively and incubated at room temperature for 5 minutes. Contents of the tubes were mixed gently and incubated for another 20 minutes at room temperature. The culture medium in the 6-well plate was replaced with 800µl of fresh DMEM containing 10% FCS. Two hundred microliters (µl) of RNAi-Dharmfect mixture were subsequently added into each well and incubated for at least 48 hours prior to other analysis. A final concentration of 50-200nM of RNAi-2 was used per well. Transient knockdown of plakoglobin and p120 were carried out following the same protocol. RNAi sequences and transfection timeline are depicted below in Table 2 and 3.

Table 2: RNAi sequences

Self-designed (40µM)	**RNAi sequences**
Human Dsg3 (RNAi-1) (Accession: NM_001944)	AAATGCCACAGATGCAGATGA
Control siRNA	AACGATGATACATGACACGAG

ON-TARGET plus SMARTpool (5nmol)	**RNAi sequences**
Human Dsg3 (RNAi-2)	GAUCCUUGCUCCCGUCUAA GAGAAACCACUUAUACUAA GUGGAUACCUAAUGAUUGA CAAGAUUACUUCAGAUUAC
Human JUP (Plakoglobin)	AGACAUACACCUACGACUC UGAGUGUGGAUGACGUCAA CCACCAACCUGCAGCGACU UGUACUCGUCGGUGGAGAA
Human BRD8 (p120)	GAGAGAUUCUACCCGCAAA GAUGAUGGCUUCAGCAUAC AAUAGUAGCUGGAGUUGUU CCGAAGCACAGCUGAAUUU

Table 3: Timeline of transfection experiment

Day 0	Day 1	Day 2	Day 3
$2x10^5$ cells/well were seeded in a 6-well plate in normal growth medium.	Transfections were carried out in triplicate wells.	Cells were trypsinised from 3 wells and pulled together into 2 wells at approximately 75% confluence.	Freshly confluent cells were sequentially treated with calcium-free and normal calcium containing medium for 1 hour and 5 hours, respectively.

3.3 Molecular biology methods

3.3.1 Preparation of E.coli competent cells

A tube of STBL2 competent *E coli* cells (Invitrogen) was thawed on ice. One microliter (µl) of EosFP-actin or Rac1N17 plasmid (generous gifts of Dr Ann Wheeler) was added to 20µl of *E coli* cells. The mixture was incubated on ice for 30 minutes, heated at 42°C for 30 sec and returned to ice for 1 minute. Subsequently, the mixture was added to a conical flask with 500µl of Super Optimal Broth (SOC) medium (Invitrogen) containing ampicillin and incubated for 24 hours at 37°C with shaking. On the next day, the *E coli* culture was transferred into a bigger conical flask with 400ml of LB medium (Invitrogen) containing ampicillin and incubated for another 24 hours at 37°C with shaking. The final concentration for ampicillin was 100µg/mL. The cells were recovered by centrifugation in Sorval GSA rotor at 4^oC for 10 minutes at 3,000 g.

3.3.2 Plasmid DNA extraction: Maxi-prep®

Plasmid DNA preps were performed using a QIAGEN® maxi-prep® kit. DNA was eluted with 50µl of elution buffer and their concentrations were measured using an ND-1000 Spectrophotometer (Nanodrop).

3.3.3. Transient transfection

Transfection was performed using Fugene6 (Roche) according to the manufacturer's instructions. A431-V and -D3 cells were transiently transfected with either the EosFP-actin construct or the dominantly inhibitory N17Rac1 mutant for 48 hours. Fugene6 transfection reagent was diluted with OPTI-MEM (Invitrogen) in a ratio of 3:2 and incubated at room temperature for 5 minutes. Two micrograms (μg) of DNA was added to the diluted Fugene6 transfection reagent, mixed well and incubated at room temperature for a further 15 minutes. Subsequently, the Fugene6-DNA complex was added to each well in a drop-wise manner and left for another 48 hours prior to other analysis.

3.4 Calcium treatment

3.4.1 Calcium-free media

De-calcificated FCS was prepared as follows: 5g of chelating resin (Sigma) was mixed with 250ml of distilled water and adjusted to pH 7.4. After 3 hours of equilibration at pH 7.4, the beads were collected by filtration through Whatman No1 filter paper. Five grams (g) of the resulting chelating resin was mixed with 50ml of FCS and stirred overnight. The resin was collected by centrifugation at 15,000 rpm for 10 minutes and the FCS was sterilised through a 0.22 um filter prior to use or storage at -20°C (Mattey & Garrod, 1986). Calcium-free medium was prepared as follows: DMEM supplemented with 10% decalcified FCS plus 3 mM EGTA (Wallis et al, 2000).

For all Src signalling experiments in Chapter 6, cells were initially grown to 90% confluence in a normal growth medium (DMEM+10% FSC) and treated with calcium-free medium for 1 hour. During this period, it was noted under the phase contrast microscope that the intercellular junctions of epithelial cells were disrupted. Cells were seen rounded up but remained attached to

the substrate. Subsequently, the cells were replenished Dulbecco's Modified Eagle Medium (DMEM) (Gibco, Invitrogen) supplemented with 10% Fetal Calf Serum (FCS) (Biosera, UK)(containing 1.8mM calcium) for 5 hours to allow the re-establishment of cell junctions prior to cell extraction and other analysis.

3.4.2 Calcium switch experiments

HaCaT cells were seeded at high density and grown to 90% confluence in a low calcium medium for 24 hours (EpiLife; Ca^{++} 60μM, Cascade Biologics). Subsequently, 2mM of calcium ions were added for different periods of time according to the individual experiments. For the extraction of the Triton soluble and insoluble fractions in Figure 15, cells were calcium switched for 2 hours, 8 hours, 16 hours, 1 day, 3 days and 6 days prior to protein extraction and Western blot analysis. For co-immunoprecipitaion experiment in Figure 18, cells were calcium switched for 0 hour, 16 hours and 48 hours prior to protein extraction and Western blot analysis. For immunofluorescence staining in Figure 23, HaCaT cells with or without Dsg3 knockdown were calcium switched for 1 hour, 8 hours and 24 hours prior to fixation.

3.5 Antibodies

Table 4: Antibodies used for Western blotting (WB) and Immunfluorescence (IF) analysis.

Antibodies	Clone	Host	Working dilution (WB)	Working dilution (IF)	Company
Anti-Dsg3	5H10	mouse	1:500	neat	Gift from Professor M Amagai
Anti-Dsg3	AHP319	rabbit	1:500	1:100	Serotec
Anti-Dsg2	10G11	mouse	1:50	1:50	Progen
Anti-Dsc3	Dsc3-U114	mouse	1:50	1:50	Progen
Anti-Dsc2a/b	Pab -Dsc2	rabbit	1:4000	1:100	Progen
Anti-Dp	115F	mouse	1:50	neat	Gift from Professor D Garrod
Anti-Dp	AHP320	rabbit	1:1000	1:100	Serotec
Anti- Pg	PG5.1	mouse	1:100	1:20	Millipore
Anti-PP2 (2a+2b)		mouse	1:50	---	Progen
Anti-E-cadherin	HECD-1	mouse	1:1000	1:100	Abcam
Anti-P-cadherin		mouse	1:500	---	Zymed laboratories Inc
Anti-β-catenin	6F9	mouse	1:2000	1:100	Sigma
Anti-p120 catenin		mouse	1:250	1:100	BD Transduction Laboratories
Anti-Myc tag		rabbit	1:500	1:100	Abcam and Novus Biologicals
Anti-phospho-Src (Tyr416)	32G6	rabbit	1:500	1:100	Cell Signaling
Anti-nonphospho-Src (Tyr416)		mouse	1:500	1:100	Cell Signaling

Anti-phospho-Tyrosine		mouse	1:500	1:100	R&D system
Anti- β-Actin	ab8227	rabbit	1:1000	1:100	Abcam
Anti- Tubulin	ab7291	mouse	1:1000	---	Abcam
AlexaFluor 488/568 conjugated goat IgGs		Mouse/ rabbit IgG	---	1:100	Invitrogen

3.6 Experiments with inhibitors

For the tyrosine phosphorylation experiment in Figure 25, cells were grown to 90% confluence and treated with calcium-free medium for 1 hour before being replenished with normal calcium-containing medium. Inhibitor was added 30 minutes after replenished with normal calcium-containing medium as a precaution to allow cells to re-establish cell-cell junctions prior to other treatments. 10μM of Src specific inhibitor, PP2 or equal volume of DMSO (vehicle control) was added into the medium for 5 hours (Nam et al, 2002) prior to co-immunoprecipitation. PP2 stock solution (Calbiochem) was dissolved in DMSO and diluted at least 1000-fold into culture medium to give a final concentration of 10μM.

For the study of actin dynamics in Figure 39-40, cells were grown to 90% confluence (without any calcium-free treatment) and treated with or without Rac1 inhibitor, NSC23766 at 30-50μM for 6 hours (Gao et al, 2004) prior to other analysis. Rac1 inhibitor stock solution (Tocris Bioscience) was dissolved in water and diluted at least 1000-fold into culture medium to give a final concentration of 30-50μM.

3.7 Protein methods

3.7.1 Determination of protein concentration

Bio-Rad Detergent Compatible (DC) protein assay was used to measure the protein concentrations. Each sample was measured in triplicate and the optical density (OD) for each sample was read out using a Wallac 1420 UV/Vis Spectrophotometer with the absorbance reading of 650nm. Protein concentration was determined using a standard curve of BSA. This assay has been shown to be compatible with our extraction buffers containing SDS, NP-40 or Triton X-100 and 10% (v/v) β-mercaptoethanol is only added to the samples after the Bio-Rad *DC* protein assay.

3.7.2 Cell extraction

3.7.2.1 Total cell extraction

Cells were grown to 90% confluence, washed with ice cold PBS and lysed on ice with either 2x sodium dodecyl sulfate (SDS) laemmli sample buffer containing 0.125M Tris-Cl pH 6.8, 4% SDS, 20% Glycerol and 10% (v/v) β-mercaptoethanol, which was added to the samples after the Bio-Rad *DC* protein assay. The cell lysate was immediately scraped from the plate, collected in a tube and centrifuged at 15,000 rpm for 10 minutes. Protein concentration was measured prior to Western blot analysis. The unused lysates were stored at -20°C.

3.7.2.2 Triton X-100 soluble and insoluble fractions

Cells were grown to 90% confluence in 100mm Petri dishes, washed with ice cold PBS and 200µl of Triton X-100 extraction buffer (10mM Tris-HCL, pH7.5, 150mM NaCl, 2mM ethyleneglycol-bis-(β-aminoethylether)-N,N,N',N' tetraacetic acid (EGTA), 5mM ethylenediamine tetraacetic acid (EDTA), 1% Triton X-100, 1mM phenylmethylsufonyl fluoride and protease inhibitor cocktail (Boehringer Mannheim)) was added and incubated on ice for 10

minutes. The cell lysate was scraped from the plate, collected in a tube and centrifuged at 15,000 rpm for 10 minutes to separate detergent-soluble from detergent-insoluble fraction. The resulting supernatant was denoted as the Triton X-100 soluble fraction. The detergent-insoluble pellet was re-suspended with 200µl SDS Laemmli sample buffer and the supernatant was denoted as the Triton X-100 insoluble fraction. For co-immunoprecipitation, RIPA buffer instead of SDS Laemmli sample buffer was used to recover proteins from the Triton insoluble fraction. Protein concentration for each fraction was measured prior to Western blot analysis. In Figure 17, the pellet collected after RIPA buffer extraction was further dissolved in a SDS Laemmli sample buffer to recover the rest of the highly insoluble proteins including the desmosomal proteins that are associated with the intermediate filaments.

3.7.2.3 Cell extraction for co-immunoprecipitation experiments

Cells were washed with ice-cold PBS, lysed with 1 x RIPA buffer (Upstate) containing 1% NP-40, protease-inhibitor cocktail (Calbiochem) and phosphase inhibitors (e.g. 10mM sodium fluoride and 2mM sodium orthovanadate) and incubated on ice for 10 minutes. The cell lysate was scraped and collected in a tube and centrifuged at 15,000 rpm for 10 minutes. Protein concentration was measured prior to co-immunoprecipitation analysis.

3.7.2.4 Cell extraction from human skin

The tissue was obtained from breast reduction following ethical approval and patient consent. The skin was washed thoroughly with PBS and cut into small pieces before incubated with 2.5mg/ml dispase in PBS for 24 hours. The epidermis was separated from dermis and lysed on ice with 1 x RIPA buffer as described in section 3.7.2.3.

3.7.3 Co-Immunoprecipitation (co-IP)

Three to twenty microliters (µl) of the indicated antibody was first incubated with 30µl of Dynabeads (Invitrogen). After 3 hours of incubation, approximately 500 to 1000µg of the protein lysates were added to the antibody-Dynabeads mixture and incubated overnight at 4°C on rotation. On the next day, the Dynabeads containing immune complexes were washed with RIPA buffer 3 x 5 minutes and re-suspended in 10µl of 2 x SDS buffer. The bead-bound complexes were boiled for 3 minutes before loading onto a Nupage Bis-Tris gel and analysed by Western blotting as described below.

3.7.4 Rho GTPase pull down assay

The CRIB domain of Pak-PBD fused with GST was used to pull down the active GTP-bound Rac1 and Cdc42 from A431-V and -D3 cells following the manufacturing protocol (Rac1/Cdc42 Activation Assay Kit, Millipore). Five hundred micrograms (µg) of protein lysates were incubated with 10µg of Rac/Cdc42 assay reagent (PAK-1 PBD, agarose) at 4°C on rotation for 60 minutes. Twenty microliters (µl) of 2 x SDS buffer was used to elute the GST-fusion protein from the glutathione resin. Bead-bound complexes were loaded onto a Nupage Bis-Tris gel and the amount of activated GTPase was analysed by Western blotting with anti-Rac1 and Cdc42 antibodies.

3.7.5 Western blotting

3.7.5.1 Sample preparation and loading

All samples were heated at 99°C for 3 - 5 minutes before loading onto a Nupage 10% or 4 - 12% gradient Bis-Tris gel (Invitrogen). Full range molecular weight Rainbow Markers (Amersham) were used to determine the molecular weight of the proteins.

3.7.5.2 Chemiluminutescent detection of antibodies

The proteins were separated by SDS gel electrophoresis and transferred to a nitrocellulose transfer membrane (Millipore) using an electrophoresis apparatus. The membrane was blocked with 5% (w/v) non-fat milk in Tris Buffered Saline containing 0.1% Tween 20 (TBS-T) for 15 minutes and incubated with primary antibody against the specific proteins either for 1 hour at room temperature or overnight at 4°C. The membrane was washed 3 x 5 minutes with TBS-T and incubated with either anti-mouse or anti-rabbit IgG horseradish peroxidase-linked antibody (Chemicon) in 5% (w/v) non-fat milk in TBS-T for 1 hour. Subsequently, the membrane was washed thoroughly with TBS-T 3 x 5 minutes at room temperature with shaking. Chemiluminutescent solution-SuperSignal® west fermto maximum sensitivity substrate (Thermo scientific) or Amersham ECL plus Western blotting detection system (GE healthcare) was added onto the membrane following the manufacturers' instructions. The membrane was then exposed to Amersham Hyperfilm ECL and developed in an AGFA Curix 60 developer.

3.8 Immunofluorescence and analysis

Cells were grown on coverslips to 90% confluence, washed with ice cold PBS and fixed with either ice-cold 1:1 methanol/acetone for 10 minutes or 4% formaldehyde for 8 minutes and permeabilised with 0.1% Triton X-100 for 3 minutes. In Figure 12, cells were first treated with ice-cold cytoskeleton (CSK) buffer containing 5mM NaCl, 300mM sucrose, 10mM PIPES (pH 6.8), 3mM $MgCl_2$, 0.5% Triton X-100 and 1.2mM PMSF for 20 minutes to strip away proteins that do not associate with the intermediate filaments prior to immunostaining. The coverslips were then blocked with 10% goat serum (Sigma) for 15 minutes and incubated with primary antibody diluted in 10% goat serum for 1 hour at room temperature. After three washes in PBS plus 0.1% Tween 20, the samples were incubated with secondary conjugated antibody (Alexa Fluor 568 and Alexa Fluor 488 or A488 conjugated phalloidin) diluted in 10% goat serum for 1 hour at room temperature. Subsequently, the

coverslips were washed, mounted on glass slides using Prolong© gold anti-fade reagent with DAPI (Invitrogen) and analysed with a Leica DM5000 epi-fluorescence microscope.

The peripheral fluorescence levels of E-cadherin across the monolayer in Figure 23 was analysed by ImageJ software and only confluence images were quantified. As demonstrated in Figure 11, the confocal images were set to 8 bits and the cytoplasmic staining was cut out from each cell using the drawing tool of ImageJ software (Figure 11B). The integrated density was determined by gating out the intracellular signal before thresholding (Figure 11C). The junctional fluorescence intensity per cell was obtained by dividing the integrated density over the number of cells found (approximately 50 cells) in each field. Four arbitrary fields in each sample were measured and presented as the mean±sd.

The degree of colocalisation in Figure 32 and 40 was analysed by ImageJ software. The colocalisation index, a merge of red and green channels, was quantified and highlighted in white (http://www.macbiophotonics.ca/).

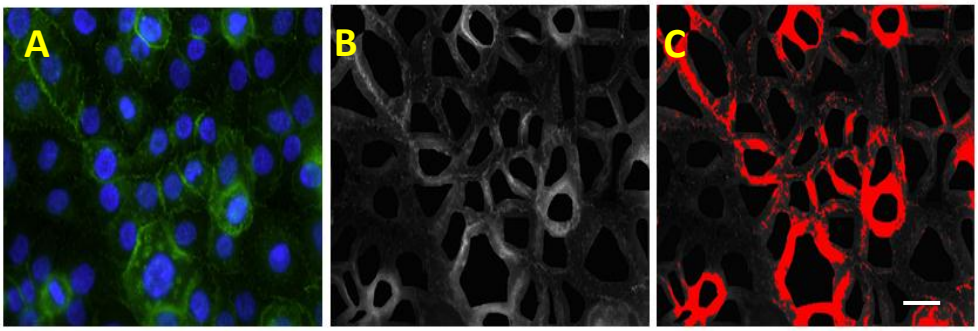

Figure 11: Quantification of peripheral E-cadherin fluorescence intensity.

A) Representative images taken by confocal microscopy. B) The cytoplasmic staining was removed from each cell using a drawing tool. C) Post-processed image using a threshold of 50 in a 8 bits grayscale.

3.9 Proximity ligation assay (PLA)

Cells were grown on coverslips to 90% confluence, washed with ice-cold PBS and fixed with 1:1 methanol/acetone for 10 minutes. The cells were blocked with 10% goat serum (Sigma) for 15 minutes and incubated with primary antibody diluted in 1× antibody diluent (Olink Bioscience) for 1 hour at room temperature. Next, the cells were co-incubated with anti-mouse PLA MINUS and anti-rabbit PLA PLUS secondary probes diluted in 1× antibody diluent at 37°C for 2 hours. The cells were sequentially incubated with 1× diluted hybridisation solution for 15 minutes, 1× diluted ligation solution for 15 minutes, duolink polymerase (1:80) in 1× amplification stock for 60 minutes and 1x diluted detection probes for 60 minutes. Subsequently, the cells were washed, mounted on a glass slide and examined with a Leica DM5000 epi-fluorescence microscope under a 40/60× objective. Washing procedures were carried out in between steps by rinsing the coverslips with TBS-T. All incubation was carried out in a humidified chamber at 37°C and all 5x stocks were diluted with high purity water in a ratio of 1:5.

3.10 Live cell imaging and analysis

3.10.1 Cell migration

A431-V and -D3 cells were grown on a 6-well plate to 90% confluence and treated with or without 30µM Rac1 inhibitor in a normal growth medium (DMEM+10% FCS) for 6 hours. Cells were then trypsinised, recovered by centrifugation and seeded onto glass-bottom cell culture dishes (WPI) at $1x10^5$ cells/dish in a low calcium medium (EpiLife). Once the cells were seeded (30 minutes), NSC23766 was added back into the medium to ensure cells were maintained in the inhibitor for the experiment's duration. During the experiment, cells were incubated in a humidified chamber at 37°C with 10% CO_2. Time-lapse imaging was carried out in an inverted microscope (Zeiss) using a 10x objective and phase contrast optics. A time-lapse series was collected every 5 minutes for 18 hours using Metamorph (Molecular Devices).

Analysis of speed was performed by manual tracking of cells over the sequence of time-lapse digital images for the first 3 hours because cells die after 3 hours of imaging. Eighty cells for each condition from three independent experiments were tracked.

3.10.2 Membrane protrusion

Spinning disk confocal microscope was used for the analysis of membrane protrusions. Cells were prepared in the same way as the above experiment. One micromole (μM) of carboxyfluorescein diacetate, succinimidyl ester (CFSE) was added to culture medium to label the cell membranes for 30 minutes before live cell imaging. A time-lapse series was collected every 5 sec for 5 minutes using a 60×1.4NA objective. Image sequences were analysed with the kymograph function in Metamorph. Three to four different regions per cell near the edge of cell protrusions were selected. Straight lines were drawn in the direction of individual protrusions and the slopes of these lines were used to calculate the velocities (Bear et al, 2002). Eight cells for each condition from two independent experiments were analysed. The total number of cell edges analysed per condition is >24.

3.10.3 Actin dynamics

A431-V and -D3 cells were transiently transfected with the photoconvertable EosFP-actin for 48 hours. Transfection was performed using Fugene6 (Promega) according to the manufacturer's instructions. At 48 hours post-transfection, cells were trypsinised, recovered by centrifugation and seeded onto glass-bottom cell culture dishes at $2x10^5$ cells/dish in a low calcium medium (EpiLife). A small region of actin was photoconverted from GFP to RFP and the dynamics of this region were followed by collecting an image every 10 sec for 10 minutes. Data were collected on a Zeiss 510LSM inverted microscope using a 63×1.4NA objective. Pre- and post-conversion images were acquired using 488 and 543 nm laser lines. Images were acquired within

10 sec after photo-conversion (Schenkel et al, 2008). The intensity profiles for each image (frames 1–10) were normalised and the mean percentage recovery was quantified. Five cells for each condition and 4-5 different regions per cell near the edge of the cell were analysed. The total number of cell edges analysed per condition is >20.

3.11 Statistical Analysis

Statistical differences between experimental groups were evaluated by 2-tailed Student t test. A P valve less than 0.05 was considered statistical significance.

CHAPTER 4

ASSOCIATION BETWEEN DSG3 AND E-CADHERIN

4.1 Results

4.1.1 Complex formation and colocalisation between Dsg3 and E-cadherin

It has long been an area of interest in understanding the cross-talk between desmosomes and adherens junctions since emerging evidence suggests that these two junctions are mutually dependent. Immunofluorescence data from our laboratory showed that Dsg3 colocalises with adherens junctional proteins such as E-cadherin, suggesting that Dsg3 may play an important role in regulating cross-talk between these junctions. To gain further insight into the nature of the Dsg3/E-cadherin interaction, I took advantage of the A431 cell line stably expressing either the full-length human Dsg3 tagged with a c-Myc epitope at the C-terminus (A431-D3) or the empty vector control (A431-V), which was established in our laboratory, to examine in detail the interaction between Dsg3 and E-cadherin, a marker for adherens junctions. As demonstrated in Figure 12, the representative confocal images clearly indicate a substantial colocalisation of E-cadherin (green) and Dsg3.myc (red) at the plasma membrane in Dsg3 overexpressing A431 cells (A431-D3). Such interaction persisted in cells treated with the cytoskeletal buffer (CSK), suggesting a high affinity of protein-protein interaction.

To examine whether Dsg3 and E-cadherin physically interacted with each other, a series of biochemical analysis such as co-immunoprecipation and proximity ligation assay (PLA) were carried out. For co-immunoprecipitation assay, freshly confluent A431-V and -D3 cells were first extracted using RIPA buffer (Upstate) containing 1% NP-40 and the resulting protein lysates were immunoprecipated with mouse anti-E-cadherin antibody, HECD-1 and Western blotted for the indicated proteins such as Dsg3, Myc-tag and E-cadherin. In Figure 12B, the Western blots of E-cadherin immunoprecipitates

show that overexpression of Dsg3 increased the association between Dsg3 and E-cadherin as compared with A431-V control cells. It was also noted that a small amount of Dsg3 and E-cadherin association was present in A431-V control cells. For the negative control, no binding of E-cadherin was seen in the mouse pre-immune immunoprecipitate (Figure 12B). The Western blot was re-probed with the same immunoprecipitating anti-E-cadherin antibody to verify immunoprecipitation efficiency and equal amount of E-cadherin was observed in each lane.

These findings were confirmed in the reverse approach (Figure 12C and D), in which the co-immunoprecipitations were carried out in A431, HaCaT cells and human breast skin. Freshly confluent A431 and HaCaT cells were extracted using RIPA buffer as described above, while the epidermis was separated from dermis using dispase and subsequently extracted with RIPA buffer. The resulting protein lysates were co-immunoprecipated individually with either mouse anti-Dsg3 antibody, 5H10 or rabbit anti-Myc tag antibody and Western blotted for β-catenin, E-cadherin and Dsg3. In Figure 12C, overexpression of Dsg3 increased the association between Dsg3 and β-catenin as compared with A431-V control cells. Similarly, the endogenous Dsg3 was immunoprecipitated with E-cadherin in HaCaT cells as well as skin lysates directly extracted from human breast epidermis (Figure 12C, bottom). No binding of Myc-tag was seen in the rabbit pre-immune immunoprecipitate and was used as the negative control (Figure 12D). Taken together, these results demonstrate that Dsg3 (both endogenous and exogenous) associates with E-cadherin in various epithelial cell lines, including normal keratinocyte HaCaT cells, A431 cancer cells as well as in human breast skin.

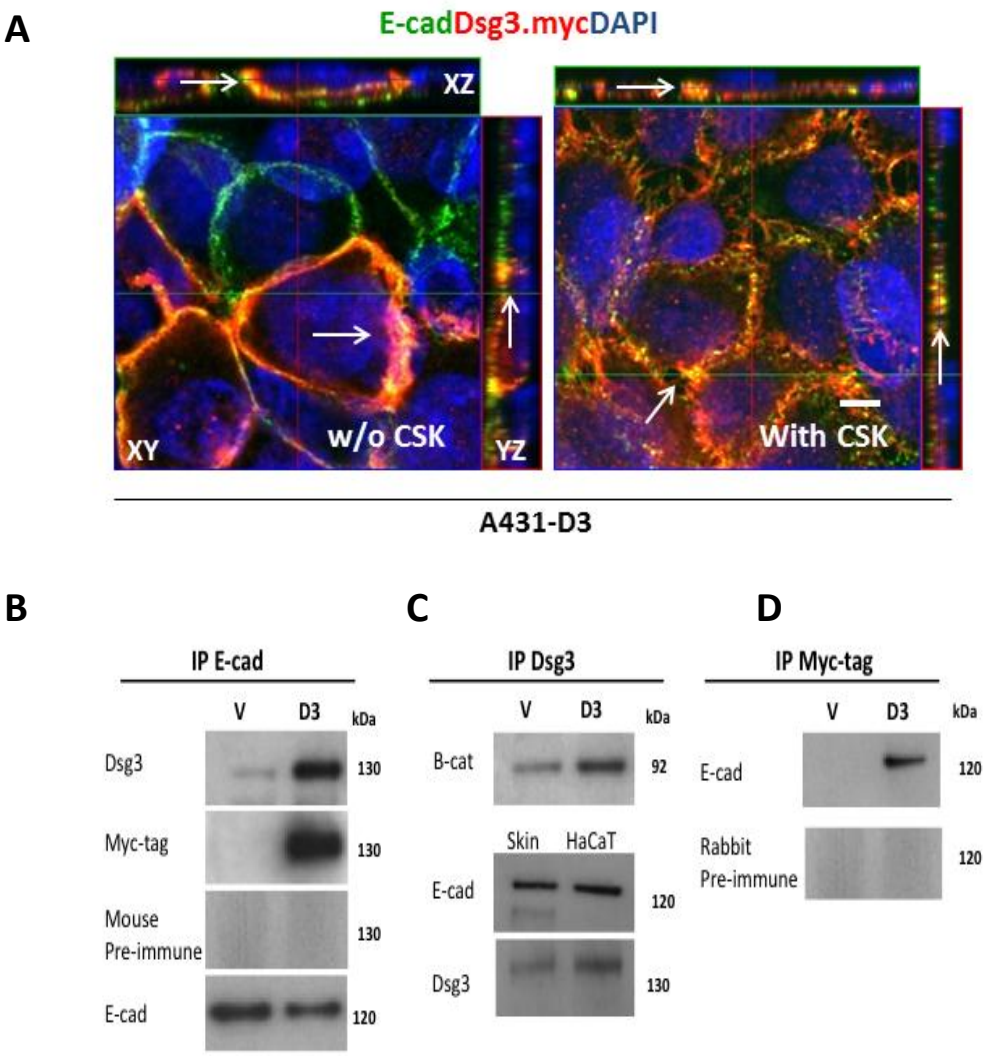

Figure 12: Dsg3 colocalises and associates with E-cadherin.

A) Confocal images of the colocalisation between Dsg3 and E-cadherin in A431-D3 cells. A431-D3 cells were treated with or without cytoskeletal buffer (CSK) prior to fixation and co-stained with rabbit anti-Myc-tag (red) and mouse anti-E-cadherin, HDEC-1 (green) antibodies. Scale bars are 10 µm. (Arrows in XY, XZ and YZ image panels, confocal images courtesy of Wan H). B, C and D) Western blots of immunoprecipitates from protein lysates of A431 cells, HaCaT cells and the epidermis of human breast skin. Freshly confluent cells and epidermis of breast skin were extracted with RIPA buffer containing 1% NP-40. Five hundred micrograms (µg) of the resulting protein lysates were subjected to co-immunoprecipation with the indicated antibody and Western blotted for Dsg3, E-cadherin, Myc-tag and β-catenin. Pre-immune rabbit and mouse serum were used as the negative control. The representative confocal images (A) and Western blots of (B, C and D) were obtained from at least two independent experiments.

To further consolidate these findings, proximity ligation assay (PLA) was carried out in A431 cells. This method not only allows one to visualise protein-protein interactions, it also offers unprecedented levels of specificity and sensitivity for protein-protein interactions in close proximity, *i.e.* less than 30-40 nm (Landegren et al, 2004). The PLA proximity probes (PLUS and MINUS) are designed to bind pairs of target proteins and a fluorescence signal is generated if these probes are brought in close proximity of each other. To begin, the freshly confluent A431-V and -D3 were fixed with 1:1 methanol/acetone, blocked with 10% goat serum and co-incubated with primary antibody. After primary antibody incubation, the cells were sequentially incubated with PLA plus and minus probes and other PLA reagents following the manufacturer's protocol (Refer to Materials and Methods Chapter 3.8). Five arbitrary images were taken by fluorescence microscopy and the number of fluorescence dots per cell was quantified by ImageJ. The positive and negative controls were A431-V and -D3 cells co-incubated with mouse anti-Dsg3, 5H10 and rabbit anti-Myc-tag antibodies. In A431-D3 positive control cells, both of these antibodies target the same protein - the anti-Dsg3 antibody binds specifically to the EC1-EC2 domains of Dsg3, while the anti-Myc-tag antibody binds to the Myc epitope at the C-terminus. However, in A431-V negative control cells, the anti-Myc-tag antibody recognises only the endogenous c-Myc in the nucleus. As expected, overexpression of Dsg3 in A431-D3 cells (positive control) significantly increased the amount of PLA signals as compared with A431-V control cells (negative control).

As for the test sample, A431-D3 cells were co-incubated with mouse anti-E-cadherin, HDEC-1 and rabbit anti-Dsg3 antibodies (Figure 13). The representative images clearly show an enhanced level of PLA signal between Dsg3 and E-cadherin in A431-D3 cells as compared with the negative control (** $p<0.01$). This result confirms that Dsg3 and E-cadherin are indeed in close proximity (<40nm) of each other. The bar chart in Figure 13 represents the average number of fluorescence dots per cell from five different images.

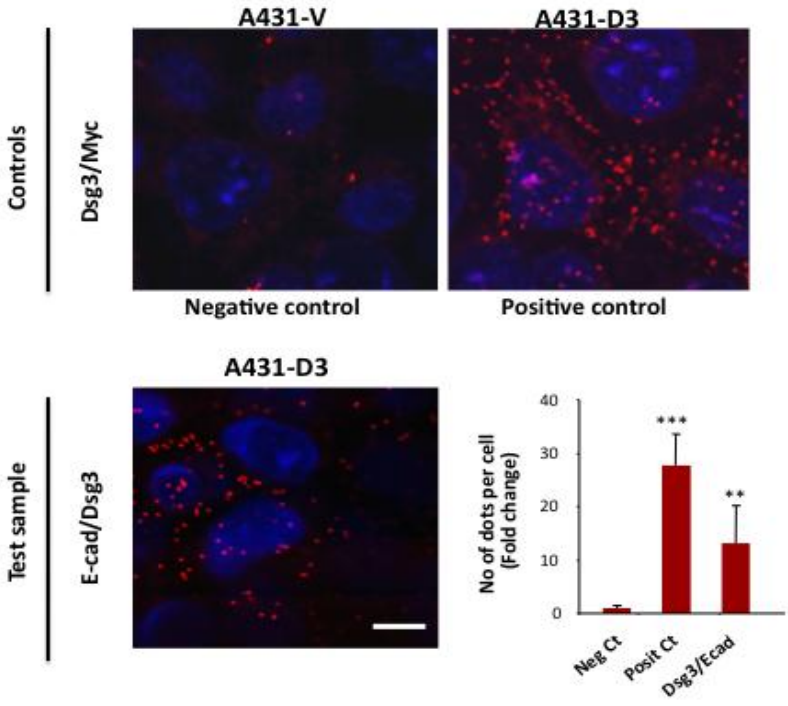

Figure 13: Proximity Ligation Analysis (PLA) demonstrates Dsg3 and E-cadherin are in close proximity of each other in A431-D3 cells.

Representative immunofluorescence images of Proximity Ligation Analysis in A431 cells. Freshly confluent A431-V and -D3 were blocked with 10% goat serum and co-incubated with primary antibodies. The positive and negative controls were A431-V and -D3 cells co-incubated with mouse anti-Dsg3, 5H10 and rabbit anti-Myc-tag, while the test sample was A431-D3 cells co-incubated with mouse anti-E-cadherin, HDEC-1 and rabbit anti-Dsg3 antibodies. Each protein-protein interaction was detected by Duolink® 100 Detection kit and represented by a fluorescence red dot. The bar chart shows the average number of fluorescence red dots per cell (** $p<0.01$). Scale bars are 10 µm. (Posit Ct, Positive control; Neg Ct, Negative control). Two independent experiments were performed and similar reproducible results were obtained.

4.1.2 Association between Dsg3 and E-cadherin is calcium dependent

Calcium is a necessary prerequisite for a variety of cellular processes such as the assembly of intercellular junctions, differentiation and stratification. To determine the biological relevance of the Dsg3/E-cadherin association, the co-immunoprecipitation assay was used to examine if such association was enhanced over the time course of calcium exposure. It was demonstrated that the complex formation between Dsg3 and E-cadherin was gradually enhanced upon calcium addition in HaCaT cells, particularly after longer calcium exposures e.g 48 hours (Tsang et al, 2012b). To verify whether the Dsg3/E-cadherin association also existed in primary cultures, co-immunoprecipitation of E-cadherin was performed in epidermal keratinocytes. Primary cells at passage 3 were initially grown to 90% confluence in a low calcium medium (EpiLife, 60μM Ca^{2+}) and 2mM of calcium was added into the medium for 16 hours and 48 hours prior to RIPA buffer extraction. The resulting protein lysates were co-immunoprecipated with mouse anti-E-cadherin antibody, HECD-1 and Western blotted for Dsg3 and other indicated proteins.

In Figure 14, the Western blots of E-cadherin immunoprecipitates show the association between E-cadherin and Dsg3 increased progressively upon the addition of extracellular calcium. To justify the immunoprecipitation efficiency, the Western blot was re-probed with β-catenin, a closely associated protein of E-cadherin and the heavy chains of antibodies and equal amount of β-catenin and the heavy chains of antibodies were observed in each lane. For input, the total lysates were Western blotted for Dsg3, E-cadherin and β-catenin with actin as the loading control. As expected, the levels of Dsg3 protein increased progressively upon the addition of calcium, while the protein levels of E-cadherin, β-catenin and actin remained relatively consistent throughout this time period (Figure 14, right). Taken together, the association between Dsg3 and E-cadherin was consistently enhanced upon the addition of calcium in primary epidermal keratinocytes and HaCaT cells (Tsang et al, 2012b), highlighting its biological relevance during the process of junction formation and cellular differentiation.

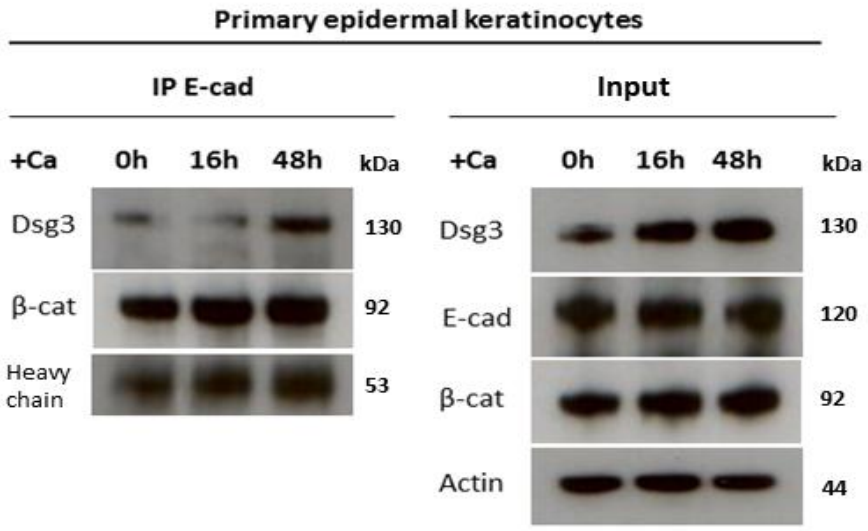

Figure 14: The Dsg3 and E-cadherin association increases upon the addition of calcium.

Western blots of E-cadherin immunoprecipitates and total lysates after a calcium switch assay in primary epidermal keratinocytes. Primary cells were initially grown to 90% confluence in a low calcium medium (EpiLife, 60μM Ca^{2+}) and 2mM of calcium was added into the medium to trigger the assembly of the intercellular junctions. Protein extraction using RIPA buffer was carried out after 0 hour, 16 hours and 48 hours of calcium exposures. Five hundred micrograms (μg) of the resulting protein lysates were co-immunoprecipated with mouse anti-E-cadherin antibody, HECD-1 and Western blotted for Dsg3, β-catenin and heavy chains of antibodies. For input, 10μg of protein lysates were loaded in each lane and Western blotted for the indicated proteins. Two independent experiments were performed and similar reproducible results were obtained.

4.1.3 Detergent solubility of Dsg3 and E-cadherin

It is known that there are two fractions of Dsg3 protein present in epithelial cells: the Triton X-100 soluble and insoluble fractions. The latter fraction is found in desmosomes, which is associated with the intermediate filaments (Aoyama et al, 1999). Hence, the next question was to determine in which cellular fraction of Dsg3 bound to E-cadherin. Before answering this question, it is important to determine the protein levels and cellular distribution of the desmosomal and adherens junctional proteins in response to the addition of extracellular calcium in HaCaT cells. To study the dynamics of junction assembly (Green & Simpson, 2007), the calcium switch assay (Hennings et al, 1980; Watt et al, 1984) and the Triton X-100 solubility assay were used. It is established that the titration of desmosomal components from the detergent-soluble to detergent-insoluble fractions reflects the recruitment of desmosomal components from the cytoplasm to plasma membrane where they form stable interactions with the intermediate filaments (Kowalczyk et al, 1994).

HaCaT is an immortalised normal human keratinocytes, which retain normal morphogenesis and differentiation features (Boukamp et al, 1988). It expresses high levels of endogenous Dsg3 and serves as an ideal model to study the formation of the intercellular junctions and cellular differentiation (Garrod & Chidgey, 2008). HaCaT cells were initially grown to 90% confluence in a low calcium medium (EpiLife, 60μM Ca^{2+}) and 2mM of calcium was added into the medium to trigger the assembly of intercellular junctions. Protein extraction of the Triton X-100 soluble and insoluble fractions was carried out after different time periods of calcium exposure (2 hours, 8 hours, 16 hours, 1 day, 3 days and up to 6 days). The soluble fraction was extracted with 1% Triton X-100 buffer (Cirillo et al, 2009), while the insoluble fraction was recovered by dissolving the pellet with SDS Laemmli sample buffer. Equal amounts of cell lysates from each fraction (5μg per lane) were loaded and analysed by Western blot analysis. In Figure 15, the Western blot analysis shows the levels of intercellular junctional proteins in both soluble and

insoluble fractions. The bar charts in Figure 16 are results of the band densitometry analysis of Figure 15, which show the average Triton solubility of Dsg3 and E-cadherin obtained from three independent experiments with β-actin as the loading control.

As shown in Figure 15, the protein levels of Dsg3 and E-cadherin exhibited distinct distribution in terms of Triton solubility. At time 0 hour before the addition of calcium, a higher partition of Dsg3 protein was observed in the Triton X-100 insoluble fraction of HaCaT cells. Upon the addition of calcium (2mM), the levels of desmosomal proteins were markedly increased, particularly after longer calcium exposures (1-6 days). For instance, the protein levels of Dsg2 and 3 increased gradually from 0 hour to 16 hours and became largely consistent after 1 day of calcium exposure. Similarly, the protein levels of Dsc2 and 3 increased progressively for up to 6 days. These results demonstrate that the levels of desmosomal proteins, including Dsg3, were enhanced by calcium in a time-dependent manner. A higher partition of desmosomal cadherins (70-80%) was observed in the Triton X-100 insoluble fraction, while the remaining fraction (20-30%) was found in the soluble fraction of cells (Figure 16). Additionally, the relative ratio of desmosomal cadherins between Triton soluble (20-30%) and insoluble fractions (70-80%) was consistent throughout the time frame of study.

As for the adherens junctions, the levels of E-cadherin and other junctional proteins such as α- and β-catenins did not increase upon the addition of calcium and remained largely in the Triton soluble fraction (Figure 15). It was observed that the relative ratio between the soluble and insoluble fractions of E-cadherin or P-cadherin was less consistent than that of Dsg3 throughout the time frame of study (Figure 16).

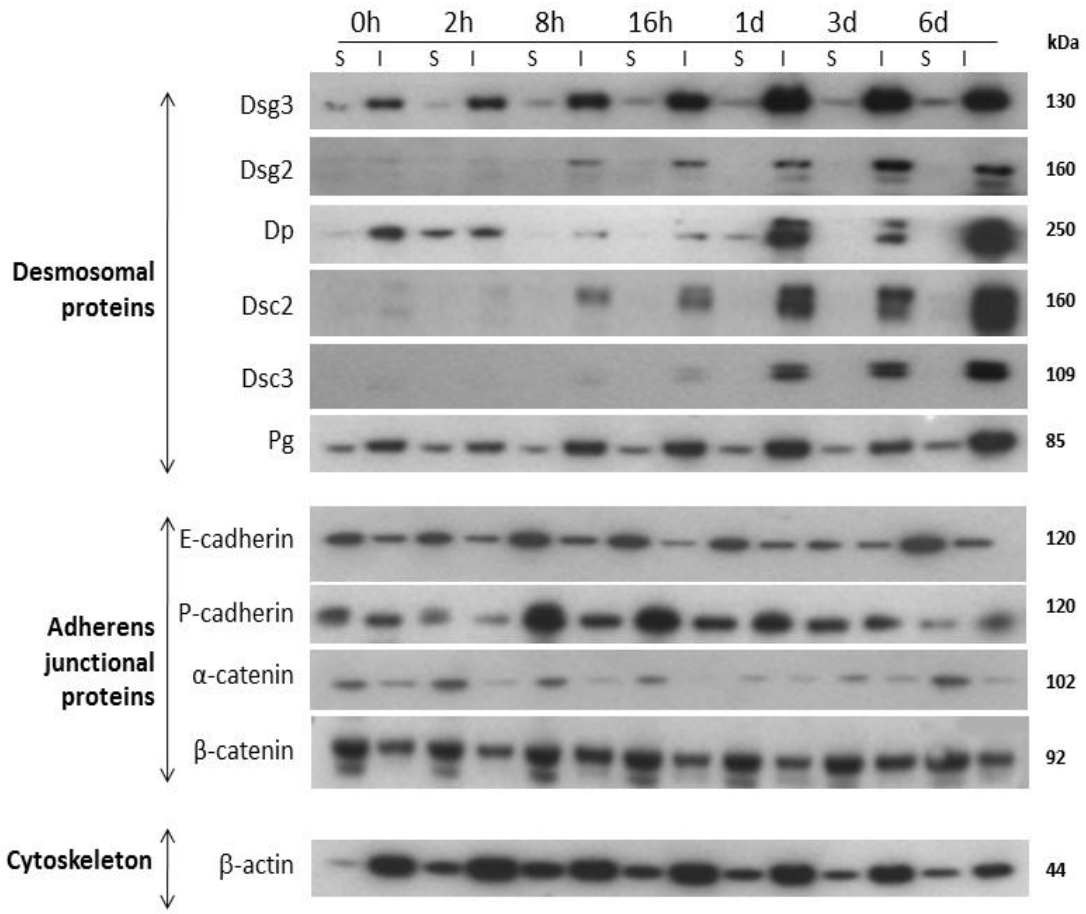

Figure 15: The protein levels of junctional cadherins in Triton soluble and insoluble fractions after a calcium switch assay.

Western blots of HaCaT cells following the calcium switch and Triton X-100 solubility assays. HaCaT cells were grown in EpiLife medium till 90% confluence. Two millimolar (mM) of calcium was added into the medium for 2 hours, 8 hours, 16 hours, 1 day, 3 days and 6 days. At each time point, cells were extracted sequentially using 1% Triton X-100 buffer and SDS Laemmli sample buffer for the soluble (S) and insoluble (I) fractions, respectively. Five micrograms (µg) of protein lysates were loaded in each lane and Western blotted for the indicated proteins. Three independent experiments were performed and similar reproducible results were obtained.

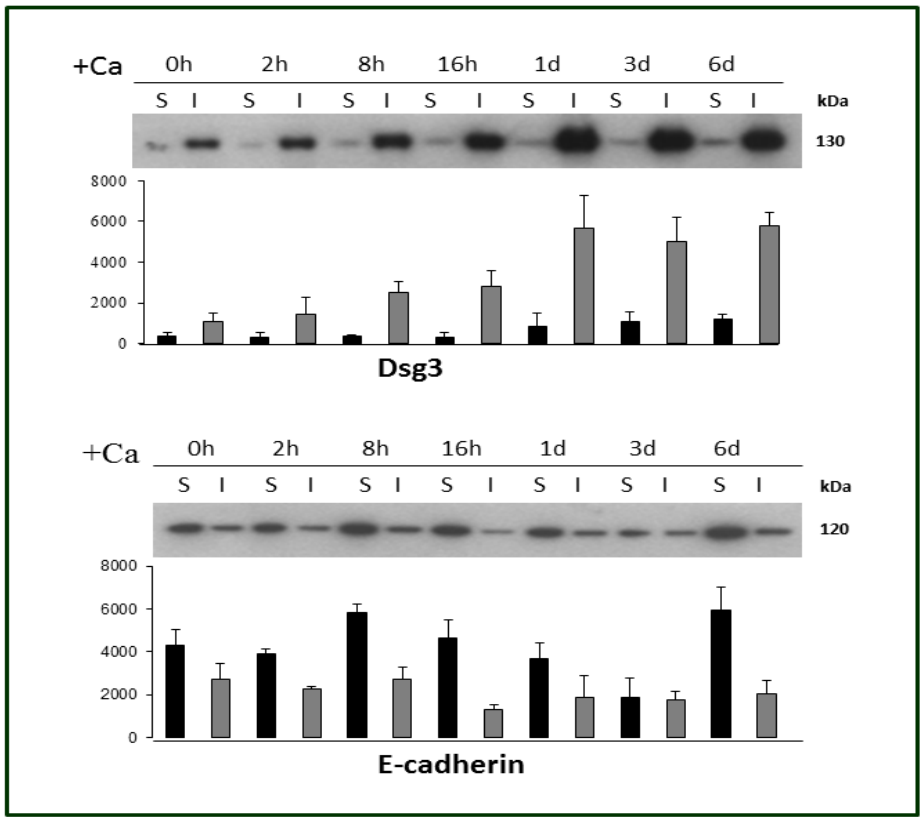

Figure 16: Dsg3 is predominantly distributed in the Triton insoluble fraction, while E-cadherin is mainly distributed in the soluble fraction.

Densitometry analysis of Western blots in Figure 15. The bar charts show the average protein levels of Dsg3 and E-cadherin in Triton soluble and insoluble fractions obtained from three independent experiments (mean+/-SD). Soluble (Black) and insoluble (Grey).

To address which cellular fraction of Dsg3 bound to E-cadherin, freshly confluent HaCaT cells were sequentially extracted with 1% Triton X-100 buffer and RIPA buffer containing 1% NP-40 for the Triton soluble and insoluble fractions, respectively. This procedure is similar to experiments described in Figure 15 but RIPA buffer instead of SDS Laemmli sample buffer was used to recover proteins from the Triton insoluble fraction. The resulting protein lysates were co-immunoprecipitated individually with mouse anti-E-cadherin antibody, HECD-1 and Western blotted for Dsg3.

In Figure 17A (left), the Western blots of E-cadherin immunoprecipitates show that the association between Dsg3 and E-cadherin was only detectable in the Triton X-100 soluble fraction and no Dsg3 band was detected in the insoluble fraction. The heavy and light chains of antibodies were used to justify for the immunoprecipitation efficiency and equal amount of heavy and light chains of antibodies were observed in each lane. This finding was in agreement with the reverse approach as shown in Figure 17A (right), where co-immunoprecipitation with rabbit anti-Dsg3 antibody was carried out and Western blotted for E-cadherin and Dsg3. Consistently, the association between E-cadherin and Dsg3 was detected only in the Triton soluble fraction. The Western blot was re-probed with the same immunoprecipitating anti-Dsg3 antibody to verify immunoprecipitation efficiency and equal amount of Dsg3 was observed in each lane. For input, freshly confluent HaCaT cells were sequentially extracted using 1% Triton X-100 buffer and RIPA buffer containing 1% NP-40. After RIPA buffer extraction, the remaining pellet was dissolved in SDS sample buffer to recover the rest of the highly insoluble proteins. In Figure 17B, the Western blots of these fractions show that Dsg3 and E-cadherin were present in both soluble and insoluble (RIPA and SDS) fractions. Taken together, the Dsg3 and E-cadherin association was detected in the Triton soluble fraction of HaCaT cells.

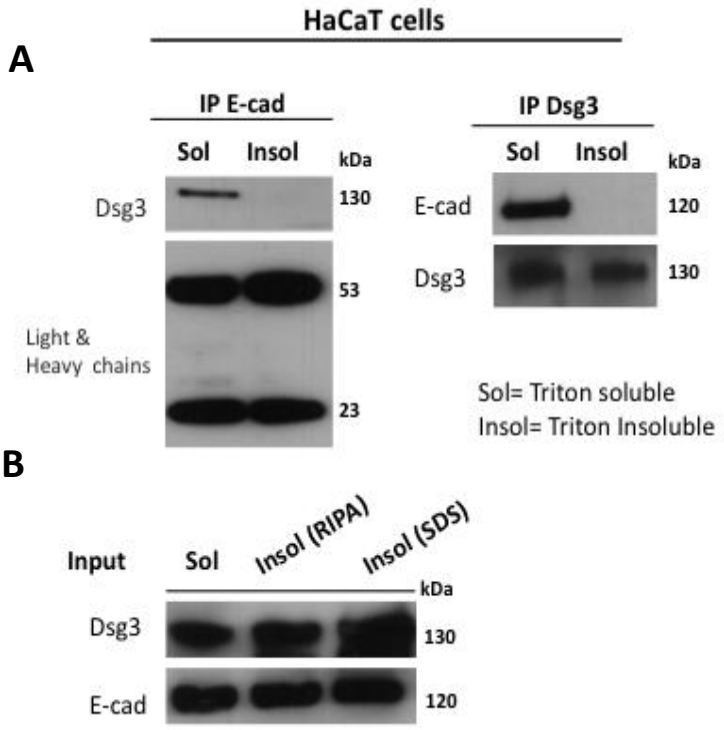

Figure 17: Dsg3 associates with E-cadherin in Triton X-100 soluble fraction.

Western blots of E-cadherin and Dsg3 immunoprecipitates and total lysates of HaCaT cells. A) Freshly confluent HaCaT cells were extracted sequentially using Triton X-100 for the soluble fraction and RIPA buffer for the insoluble fraction. Five hundred micrograms (µg) of the resulting protein lysates were co-immunoprecipitated with mouse anti-E-cadherin, HDEC-1 or rabbit anti-Dsg3 antibody and Western blotted for Dsg3 and E-cadherin. B) For input, freshly confluent HaCaT cells were sequentially extracted in a series of buffers as described above. After RIPA buffer extraction, the remaining pellet was dissolved in SDS sample buffer to recover the rest of the highly insoluble proteins. Ten micrograms (µg) of protein lysates were loaded in each lane and Western blotted for Dsg3 and E-cadherin. Two independent experiments (both direct and reverse co-immunoprecipitations) were performed and similar reproducible results were obtained.

4.1.4 Plakoglobin and p120 catenins are required for the association between Dsg3 and E-cadherin

It was demonstrated that the association between Dsg3 and E-cadherin existed in HaCaT cells, A431 cells and human breast skin. I further speculated that such association might involved other junctional proteins such as plakoglobin (Pg) and p120 catenin, which are known to bind to both desmosomal and adherens junctional proteins (Kanno et al, 2008b; Roh & Stanley, 1995). It was demonstrated that co-expression of plakoglobin with E-cadherin is essential for the initiation of desmosome assembly in A431 cells (Lewis et al, 1997), while p120 was shown to interact with Dsg3 at the same IA domain that binds E-cadherin (Kanno et al, 2008b). To address this question, siRNA-mediated knockdown of these catenins was performed. HaCaT cells were transiently transfected with p120 or Pg siRNA (smartpool) or control siRNA for 48 hours prior to co-immunoprecipitation with mouse anti-E-cadherin antibody, HECD-1 and Western blotted for Dsg3. In Figure 18 (left), the Western blots of E-cadherin immunoprecipitates show that knockdown of p120 or Pg greatly reduced the association between E-cadherin and Dsg3. The Western blot was re-probed with same immunoprecipitating anti-E-cadherin antibody to verify immunoprecipitation efficiency and equal amount of E-cadherin was observed in each lane.

For input, the total lysates were Western blotted for a number of junctional proteins. The best knockdown result out of the three experiments was shown in Figure 18. On the average, there were an approximately 40% reduction of p120 protein in p120-depleted cells and a 80% reduction of Pg protein in Pg-depleted cells as compared with their respective control siRNA-treated cells. No significant change was observed in the protein levels of Dsg3 and E-cadherin in neither of the knockdown cells with actin as the loading control. Taken together, knockdown of these proteins exert a negative effect on the Dsg3/E-cadherin association, suggesting that both p120 and Pg are required for the association between Dsg3 and E-cadherin.

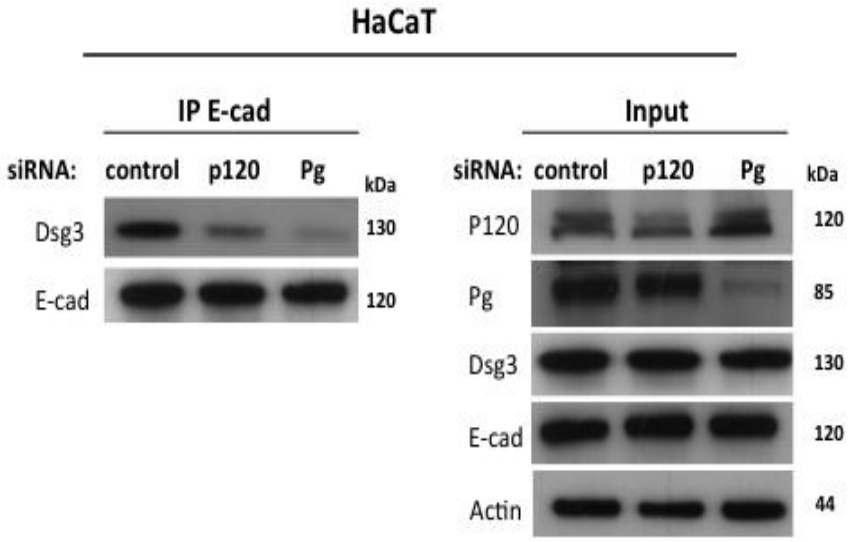

Figure 18: p120 and Pg catenins are required for the association between Dsg3 and E-cadherin.

Western blots of E-cadherin immunoprecipitates and total lysates of HaCaT cells with or without p120 or Pg knockdown. siRNA-mediated knockdown of p120 or Pg (smartpool) was performed in HaCaT cells for 48 hours prior to RIPA buffer extraction. Five hundred micrograms (µg) of the resulting protein lysates were immunoprecipitated with anti-E-cadherin antibody, HECD-1 and Western blotted for Dsg3. For input, 10 µg of protein lysates were loaded in each lane and Western blotted for the indicated proteins with actin as the loading control. Two (co-IP) and three (input) independent experiments were performed and similar reproducible results were obtained. Pg, Plakoglobin.

4.2 Discussion

4.2.1 The interaction between Dsg3 and E-cadherin

CSK buffer is commonly used to remove the soluble component of junctional proteins, but not the intermediate filaments and its associated proteins. It has been shown that cell extraction using CSK buffer retains many of the morphological characteristics of the intact cells such as intercellular junctional complexes and permits visualising the internal network with great clarity (Fey et al, 1984). In this experiment, cells were treated with ice-cold CSK buffer containing 0.5% Triton X-100 for 20 minutes to strip away proteins that do not associate with the intermediate filaments prior to immunostaining. The CSK buffer removed most of the Dsg3/E-cadherin colocalisation and a significant lesser amount of Dsg3 and E-cadherin colocalisation was present in the CSK-treated A431 cells as compared to the CSK-untreated cells (Figure 12A). This experiment does suggest that a larger proportion of Dsg3/E-cadherin colocalisation was present in the Triton soluble fraction, which is not associated with the intermediate filaments.

To confirm the protein-protein interaction between Dsg3 and E-cadherin, co-immunoprecipitation was carried out using Dynabeads (Invitrogen). It was demonstrated that Dsg3 could be immunoprecipitated with E-cadherin or β-catenin in cultured A431 cells, HaCaT cells and/or human breast skin (Figure 12B). This finding is in contrast with the work of Plott and colleagues, who showed that Dsg3 is immunoprecipitated only with plakoglobin using radio-isotope labelled human keratinocytes (Plott et al, 1994). To ensure proper experimental controls were in place, co-immunoprecipitation with mouse/rabbit pre-immune serum was carried out and no binding of Dsg3 or E-cadherin was seen in either of the controls. Furthermore, it was tested that Dsg3 was unable to co-immunoprecipitate with desmoplakin or desmocollins (internal communication), confirming that the association between Dsg3/E-cadherin is unlikely to be an artifactual interaction e.g Dsg3 does not bind to all junctional proteins.

To further support this novel Dsg3 and E-cadherin interaction, the proximity ligation assay (PLA) was used to detect protein proximity *in situ*. This method not only depends upon the use of antibodies from two different species targeting on the same or different protein(s) of interest, but also requires two species-specific PLA probes to be in close proximity of each other before a signal is generated. Overexpression of Dsg3 significantly enhanced the PLA signal between Dsg3 and E-cadherin in A431-D3 cells as compared to the negative control (Figure 13), indicating that Dsg3 and E-cadherin were in a close proximity of each other (<30-40 nm). Our results were normalised against the signals from the negative controls and thus minimising the non-specific signals. This method provides supporting evidence to the co-immunoprecipitation studies, proving that Dsg3 and E-cadherin interaction was less than 40nm of each other. However, due to the lack of a cell surface marker in this assay, we were unable to demonstrate that the detected PLA signals were located on the cell surface or in the cytoplasm by this technique. Immunostaining in conjunction with cell surface markers are needed to determine whether the Dsg3/E-cadherin interaction was present in the cytoplasm. Therefore, we are more inclined to believe that the Dsg3/E-cadherin interaction is present at cell-cell contacts as shown by the immunofluorescence data (Figure 12).

We speculated that the association between Dsg3 and E-cadherin was facilitated by plakoglobin and p120 catenin, which are known to interact with both cadherins (Kanno et al, 2008b; Roh & Stanley, 1995). To determine whether these catenins was required for the Dsg3/E-cadherin association, siRNA-mediated knockdown of plakoglobin or p120 was performed in HaCaT cells prior to co-immunoprecipitation (Figure 18). Knockdown of p120 and plakoglobin greatly reduced the binding between E-cadherin and Dsg3 (Figure 18), suggesting that both p120 and plakoglobin are involved in mediating such an interaction. Dave and colleagues reported that knockdown of p120 affects both the total and cell surface protein levels of E-cadherin (Davis et al, 2003). In my experiment, no significant difference was observed in the levels of E-

cadherin protein in p120-depleted cells (Figure 18). However, a slight decrease of plakoglobin protein was observed and future work is needed to examine the efficiency of p120-RNAi on the levels of plakoglobin protein.

Collectively, my study does demonstrate that both plakoglobin and p120 catenin are involved in the association between Dsg3 and E-cadherin. It is known that p120 interacts with Dsg3 in the same region as E-cadherin (Kanno et al, 2008a) and its crucial role in the adherens junctions is associated with the dynamic regulation of cadherin adhesiveness (Anastasiadis & Reynolds, 2001). We hypothesise that p120 may play a similar stabilising role in promoting the complex formation between Dsg3 and E-cadherin. As the co-immunoprecipitation technique is unable to distinguish a direct from an indirect interaction, other techniques are needed to confirm the nature of the Dsg3 and E-cadherin interaction and examine whether p120 and Pg are directly involved.

Taken together, my colleagues and I have used a variety of different techniques to confirm the interaction between Dsg3 and E-cadherin and hence, the reason for the discrepancy with the work of Plott and colleagues might well be due to different culture conditions, different detection methodologies and/or the sensitivity of each technique.

4.2.2 The biological significant of the Dsg3 and E-cadherin complex formation

To determine the biological relevance of the Dsg3/E-cadherin association, a series of co-immunoprecipitations were carried out to examine if such an association was enhanced upon the addition of extracellular calcium. Consistently, the Dsg3/E-cadherin interaction in primary epidermal keratinocytes was shown to increase progressively upon the addition of calcium in a time-dependent manner. This finding helps to rule out the possibility that the calcium-induced Dsg3/E-cadherin complex formation was regulated differently in different cell systems i.e HaCaT cells and primary

epidermal keratinocytes. It is believe that the increased stability of the Dsg3 protein after calcium introduction plays an important role in enhancing the complex formation between Dsg3 and E-cadherin. Since calcium is known to be involved in the regulation of early keratinocyte differentiation including junction formation, polarisation and stratification, we thus speculate the Dsg3/E-cadherin complex formation is likely one of the key molecular events that is required for early keratinocyte differentiation.

4.2.3 Detergent solubility of the desmosomal and classical cadherins

There are two fractions of Dsg3 proteins: one in desmosomes and the other outside of desmosomes that does not associate with the intermediate filaments (non-junctional Dsg3) (Aoyama et al, 1999). The calcium switch assay (Hennings et al, 1980; Watt et al, 1984) and the Triton X-100 solubility assay (Green & Simpson, 2007) were used to study the changes in the protein levels and cellular distribution of the desmosomal and adherens junctional proteins upon the addition of calcium. HaCaT cells, a normal keratinocyte cell line, which express a high level of endogenous Dsg3 was used. It was tested that the endogenous levels of Dsg3 proteins in HaCaT and primary oral keratinocytes were much higher than that of the A431-D3 cells (Tsang et al, 2010).

At time 0 hour before the addition of calcium, a higher partition of Dsg3 was noted in the Triton X-100 insoluble fraction of HaCaT cells (Figure 15 and 16). This observation may add support to the hypothesis proposed by Demlehner and colleagues, where desmosomal components in low calcium medium are co-assembled on the cell surface in the form of half-desmosomes. It is believed that these structures are unable to participate in adhesive binding and are quickly internalised and degraded (Demlehner et al, 1995). Upon the addition of calcium (2mM), my results showed that the levels of desmosomal proteins, including Dsg3, were markedly increased in a time-dependent manner for both soluble and insoluble fractions. As mentioned earlier, calcium plays an essential role in the stability of desmosomal proteins and

proper assembly of intercellular junctions. These results support the view made by others in the field that extracellular calcium enhances the levels of desmosomal proteins, most probably through protein stabilisation (Denning et al, 1998; Garrod et al, 2002). Additionally, it was observed that the desmosomal proteins were mostly detergent-insoluble with only a small fraction (20-30%) presented in the soluble fraction of HaCaT cells. These findings are in agreement with the general notion that desmosomal proteins are being recruited from the cytoplasm to the plasma membrane upon calcium addition, where they are incorporated into the desmosomes and become highly insoluble in non-ionic detergents.

As for the adherens junctions, the levels of adherens junctional proteins did not increase upon calcium addition and were distributed mainly in the soluble fraction of HaCaT cells (Figure 15 and 16). Wheelock and colleagues demonstrated that the levels of E-cadherin protein are not affected by the addition of extracellular calcium, but greatly enhanced in confluent cultures (Wheelock & Jensen, 1992). This finding is in agreement with our Western blot analysis, in which enhanced levels of E-cadherin protein were observed in the confluent cultures as compared with the sub-confluent cultures (internal communication). It was noted that the relative ratio between soluble and insoluble fractions was less consistent throughout the time frame of analysis. The reason for this variability cannot be explained as yet, we hypothesise that the spatiotemporal pattern of cadherin expression is correlated to the dynamic processes necessary for tissue morphogenesis such as epithelial polarisation, stratification and differentiation.

Desmosomal proteins are highly insoluble and they are often treated with an extremely harsh buffer containing SDS and urea to aid solubility during protein purification. However, this method is not suitable for the analysis of protein interactions as it would disrupt the protein-protein interactions and does not provide information relating to intact desmosomes per se (Garrod, 2010). In Figure 17, the Dsg3 and E-cadherin interaction was biochemically

undetectable in the Triton insoluble fraction and this could be due to several reasons. Firstly, RIPA buffer containing 1% NP-40 was unable to fully dissolve the detergent-insoluble proteins and the undissolved pellet was excluded from the analysis. Thus after RIPA extraction, the cell lysates that were used for co-immunoprecipitation may contain low levels of the insoluble proteins and hence cannot truly represent all the proteins found in the Triton X-100 insoluble fraction. Secondly, the co-immunoprecipitation techique is not feasible to assess interactions of protein in the insoluble fraction as this method requires the target proteins to be soluble in the buffer that was used (Ueki et al, 2011) e.g RIPA buffer in our studies. Thirdly, boiling the sample in SDS buffer before Western blot analysis could disrupt the stable protein-protein interaction and hence, unable to yield any interaction. As demonstrated in Figure 12A, we showed that there were a subset of Dsg3 and E-cadherin association persisted in cells treated with CSK buffer, suggesting that the Dsg3/E-cadherin interaction is likely present in both soluble and insoluble fractions of HaCaT cells.

4.2.4 Future work

It is still not clear whether the association between Dsg3 and E-cadherin was direct or indirect as the co-immunoprecipitation technique is unable to distinguish a direct from an indirect interaction. Future experiments such as a GST pull-down assay can be use to confirm the existence interactions as demonstrated by co-immunoprecipitation. Using this method, a purified protein is used to capture its protein-binding partner and we can establish if E-cadherin or plakoglobin or p120 is directly interacted with the purified GST fusion protein containing the full-length or C-terminus of the Dsg3 protein immobilised on glutathione-agarose beads. To further identify which domains are involved, GST fusion proteins carrying various portions of the cytoplasmic domain of Dsg3 can be used to pull down with E-cadherin or other junctional proteins. Another limitation of co-immunoprecipitation is that this technique is not feasible to assess interactions of the insoluble proteins. Other

techniques such as electron microscopy and the use of chemical cross-linking agents to stabilise *in vivo* protein interactions may provide additional information about the insoluble proteins. As for the knockdown experiments in Figure 18, titrating the siRNA and use it at its lowest effective concentration may help ensure target specificity and minimise the non-specific silencing effects of p120-RNAi.

4.2.5 Summary

I have shown that the association between Dsg3 and E-cadherin 1) occurred in cultured A431 cells, HaCaT cells, primary keratinocytes and human breast skin; 2) required both P120 and plakoglobin since depletion of either catenin attenuated the complex formation dramatically; and most importantly 3) enhanced in a calcium-dependent manner in both HaCaT cells and primary epidermal keratinocytes. These findings suggest that the Dsg3 and E-cadherin association is biologically relevant and most likely occurs during the process of early keratinocyte differentiation.

CHAPTER 5

RELATIONSHIP BETWEEN THE LEVELS OF DSG3 PROTEIN AND OTHER JUNCTIONAL PROTEINS

5.1 Results

5.1.1 Western blot analysis of desmosomal and adherens junctional proteins

Misexpression of desmosomal cadherins is strongly associated with altered stability of cell-cell junctions and disturbance of keratinocyte differentiation and barrier function (Hardman et al, 2005). Figure 19 shows that overexpression of Dsg3 reduced the protein levels of classical E-cadherin and a lesser extent on the reduction of P-cadherin as compared with control cell lines such as A431 parental and A431 expressing the empty vector or GFP transgene (Tsang et al, 2010). No significant difference was observed in the protein levels of β-catenin and p120 with α-tubulin as the loading control. As for the desmosomal proteins, a slight reduction was observed in the protein levels of Dsg2 and Dsc2. To confirm that this was not a specific feature of the highly malignant, tumour-derived A431 cells, I sought to determine whether knockdown of Dsg3 affected the levels of other junctional proteins in HaCaT cells, which expresses high levels of Dsg3 protein. The siRNA transfection has been optimised and efficient suppression of Dsg3 protein by RNAi-1/2 was demonstrated by Western blot analysis (Tsang et al, 2010).

siRNA-mediated knockdown of Dsg3 was performed in HaCaT cells prior to Western blot analysis. HaCaT cells were transiently transfected with Dsg3 RNAi-2 or control siRNA for 48 hours prior to SDS sample buffer extraction and Western blotted for various desmosomal and adherens junctional proteins. As shown in Figure 20, knockdown of Dsg3 effectively reduced the levels of Dsg3 protein and other desmosomal proteins including desmocollin 2/3 (Dscs), desmoplakin (DP), plakoglobin (Pg), plakophilins 1-3 (PKPs) and a lesser extent on the reduction of Dsg1/2 as compared with control siRNA-

treated cells. As for the adherens junctional proteins, no significant difference was observed in the protein levels of E-cadherin, β-catenin and p120 with actin as the loading control. Similar results were obtained with RNAi-1 (Tsang et al, 2010).

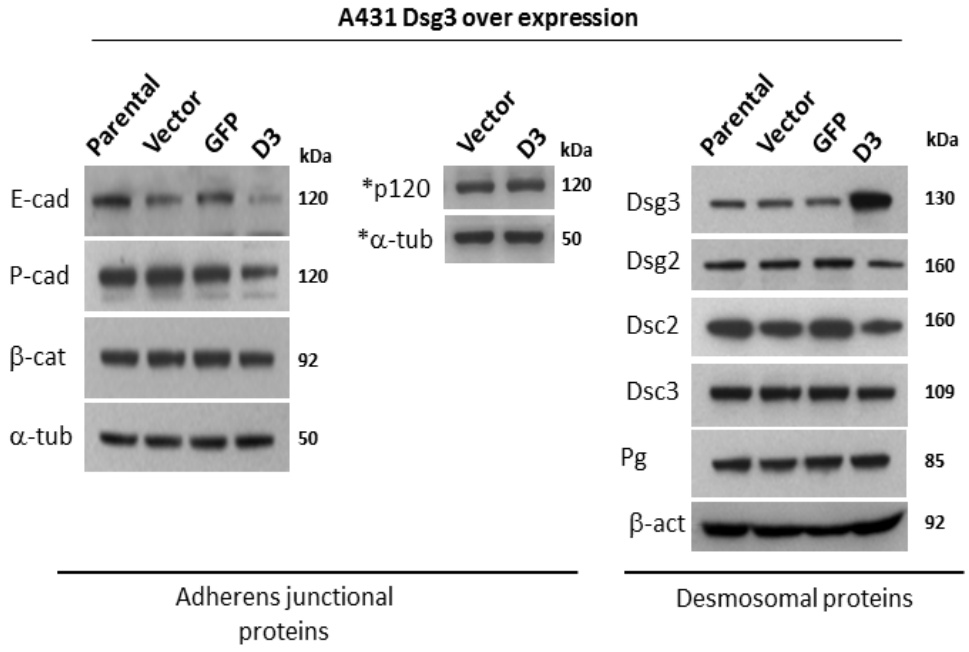

Figure 19: **Overexpression of Dsg3 reduces the levels of classical and desmosomal cadherins.**

Western blot analysis of total lysates of A431 cells with or without Dsg3 overexpression. Freshly confluent A431-D3 and control cells (A431 parental and A431 expressing the empty vector or GFP transgene) were extracted with SDS sample buffer. Ten micrograms (μg) of protein lysates were loaded in each lane and Western blotted for desmosomal and adherens junctional proteins with α-tubulin and β-actin as the loading control (Western blots courtesy of Wan H). *Western blots of p120 and α-tubulin were carried out in a separate experiment. Two independent experiments with similar results were obtained. α-tub, α-tubulin; Dscs, Desmocollins; Dp, Desmoplakin; Pg, Plakoglobin; and PKPs, Plakophilins.

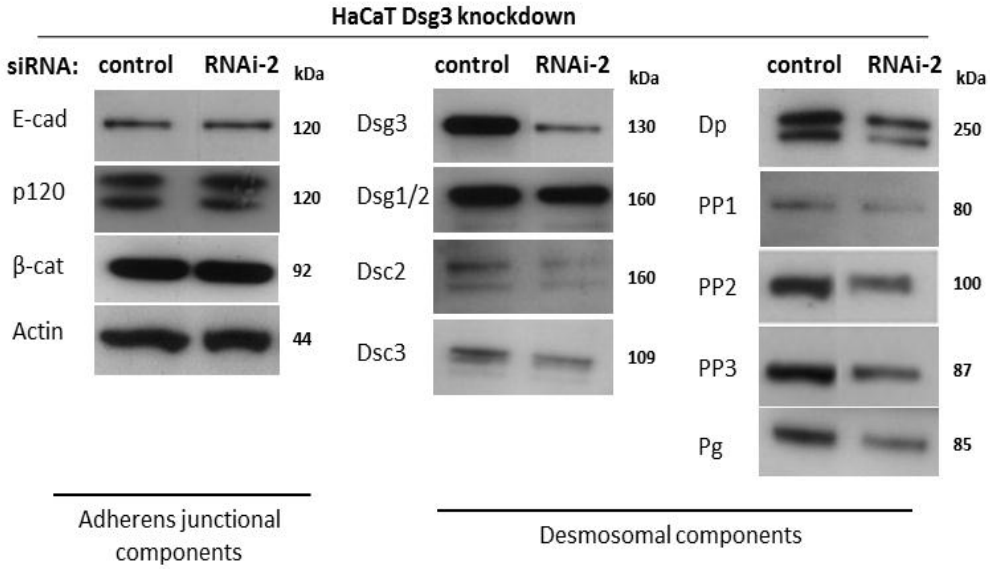

Figure 20: Knockdown of Dsg3 reduces the levels of desmosomal proteins but not the adherens junctional proteins.

Western blot analysis of total lysates of HaCaT cells with or without Dsg3 knockdown. Knockdown of Dsg3 (RNAi-2) was performed in HaCaT cells for 48 hours prior to SDS sample buffer extraction. Ten micrograms (μg) of protein lysates were loaded in each lane and Western blotted for desmosomal and adherens junctional proteins with actin as the loading control. Three independent experiments with similar results were obtained using both Dsg3 RNAi-1 (data not shown) and RNAi-2. Dscs, Desmocollins; Dp, Desmoplakin; Pg, Plakoglobin; and PKPs, Plakophilins.

5.1.2 Overexpression of Dsg3 enhances the E-cadherin-catenin complex formation

The E-cadherin-catenin complex plays a crucial role in the maintenance of tissue architecture including regulation of cell polarity, cell migration and proliferation. Hinck and colleagues showed that at least five additional proteins were incorporated into the cadherin/catenin complexes by cross-linking experiments, which also suggest that desmosomal proteins might be involved (Hinck et al, 1994). Hence, the next question was to determine whether altering the levels of Dsg3 protein, either by Dsg3 knockdown or overexpression, would affect the E-cadherin-catenin complex formation using my routine co-immunoprecipitation approach.

Co-immunoprecipitiations were carried out using cell lysates prepared from overexpression and knockdown Dsg3 cells. Freshly confluent A431-V and -D3 cells were subjected to RIPA buffer extraction and the resulting protein lysates were immunoprecipitated with mouse anti-E-cadherin antibody, HECD-1 and Western blotted for Dsg3 and a number of adherens junctional proteins such as p120, β-catenin and E-cadherin. As shown in Figure 21, the Western blots of E-cadherin immunoprecipitates clearly show that overexpression of Dsg3 increased the association between E-cadherin and p120 or β-catenin as compared with A431-V control cells. The Western blot was re-probed with the same immunoprecipitating anti-E-cadherin antibody to verify immunoprecipitation efficiency and equal amount of E-cadherin was observed in each lane. For input, the total lysates were Western blotted for Dsg3. As expected, overexpression of Dsg3 enhanced the levels of Dsg3 protein as compared with A431-V control cells.

In parallel, siRNA-mediated knockdown of Dsg3 was performed. HaCaT cells were transiently transfected with Dsg3 siRNA (RNAi-1 and RNAi-2) or control siRNA for 48 hours prior to RIPA buffer extraction. The resulting protein lysates were co-immunoprecipitated with mouse anti-E-cadherin antibody, HDEC-1 as described above. As shown in Figure 22, no significant change was observed in association between E-cadherin and β-catenin or p120 in Dsg3-

depleted cells treated with either RNAi-1/2 (Figure 22). The Western blot was re-probed with same immunoprecipitating anti-E-cadherin antibody to verify immunoprecipitation efficiency and equal amount of E-cadherin was observed in each lane. For input, efficient suppression of Dsg3 protein by RNAi-1/2 was demonstrated by Western blot analysis. No significant difference was seen in the protein levels of β-catenin and p120. Taken together, my results show that overexpression of Dsg3 promotes the association between E-cadherin and p120 or β-catenin, while knockdown of Dsg3 has no significant effect on either of these associations.

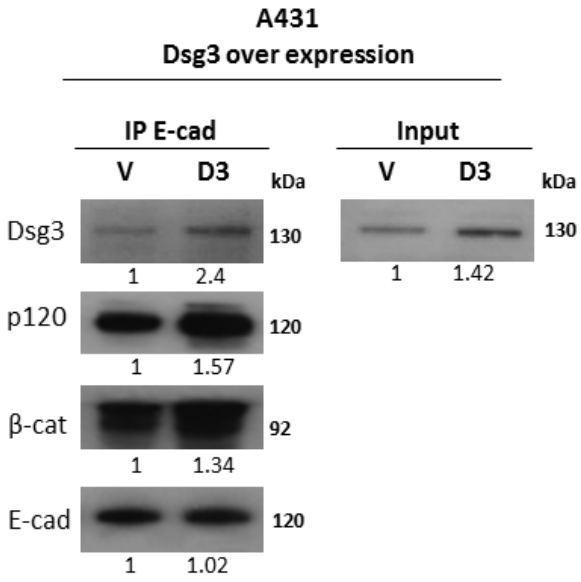

Figure 21: Overexpression of Dsg3 promotes the association between E-cadherin and p120 or β-catenin.

Western blots of E-cadherin immunoprecipitates and total lysates of A431 cells. Freshly confluent A431-V and -D3 were extracted using RIPA buffer. Five hundred micrograms (μg) of the resulting protein lysates were immunoprecipitated with mouse anti-E-cadherin antibody, HECD-1 and Western blotted for the adherens junctional proteins. For input, 10μg of protein lysates were loaded in each lane and Western blotted for Dsg3. Two independent experiments were performed and similar reproducible results were obtained.

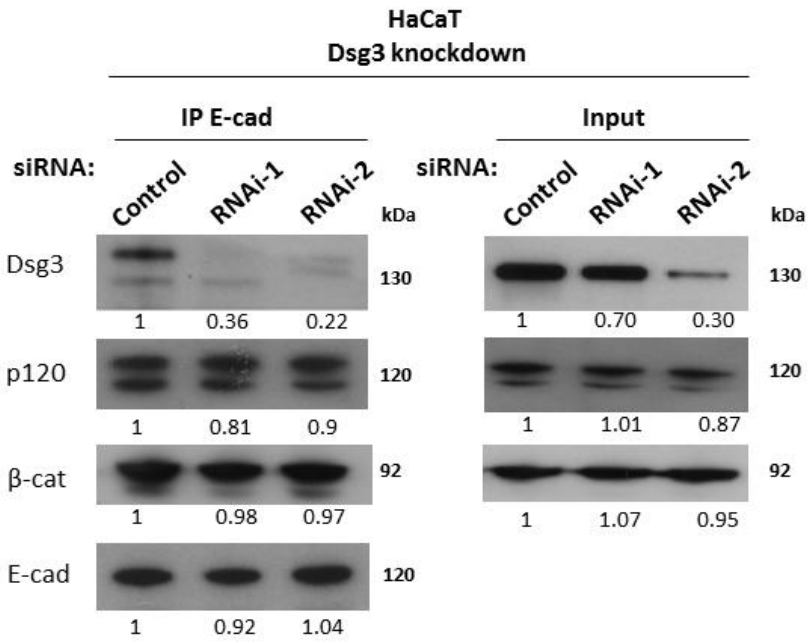

Figure 22: Knockdown of Dsg3 does not affect the association between E-cadherin and p120 or β-catenin.

Western blots of E-cadherin immunoprecipitates and total lysates of HaCaT cells with or without Dsg3 knockdown. HaCaT cells were transiently transfected with Dsg3 RNAi-1/2 or control siRNA for 48 hours prior to RIPA buffer extraction. Five hundred micrograms (μg) of the resulting protein lysates were used and subjected to the same procedures as described in Figure 21. For input, 10μg of protein lysates were loaded in each lane and Western blotted for Dsg3, p120 and β-catenin. Two independent experiments were performed and similar reproducible results were obtained.

5.1.3 Knockdown of Dsg3 affects the calcium-induced E-cadherin junction formation.

Next, I sought to determine if knockdown of Dsg3 affected the E-cadherin junction formation during the process of calcium induced cell-cell contacts. To analyse the E-cadherin membrane staining in response to the extracellular calcium (2mM), immunofluorescence of E-cadherin was carried out in HaCaT cells with or without Dsg3 knockdown. HaCaT cells were first transiently transfected with Dsg3 siRNA (RNAi-1) or control siRNA and subsequently grown on coverslips in a low calcium medium (EpiLife) to reach freshly confluence. At 36 hours post-transfection, 2mM of calcium was added into the medium to trigger the assembly of the intercellular junctions. Cells were fixed after 1 hour, 8 hours and 24 hours of calcium exposures and immunostained for E-cadherin. Four arbitrary images were acquired in each sample using a confocal microscope by Wan H. The periphery fluorescence intensity of E-cadherin was analysed by ImageJ and compared between Dsg3 knockdown and control cells (Refer to Materials and Methods Chapter 3.8). As shown in Figure 23A, the Western blot analysis demonstrates efficient suppression of Dsg3 protein by RNAi-1 with no significant difference in the total levels of E-cadherin protein at 24 hours. Unfortunately, due to the poor quality of the Western blot, the total levels of E-cadherin protein at 1 hour and 8 hours were not shown.

Representative immunofluorescence images of E-cadherin show that knockdown of Dsg3 significantly reduced the E-cadherin staining at the cell periphery especially at 8 hours as compared with control siRNA-treated cells. At 1 hour post-calcium addition, the junctional E-cadherin appeared to be substantially reduced in the Dsg3-depleted cells. At 8 hours, the E-cadherin staining remained largely cytoplasmic with evident intercellular gaps. At 24 hours, the cytoplasmic aggregates of E-cadherin were still obvious and a weaker E-cadherin staining was observed in cells surrounding those areas. Conversely, in control siRNA-treated cells, the localisation of E-cadherin at cell-cell contacts could be seen after 1 hour of calcium exposure. Gradual

decrease of the cytoplasmic staining became progressively more evident over the time course of calcium exposure. At 24 hours, enhanced and more continuous distribution of peripheral E-cadherin staining could be detected at sites of cell-cell contacts.

In Figure 23B, the bar chart shows the quantitation analysis of the peripheral E-cadherin fluorescence levels obtained from four arbitrary confocal images. The peripheral E-cadherin staining was significantly lower in the Dsg3 knockdown cells after 8 hours of calcium exposure, suggesting that Dsg3 is involved in the regulation of calcium-induced E-cadherin junction formation.

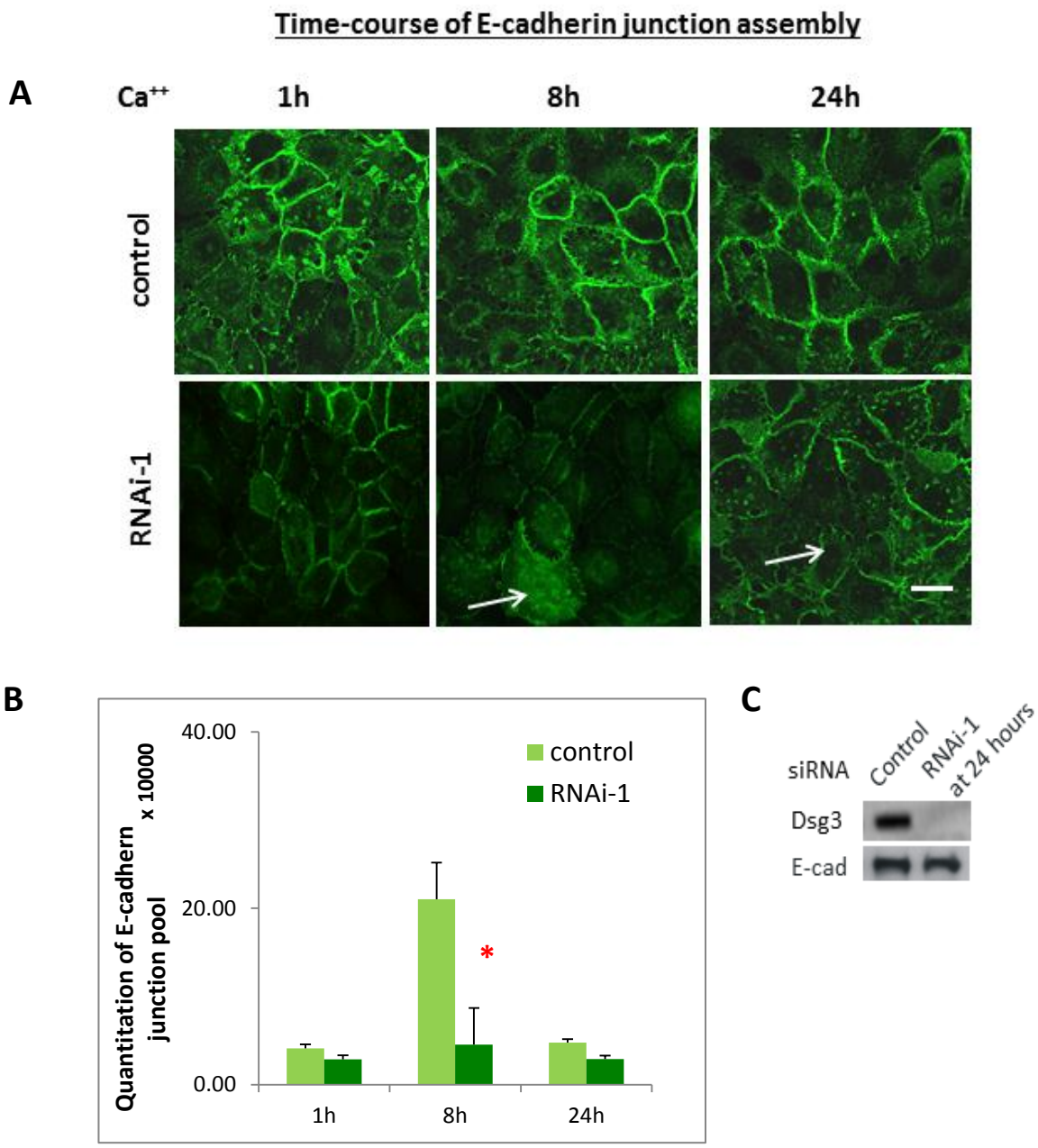

Figure 23: Knockdown of Dsg3 reduces the peripheral E-cadherin staining during calcium induced cell-cell contacts.

A) Representative fluorescence images of E-cadherin staining in HaCaT cells with or without Dsg3 knockdown. Cells were transiently transfected with Dsg3 siRNA (RNAi-1) or control siRNA. At 24 hours post-transfection, cells were transferred onto the coverslips and allowed to grow in a low calcium medium (EpiLife) overnight. At 36 hours post-transfection, 2mM of calcium was added and cells were fixed after 1 hour, 8 hours and 24 hours of calcium exposures. All coverslips were processed for immunofluorescence for E-cadherin. B) The bar chart shows the average peripheral E-cadherin fluorescence intensity obtained from four arbitrary confocal images (courtesy to Wan H). (* $p<0.05$). Scale bars are 20 µM. C) Western blots of total Dsg3 and E-cadherin at 24 hours post-calcium addition.

5.2 Discussion

5.2.1 Overexpression of Dsg3

I demonstrated that overexpression of Dsg3 reduced the levels of classical proteins and a lesser extent on the reduction of the desmosomal proteins in A431 cells (Figure 19). E-cadherin plays a crucial role in epithelial cell-cell adhesion and the loss of E-cadherin in tumourgenesis is associated with increased motility and invasive potential, a characteristic of epithelial-mesenchymal transition (EMT) (Menke & Giehl, 2012). Since upregulation of desmosomal cadherins such as Dsg2 and Dsg3 has also been reported in squamous cell carcinoma (Chen et al, 2007; Savci-Heijink et al, 2009), we speculate that the mechanism(s) by which overexpression of Dsg3 is involved in tumourgenesis might be associated with the loss of E-cadherin protein. Our speculation is in line with the scratch wound assay, which showed that overexpression of Dsg3 enhanced the rate of cell migration as compared to A431 control cells (Tsang et al, 2010).

It is acknowledged that the degree of decrease in the levels of E-cadherin protein in A431-D3 cells was somewhat variable between different experiments with no significant statistical difference. However, a slight decrease was consistently observed in the total levels of E-cadherin protein of A431-D3 cells as compared with A431-V control cells. We speculate that such variability could be related to the spatiotemporal regulation of cadherin expression as mentioned earlier in Chapter 4.2.3 Discussion.

Based on a large body of studies on *pemphigus vulgaris,* Dsg3 is believed to play a paramount role in maintaining strong adhesion and junctional integrity. Hence, we were surprised that overexpression of Dsg3 also resulted in reduced levels of desmosomal proteins. Further studies are needed to clarify the underlying molecular mechanism(s) and we do not exclude the possibility that these results are cell-context dependent (Refer to Chapter 8 Final discussion).

5.2.2 Knockdown of Dsg3

Next, we examined whether knockdown of Dsg3 would affect the levels of other junctional proteins in HaCaT cells. Ideally, A431 cells should be used for the loss of function studies. However, siRNA-mediated knockdown of junctional proteins in A431-V or -D3 cells resulted in a loss of cell morphology. These cells were less healthy and a longer period of time is required to reach confluence in the culture. Hence, we performed the loss of function studies in HaCaT cells, in which significant knockdown was routinely achieved and was used throughout all our experiments except Figure 25.

Before the start of my experiment, real-time PCR was carried out by Dr Muy-Teck Teh to confirm the efficiency of Dsg3 siRNA. It was demonstrated that Dsg3 siRNA does not cause non-specific silencing effects on other desmosomal cadherins, particularly on the closely related isoform Dsg2 (Teh et al, 2011). The Western blot analysis (Figure 20) showed that knockdown of Dsg3 reduced the levels of desmosomal proteins such as desmocollin 2/3 (Dscs), desmoplakin (DP), plakoglobin (Pg), plakophilins 1-3 (PKPs) and a lesser extent on the reduction of the Dsg1/2 protein. No significant difference was observed on the levels of adherens junctional proteins such as E-cadherin and β-catenin. This set of experiment has been confirmed by other colleagues using Dsg3-specific RNAi-1, which gave reproducible results (Tsang et al, 2012b). The slight reduction in the levels of Dsg1/2 protein could be partly due to its high endogenous protein levels in HaCaT cells (Chitaev & Troyanovsky, 1997).

The second question was to examine if knockdown of Dsg3 affected the E-cadherin junction formation during the process of calcium induced cell-cell contacts. It is acknowledged that some of the RNAi images were in sub-confluent density and hence, the data was re-analysed and only confluence images were quantified. Knockdown of Dsg3 significantly reduced the peripheral E-cadherin staining especially after 8 hours of calcium exposures (Figure 23). Although the difference in the peripheral fluorescence levels of E-

cadherin at 24 hours was not as significant as at 8 hours, this finding suggests that knockdown of Dsg3 delays the early phase of the E-cadherin-mediated junction assembly. We postulate that the decrease in the amount of E-cadherin at the plasma membrane is most likely due to reduction or retardation of the E-cadherin recruitment at the plasma membrane. The possible mechanism by which knockdown of Dsg3 interferes with the assembly of E-cadherin-mediated adherens junctions will be discussed in the Final Discussion.

5.2.3 E-cadherin-catenin complex formation

It is known that the E-cadherin-catenin complex plays a crucial role in the maintenance of cell-cell adhesion and tissue architecture. I examined whether altering the levels of Dsg3 protein, either by Dsg3 knockdown or overexpression, would affect the E-cadherin-catenin complex formation. It was showed that overexpression of Dsg3 enhanced the endogenous binding of E-cadherin with p120 or β-catenin (Figure 21), while knockdown of Dsg3 had no significant effect on the formation of cadherin complexes as compared to control cells (Figure 22). It is acknowleged that overexpression of Dsg3 promoted the formation of cadherin complexes was inconsistent with the results shown in Figure 19 and 20, in which both overexpression and knockdown of Dsg3 did not affect the protein levels of p120 or β-catenin. In addition, the total lysates (input) of E-cadherin, p120 and β-catenin were not available in Figure 21, which could affect the overall reliability of this result. Hence, it is difficult to explain how on one hand overexpression of Dsg3 reduced the levels of E-cadherin protein, and on the other hand promote the formation of E-cadhein/catenin complexes. The apparent contradictory results between overexpression and knockdown studies could be due the use of two different cell lines and the results presented here might be of cell line specific. Alternatively, the results of this study could suggest a complex process, in which the levels of E-cadherin protein might not be directly related the formation of the E-cadherin/catenin complex.

In addition, my results are in contrast with a number of studies, which established that the complex stoichiometry between E-cadherin, β-catenin and α-catenin is 1:1:1 (Aberle et al, 1994; Drees et al, 2005; Hinck et al, 1994). As the co-immunoprecipitation technique is unable to distinguish a direct from an indirect interaction, it is possible that the enhanced binding of E-cadherin with p120 or β-catenin was mediated through a third-party protein that contacts with both E-cadherin and p120 or β-catenin. Taken together, the results from this set of experiments are inconclusive and require further experimental supports. It is likely that manipulation the levels of Dsg3 protein can lead to divergent outcomes and a single mechanism is not sufficient to explain the relationship between the levels of Dsg3 protein and other junctional proteins.

5.2.4 Future work

It will be interesting to repeat the same experiment in Figure 23 and examine whether overexpression of Dsg3 would affect the assembly of E-cadherin-mediated adherens junctions. We do not exclude the possibility that this result is also cell-context dependent.

5.2.5 Summary

Overexpression of Dsg3 reduced the levels of E-cadherin protein and a lesser extent on the desmosomal proteins in A431 cell. On the other hand, knockdown of Dsg3 reduced the majority of the desmosomal proteins and affected the calcium-induced E-cadherin junction formation in HaCaT cells. Perhaps, different mechanisms are involved in each case, which warrant further investigation.

CHAPTER 6

DSG3 ASSOCIATES WITH SRC AND REGULATES ITS ACTIVATION

6.1 Results

6.1.1 Overexpression of Dsg3 enhances tyrosine phosphorylation of E-cadherin, p120 and β-catenin.

Among the mechanisms involved in the remodelling of E-cadherin mediated-adherens junctions and cellular differentiation, tyrosine phosphorylation of adherens junctional proteins plays an important role (Yap & Kovacs, 2003b). It was demonstrated that overexpression of Dsg3 not only suppresses the levels of E-cadherin protein (Chapter 5), but also enhances the membrane protrusions and cell migration (Tsang et al, 2010). These morphological and functional alterations resemble the phenotypic changes induced by constitutively active Src with the consequent de-regulation of cadherin-mediated cell-cell contacts (Avizienyte et al, 2002).

Hence, the first question was to determine whether overexpression of Dsg3 would affect the levels of phospho-tyrosine protein as compared to A431-V control cells. To address this question, co-immunoprecipitation with the phospho-tyrosine antibody was carried out in A431 cells. Freshly confluent A431-V and -D3 cells were treated with calcium-free medium for 1 hour to disrupt the intercellular junctions before being replenished with normal calcium containing medium for 5 hours to trigger signalling events associated with the junction assembly. Cell extraction was carried out using RIPA buffer. The resulting protein lysates were co-immunoprecipitated with mouse anti-phospho-tyrosine (pTyr) antibody and Western blotted for total Src and other adherens junctional proteins. For input, the total lysates were Western blotted for the indicated proteins. Phospho- and non-phospho-specific

antibody to Src Tyr416, a phosphorylation marker for Src activation (Obergfell et al, 2002) were used.

In Figure 24A, the Western blots of phospho-tyrosine immunoprecipitates clearly show that overexpression of Dsg3 enhanced the phospho-tyrosine levels of Src and adherens junctional proteins such as E-cadherin, β-catenin and p120 catenin as compared with A431-V control cells. No significant difference was observed in the phospho-tyrosine levels of EGFR between A431-V and -D3 cells in my culture condition and thus served as the negative control. For input, the Western blots of total lysates show that overexpression of Dsg3 enhanced the phosphorylation levels of Src (pY416), with a concomitant reduction of non-phospho-Src in A431-D3 cells as compared with A431-V control cells. No significant difference was observed in the total protein levels of Src, β-catenin, p120, α-catenin and EGFR. As expected, a small decrease in E-cadherin protein level was observed in A431-D3 cells.

These results were confirmed in the reverse co-immunoprecipitation approach as shown in Figure 24B, where adherens junctional proteins including E-cadherin, p120 and β-catenin were immunoprecipited individually from the lysates of A431-V and -D3 cells and Western blotted for phospho-tyrosine (pTyr). Consistent with the above findings, overexpression of Dsg3 enhanced the tyrosine phosphorylation of E-cadherin, p120 and β-catenin as compared with A431-V control cells. For input, no significant difference was observed in the total protein levels of p120 and β-catenin, while a small decrease in E-cadherin protein level was noted in A431-D3 cells. Taken together, my results strongly suggest that Dsg3 functions as an upstream regulator of Src signalling and tyrosine phosphorylation of E-cadherin, p120 and β-catenin.

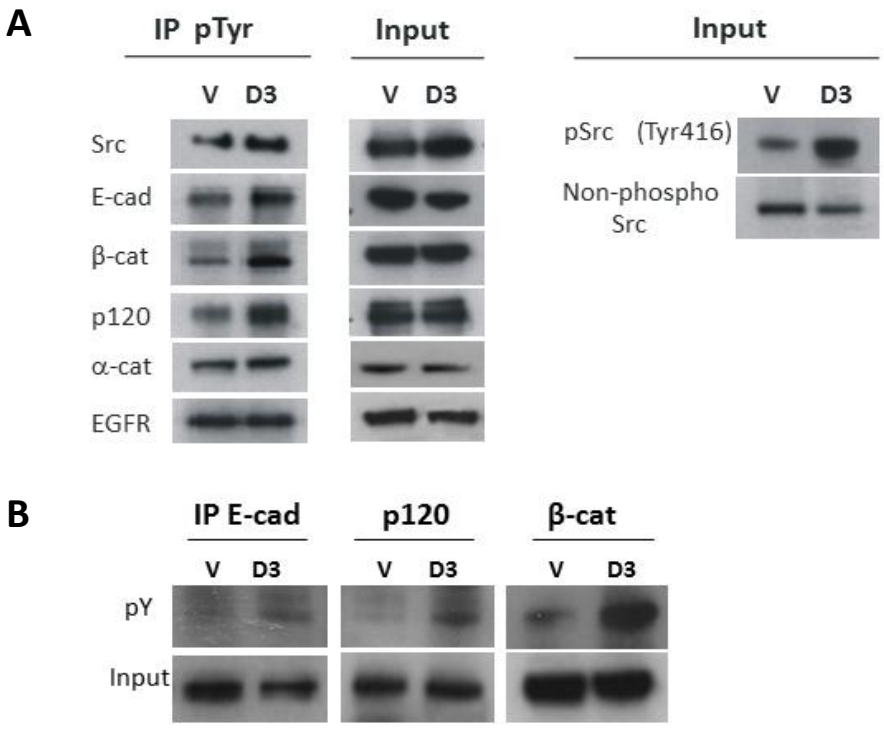

Figure 24: **Overexpression of Dsg3 increases tyrosine phosphorylation of Src and its downstream adherens junctional proteins such as E-cadherin, p120 and β-catenin**.

A) Western blots of phospho-tyrosine immunoprecipitates and total lysates of A431 cells. Freshly confluent A431-V and -D3 cells were sequentially treated with calcium-free medium for 1 hour and normal calcium containing medium for 5 hours. Protein extraction was carried out using RIPA buffer. Five hundred micrograms (µg) of the resulting protein lysates were immunoprecipitated with mouse anti-phospho-tyrosine (pTyr) antibody and Western blotted for E-cadherin/catenins proteins. For input, 10µg of protein lysates were loaded in each lane and Western blotted for the indicated proteins. B) Western blots of the reverse co-immunoprecipitation. E-cadherin, p120 and β-catenins were co-immunoprecipitated with 500µg of the protein lysates from A431-V and -D3 cells and Western blotted for tyrosine phosphorylation. For input, 10µg of protein lysates were loaded in each lane and Western blotted for E-cadherin, p120 and β-catenin. Two independent experiments (A and B) were performed and similar reproducible results were obtained.

To verify that the enhanced tyrosine phosphorylation seen in Figure 24 was indeed Src and Dsg3 specific, pharmacological inhibition of Src kinase activity and siRNA-mediated knockdown of Dsg3 were used. Freshly confluent A431-V and -D3 cells were treated routinely with calcium-free medium for 1 hour before being replenished with normal calcium-containing medium. During the calcium-free treatment, cells were seen significantly rounded up and easily detachable from the flask and hence, inhibitors were added 30 minutes after replenished with normal calcium-containing medium as a precaution to allow cells to re-establish cell-cell junctions prior to other treatments. 10µM of Src specific inhibitor, PP2 or same volume of vehicle control, DMSO was added into the medium for another 5 hours. The cells were then extracted following the routine procedures and analysed by co-immunoprecipitation with mouse anti-phospho-tyrosine antibody and Western blotted for total Src and E-cadherin.

In Figure 25A, the Western blots of phospho-tyrosine immunoprecipitates show a substantial inhibition of Src phosphorylation in both PP2-treated A431-V and -D3 cells as compared with vehicle control-treated cells. Correspondingly, the enhanced tyrosine phosphorylation of E-cadherin in A431-D3 cells was diminished by the PP2 treatment. For input, the total lysates were Western blotted for the indicated proteins. In the absence of PP2 treatment (Figure 25B), a slight reduction of E-cadherin protein was seen in A431-D3 cells, as expected. However, in the presence of PP2 treatment, equal levels of E-cadherin protein was observed in both A431-V and -D3 cells. Although there is no statistical difference, the reduced levels of E-cadherin protein in A431-D3 cells appears to be recovered by the PP2 treatment. The bar chart in Figure 25B represents the average densitometry reading of E-cadherin obtained from three independent experiments.

To determine if the depletion of Dsg3 was able to reduce the Src phosphorylation, siRNA-mediated knockdown of Dsg3 was performed. Both A431-V and -D3 cells were transiently transfected with Dsg3 siRNA (RNAi-1) or control siRNA. At 48 hours post-transfection, cells were treated with calcium-

free medium for 1 hour before being replenished with normal calcium-containing medium for 5 hours. The total lysates were extracted with SDS sample buffer and Western blotted for Dsg3, phospho-Src (pY416), total Src and E-cadherin. As showed in Figure 25C, knockdown of Dsg3 not only reduced the levels of Dsg3 protein in both A431-V and -D3 cells, but also substantially attenuated the increased phosphorylation levels of Src in A431-D3 cells. No significant difference was observed in total protein levels of Src between these cells.

Taken together, both the pharmacological inhibition of Src kinase activity and siRNA-mediated knockdown of Dsg3 abrogated the enhanced tyrosine phosphorylation of E-cadherin in A431-D3 cells, suggesting that the enhanced tyrosine phosphorylation of E-cadherin is indeed Dsg3 and Src specific.

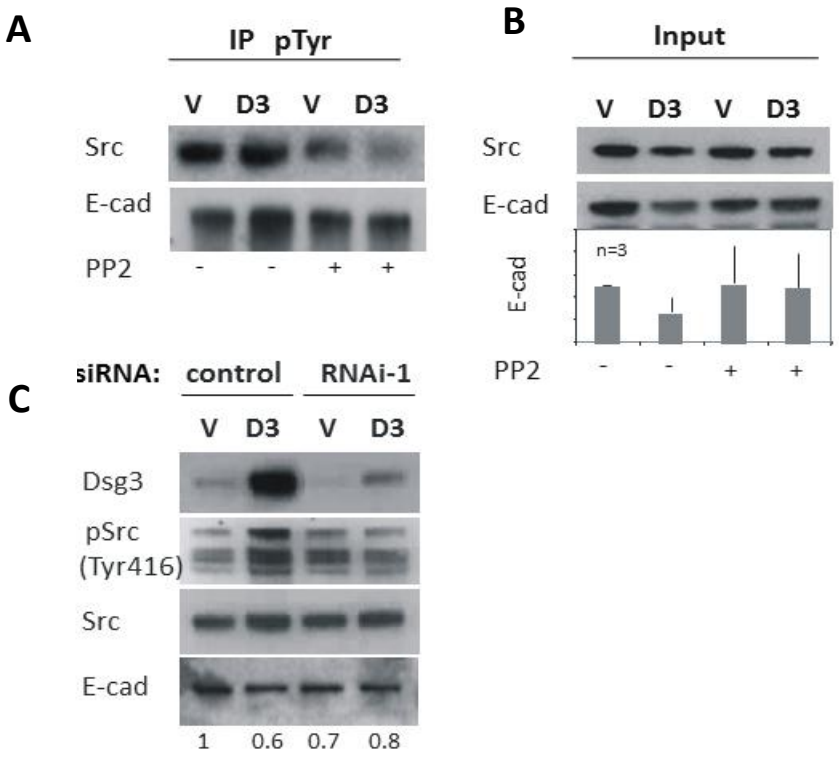

Figure 25: The enhanced tyrosine phosphorylation of E-cadherin is attenuated by both Src specific inhibition and Dsg3-mediated knockdown.

A) Western blots of phospho-tyrosine immunoprecipitates and total lysates of A431 cells pre-treated with or without Src specific inhibitor, PP2. Freshly confluent A431-V and A431-D3 cells were treated with calcium-free medium for 1 hour before being replenished with normal calcium-containing medium. After 30 minutes of medium replenishment, cells were treated with 10μM of Src specific inhibitor, PP2 or equal volume of vehicle control, DMSO for 5 hours. Protein extraction was carried out using RIPA buffer. Five hundred micrograms (μg) of the resulting protein lysates were co-immunoprecipitated with mouse anti-phospho-tyrosine antibody and Western blotted for Src and E-cadherin. B) For input, 10μg of protein lysates were loaded in each lane and Western blotted for the indicated proteins. The bar chart represents the average densitometry reading of E-cadherin obtained from three independent experiments. C) Western blots of A431 cells with or without Dsg3 knockdown. Both A431-V and -D3 cells were transiently transfected with Dsg3 siRNA (RNAi-1) or control siRNA. At 48 hours post-transfection, cells were subjected to routine calcium treatment and SDS sample buffer extraction. Ten micrograms (μg) of protein lysates were loaded in each lane and Western blotted for the indicated proteins. Two (A and C) and three (B) independent experiments were performed and similar reproducible results were obtained.

6.1.2 Overexpression of Dsg3 increases the association between E-cadherin and total Src or pSrc.

The results from the above experiments strongly suggest that Dsg3 functions as an upstream regulator of Src signalling in the E-cadherin-mediated junction formation. As such, I predicted that Dsg3 would associate with Src co-purified with E-cadherin. To address this question, co-immunoprecipitation of E-cadherin was carried out in A431 cells in the following experiments.

Freshly confluent A431-V and -D3 cells were subjected to routine calcium treatment and extracted with RIPA buffer prior to co-immunoprecipitation with mouse anti-E-cadherin antibody, HECD-1 and Western blotted for Dsg3, pSrc (Tyr416), total Src and E-cadherin. In Figure 26, the Western blots of E-cadherin immunoprecipitates show a substantial increase in the levels of total Src (also the phosphorylated form) co-purified with E-cadherin in Dsg3 overexpressed A431-D3 cells as compared with A431-V control cells. The Western blot was re-probed with the same immunoprecipitating anti-E-cadherin antibody to verify immunoprecipitation efficiency and equal amount of E-cadherin was observed in each lane. For input, the Western blots of total lysates show enhanced protein levels of Dsg3 and pSrc (pY416) as compared with A431-V control cells and no significant difference was observed in the protein levels of Src. Taken together, overexpression of Dsg3 substantially increases the association between E-cadherin and Src or pSrc, providing evidence that Dsg3 functions as an upstream regulator of the Src-E-cadherin signalling pathway in A431 cells.

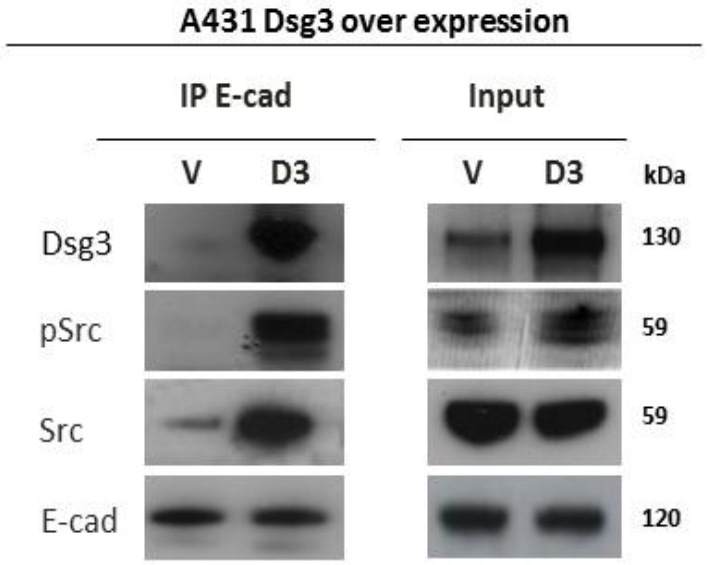

Figure 26: Overexpression of Dsg3 enhances the association between E-cadherin and total Src or pSrc.

Western blots of E-cadherin immunoprecipitates and total lysates of A431 cells. Freshly confluent A431-V and -D3 cells were treated with calcium-free medium for 1 hour before being replenished with normal calcium-containing medium for 5 hours. Five hundred micrograms (µg) of the resulting protein lysates were co-immunoprecipitated with mouse anti-E-cadherin antibody, HECD-1 and Western blotted for Dsg3, pSrc, Src and E-cadherin. For input, 10µg of protein lysates were loaded in each lane and Western blotted for the indicated proteins. Three independent experiments were performed and similar reproducible results were obtained.

6.1.3 Knockdown of Dsg3 reduces the association between E-cadherin and total Src or pSrc.

To consolidate my finding as demonstrated in Figure 26, the co-immunoprecipitation was repeated in HaCaT cells with knockdown of Dsg3. HaCaT cells were transiently transfected with Dsg3 siRNA (RNAi-2) or control siRNA for 48 hours prior to routine calcium treatment, RIPA buffer extraction and co-immunoprecipitation with E-cadherin antibody as described above. In Figure 27 (left), the Western blots of E-cadherin immunoprecipitates show that knockdown of Dsg3 reduced the association between E-cadherin and total Src or pSrc in Dsg3-depleted cells as compared with control siRNA-treated cells. Similar results of reduced pSrc and Src were obtained in cells treated with RNAi-1 (Tsang et al, 2010). The Western blot was re-probed with the same immunoprecipitating anti-E-cadherin antibody to verify immunoprecipitation efficiency and equal amount of E-cadherin was observed in each lane. For input, the total lysates were Western blotted for Dsg3, phospho-Src (Tyr416), total Src and E-cadherin. Figure 27 (right) shows that knockdown of Dsg3 reduced the protein levels of Dsg3 and pSrc, while no significant difference was observed in the protein levels of total Src and E-cadhern between Dsg3-depleted and control siRNA-treated cells. My results indicate that knockdown of Dsg3 reduces the levels of total Src and pSrc co-purified with the E-cadherin antibody as compared with A431-V control cells.

Next, I sought to examine whether knockdown of Dsg3 would affect the levels of phospho-tyrosine protein of the adherens junctional proteins. To address this question, siRNA-mediated knockdown of Dsg3 was carried out prior to co-immunoprecipitation with mouse anti-phospho-tyrosine (pTyr) antibody and Western blotted for Dsg3, E-cadherin, p120 and β-catenins (same analysis as Figure 24). Figure 28 shows that knockdown of Dsg3 significantly reduced the phospho-tyrosine levels of E-cadherin, p120 and β-catenins as compared with control siRNA-treated cells. For input, the total lysates were Western blotted for the indicated proteins. Efficient suppression of Dsg3 protein was observed in RNAi-treated cells with no significant change in the protein levels of E-

cadherin, p120 and β-catenins between these cell lines (Figure 28, right). Taken together, knockdown of Dsg3 significantly reduces the phospho-tyrosine levels, but not the total protein levels of E-cadherin, p120 and β-catenins in HaCaT cells.

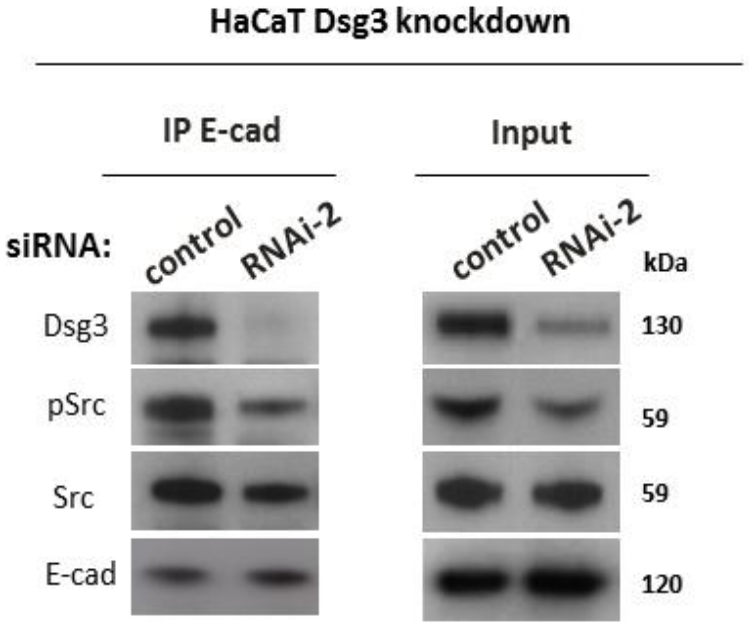

Figure 27: Knockdown of Dsg3 reduces the association between E-cadherin and total Src or pSrc.

Western blots of E-cadherin immunoprecipitates and total lysates of HaCaT cells with or without Dsg3 knockdown. HaCaT cells were transiently transfected with Dsg3 siRNA (RNAi-2) or control siRNA for 48 hours and were treated with calcium-free medium for 1 hour and normal calcium-containing medium for 5 hours. The total lysates were extracted with RIPA buffer. Five hundred micrograms (µg) of the resulting protein lysates were co-immunoprecipitation with mouse anti-E-cadherin antibody, HDEC-1 and Western blotted for Dsg3, pSrc, Src and E-cadherin. For input, 10µg of protein lysates were loaded in each lane and Western blotted for the indicated proteins. Three independent experiments were performed and similar reproducible results were obtained.

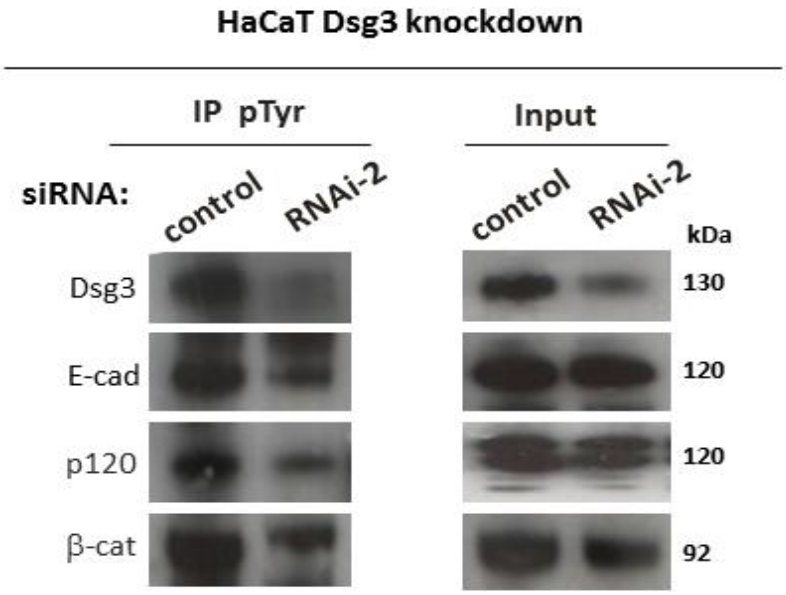

Figure 28: **Knockdown of Dsg3 decreases the phospho-tyrosine levels of p120, β-catenin and E-cadherin**.

Western blots of phospho-tyrosine immunoprecipitates and total lysates of HaCaT cells with or without Dsg3 knockdown. Cells were transiently transfected with Dsg3 siRNA (RNAi-2) or control siRNA for 48 hours and were treated with calcium-free medium for 1 hour and normal calcium-containing medium for 5 hours. The total lysates were extracted with RIPA buffer. Five hundred micrograms (μg) of the resulting protein lysates were co-immunoprecipitation with mouse anti-phospho-tyrosine antibody and Western blotted for Dsg3, E-cadherin, p120 and β-catenin. For input, 10μg of protein lysates were loaded in each lane and Western blotted for the indicated proteins. Two independent experiments were performed and similar reproducible results were obtained.

6.1.4 Dsg3 colocalises and associates with caveolin-1

The exact molecular mechanism(s) by which Dsg3 regulates Src signalling remains unclear. A possible candidate protein that might be involved in this process is caveolin-1, which is known to interact with Src-family tyrosine kinases (Li et al, 1996) and Dsg2 (Brennan et al, 2011). Based on these findings, I hypothesised that caveolin-1 is involved in the Dsg3-induced Src activation.

First, I sought to determine whether Dsg3 colocalised with caveolin-1 in A431 cells. A431-V and -D3 cells were co-stained with mouse anti-Dsg3, 5H10 (green) and rabbit anti-caveolin-1 (red) antibodies. In Figure 29A, the representative confocal images show an enhanced co-localisation between Dsg3 and caveolin-1, particularly at the cell borders in A431-D3 cells. This finding is confirmed using the proximity ligation assay (PLA), in which the fixed HaCaT cells were co-incubated with mouse anti-Dsg3, 5H10 and rabbit anti-caveolin-1 or rabbit anti-Src or rabbit anti-Myc tag antibodies. In Figure 29B, the representative immunofluorescence images show that the detected PLA signal for Dsg3 and caveolin-1 was significantly higher compared to the signal between Dsg3 and Myc-tag (negative control). Taken together, these data suggest that Dsg3, Src and caveolin-1 is in close proximity (<40nm) of each other.

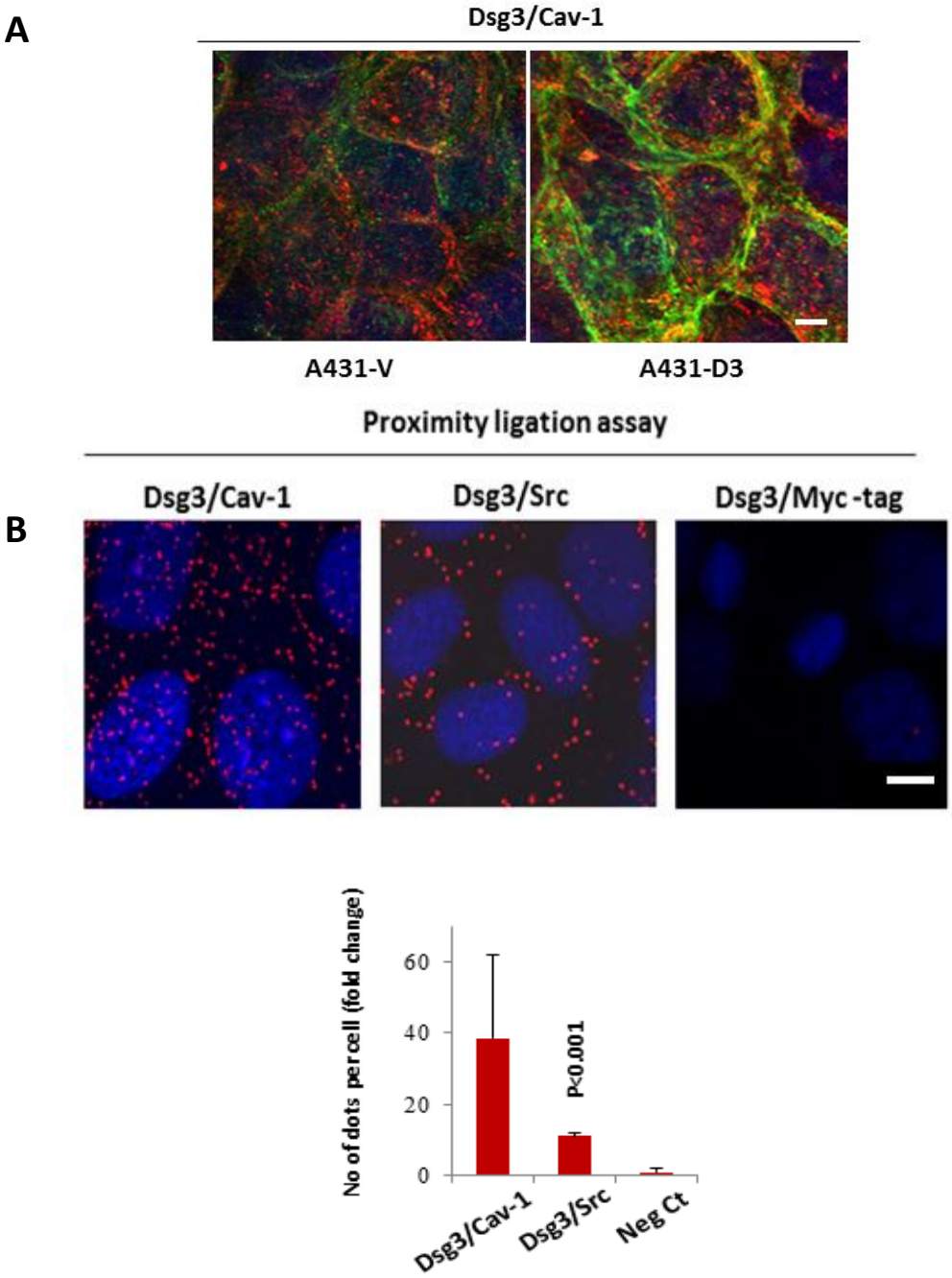

Figure 29: **Dsg3 colocalises and associates with caveolin-1 in HaCaT cells.**

A) Confocal images of A431-V and -D3 cells co-stained with mouse anti-Dsg3, 5H10 (green) and rabbit anti-caveolin-1 (red) antibodies (Confocal images courtesy of Wan H). Scale bars are 10 µM. B) Representative fluorescence images of PLA in HaCaT cells. The fixed HaCaT cells were co-incubated with mouse anti-Dsg3, 5H10 and rabbit anti-caveolin-1 or rabbit anti-Src or rabbit anti-Myc-tag antibodies. The bar chart shows the average number of fluorescence red dots per cell from four arbitrary images (** $p<0.01$, n=3). Scale bars are 10 µM. (Neg Ct, Negative control).

6.1.5 A possible model of Dsg3 in the regulation of Src activation via Caveolin-1

I hypothesised that Dsg3 might regulate Src activation by competing with the inactive Src for a common binding site on the scaffolding domain of caveolin-1 and in turn triggers the release and auto-phosphorylation (activation) of Src tyrosine kinase. If this hypothesis is correct, I would expect to see an increased binding of Dsg3 with caveolin-1 in Dsg3 overexpressing cells as compared with control cells. Correspondingly, knockdown of Dsg3 would increase the binding between Src and caveolin-1 and thus functionally inhibits the auto-activation of Src.

To address these questions, co-immunoprecipitiations were carried out in both Dsg3 overexpressed A431 and Dsg3 knockdown HaCaT cells. Both cell lines were grown to freshly confluent and subjected to calcium treatment. The resulting protein lysates were extracted with RIPA buffer prior to co-immunoprecipitation with rabbit anti-caveolin-1 antibody. In Figure 30A, the Western blots of caveolin-1 immunoprecipitates show that overexpression of Dsg3 not only enhanced its binding with caveolin-1, but also concomitantly reduced the binding between Src and caveolin-1 as compared with A431-V control cells. For input, the total lysates were Western blotted for Dsg3 and Src with actin as the loading control. No significant difference was observed in the protein levels of Src and actin between these cell lines.

This finding is confirmed in the reverse approach (Figure 30B), in which knockdown of Dsg3 increased the binding of Src with caveolin-1 as compared with control siRNA-treated cells. The Western blot was re-probed with same immunoprecipitating anti-caveolin antibody to verify immunoprecipitation efficiency and equal amount of caveolin-1 was observed in each lane. For input, the Western blots of total lysates show efficient suppression of Dsg3 by RNAi-1 with no significant change in the protein levels of Src and actin. Several attempts have been made to probe for pSrc in the caveolin-1 immunoprecipitates of A431 and HaCaT cells, but no detection of pSrc was observed under my experimental conditions. Further experimental

investigations are needed to clarify this issue. Taken together, these preliminary results *s*uggest a close relationship between Dsg3, Src and caveolin-1.

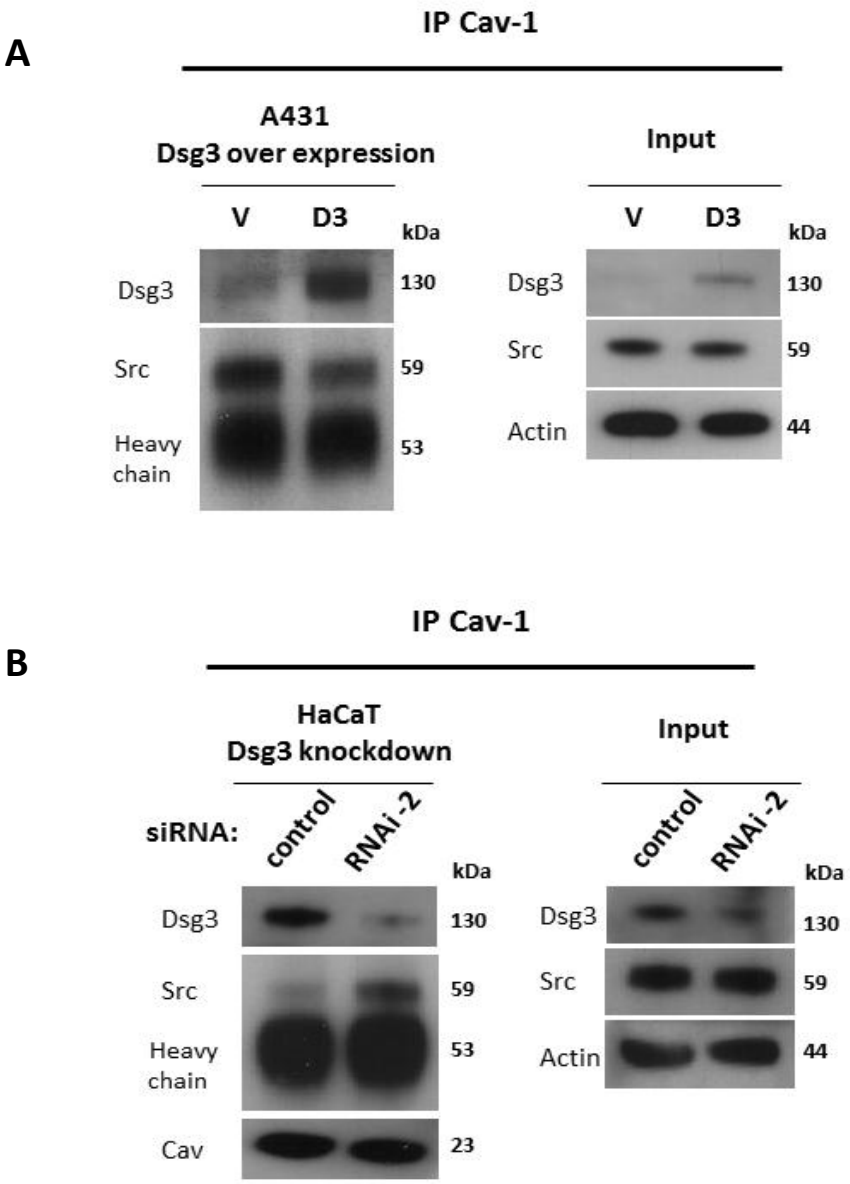

Figure 30: Dsg3 regulates the caveolin-1 and Src complex formation.

Western blots of caveolin-1 immunoprecipitates and total lysates of A431 and HaCaT cells. Both Dsg3 overexpressed A431 and knockdown HaCaT cells were grown to freshly confluence, subjected to routine calcium treatment and RIPA buffer extraction. Five hundred micrograms (µg) of the resulting protein lysates were co-immunoprecipitated with rabbit anti-caveolin-1 antibody and Western blotted for Dsg3 and total Src. For input, 10µg of protein lysates were loaded in each lane and Western blotted for the indicated proteins. One experiment (A and B) was performed with actin as the loading control.

6.2 Discussion

6.2.1 Dsg3 acts as an upstream regulator of Src activation

It is known that Src family tyrosine kinases have both positive and negative regulatory role on cell-cell adhesion and tissue integrity (Kovacs et al, 2002b). However, little is known about the upstream mechanism(s) or receptor(s) that activate these signalling activities during the process of E-cadherin-mediated junction assembly.

I showed that overexpression of Dsg3 enhanced the phospho-tyrosine levels of Src and its target effector proteins such as E-cadherin, p120 and β-catenin as compared with A431-V cells (Figure 24A). This result was confirmed in the reverse co-immunoprecipitation, where antibodies against E-cadherin or p120 or β-catenin were used for immunoprecipitation and Western blotted for phospho-tyrosine antibody. As expected, overexpression of Dsg3 enhanced tyrosine phosphorylation of adherens junctional proteins (Figure 24B). The specificity of this effect was further confirmed by pre-treating the A431 cells with an Src-specific inhibitor, PP2 or siRNA-mediated Dsg3 knockdown. PP2 was tested not to affect the levels of Dsg3 protein. Both experiments showed that the enhanced tyrosine phosphorylation of E-cadherin in A431-D3 cells was indeed Dsg3-and Src-specific (Figure 25). I depict that the enhanced levels of phospho-tyrosine proteins in A431-D3 cells was mediated via an EGFR-independent pathway since no significant difference was seen in the phospho-tyrosine or total protein levels of EGFR between A431-D3 and -V control cells.

Based on these findings, we speculate that Dsg3 functions as an upstream regulator of the E-cadherin-Src signalling pathway. Using both a gain and loss of function analysis, I showed that overexpression of Dsg3 increased the binding of E-cadherin with Src or pSrc, while knockdown of Dsg3 reversed this effect with reduced binding of E-cadherin with Src or pSrc (Figure 26 and 27). Furthermore, I showed that depletion of Dsg3 significantly reduced the phospho-tyrosine levels of adherens junctional proteins, indicating that Dsg3 is indeed involved in the regulation of Src activation and phosphorylation of

its downstream effector proteins (Figure 28). It is acknowledged that immunoprecipitation with phospho-tyrosine antibody would subject to caveats concerning non-specific effects and future experiment is needed to confirm this result. Taken together, I present new insight into the E-cadherin-Src signalling and show that Dsg3 acts as an upstream regulator of Src signalling.

It is noted that PP2 treatment seemed to recover the reduced levels of E-cadherin protein in Dsg3 overexpressed A431 cells (Figure 25B), suggesting that Src may be involved in the molecular mechanism underlying the loss of E-cadherin in the A431 cells. This suggestion is consistent with a study by Nam and colleagues, who showed that the inhibition of Src by PP2 can restore E-cadherin-mediated cell adhesion possibility through up-regulation of E-cadherin/catenin gene expression or other mechanisms involving downstream effector, Rho (Nam et al, 2002). Alternatively, the reduced levels of E-cadherin protein could be related to an E3 ubiquitin-ligase Hakai, which is known to interact with the tyrosine phosphorylated E-cadherin and causes ubiquitination and endocytosis of E-cadherin (Fujita, 2002).

It is acknowledged that there is insufficient loading control for immunoprecipitation efficiency and total lysates in some of my experiments. To verify immunoprecipitation efficiency, the Western blot should be re-probed with the same immunoprecipitating antibody to ensure equal amount of immunoprecipitation was carried out in each lane i.e anti-phospho-tyrosine antibody in Figure 24A and 25A; anti-E-cadherin, -p120 and -β-catenin antibodies in Figure 24B, C and D and anti-caveolin-1 antibody in Figure 30A. Similarly, the appropriate loading control for total lysates in Figure 25B, 25C, 26, 27 and 28 were not available. Re-probing the Western blot with anti-actin or anti-tubulin antibodies will improve the reliability of the results. However, in these experiments, no significant change was observed in the levels of total Src protein between A431-V and -D3 and hence we argue that the total Src could be used to demonstrate relatively equal protein loading. In Figure 24B and 28, anti-phospho-tyrosine was used as the immunoprecipitating antibody

and a very high background was observed, which affected the quality of my Western blots. Nevertheless, the changes in the signal intensities of the test samples could still be observed and compared with the control cells.

6.2.2 The involvement of Caveolin-1

The Dsg3 protein does not possess a tyrosine kinase domain and hence another protein that associates with both Src and Dsg3 is likely involved in the Dsg3-induced Src activation. One of the possible candidates is caveolin-1, a ubiquitously expressed integral membrane protein, which plays a major physiological function, including endocytosis and transcytosis processes, signal transduction and cholesterol homeostasis (Williams & Lisanti, 2005). It was suggested that caution must be taken when interpreting the data relating to the multiple actions of caveolin as the list of putative caveolin interacting partners is extensive. For instance, it was shown that depletion of caveolin-1 is associated with changes in the expression or phosphorylation of Akt, glycogen synthase kinase 3β, Paxillin, Src, c-Jun N-terminal kinase and mitogen-activated protein kinase (Hehlgans et al, 2009).

To demonstrate that Dsg3 is capable of interacting with caveolin-1, immunofluorescence and PLA assay were carried out. I showed that overexpression of Dsg3 enhanced the colocalisation between Dsg3 and caveolin-1 as compared to A431-V control cells. This result was also validated by the PLA assay, confirming that Dsg3 and caveolin-1 were indeed in close proximity of each other (Figure 29A and B). Furthermore, other result based on sequence analysis suggested that the interaction between Dsg3 and Cav-1 is likely mediated via a potential binding site at the residues 789-899 in the C-terminal of Dsg3 (internal communication), the same site in Dsg2 that has been shown to bind to Cav-1 (Brennan et al, 2011).

Wei and colleagues proposed a integrin clustering theory, in which integrins functionally modify the physical interaction between caveolin-1 and Src and in

turn lead to the release of Src and its subsequent autoactivation (Wei et al, 1999). Based on this study, we hypothesise that Dsg3 might activate Src by a similar mechanism, i.e. Dsg3 competes with Src for a potential binding site on the scaffold domain of caveolin-1 protein (Couet et al, 1997) and in turn leads to the release and auto-activation of Src. Using both a gain and loss of Dsg3, I showed that overexpression of Dsg3 enhanced its binding with caveolin-1 and reduced the association between caveolin-1 and Src compared to that of A431-V control cells (Figure 30). This finding was confirmed in HaCaT cells with Dsg3 depletion, in which knockdown of Dsg3 reduced its associaton with caveolin-1 and increased the binding of caveolin-1 and Src as compared with control siRNA-treated cells.

My attempts to probe for pSrc that was co-purified with caveolin-1 were unsuccessful. We speculate that Src is released from or loss its binding capacity with the caveolin-1 complex upon activation, allowing Src to associate preferentially with the E-cadherin/catenins complex and engages in E-cadherin-Src signalling. Alternatively, this could be due to the sensitivity of the Western blot analysis, which precludes the limited amount of pSrc protein or spatial analysis of phosphorylation. Although my model offers a possible molecular explanation of how caveolin-1 is involved in the Dsg3 induced-Src activation, this requires considerable further investigation.

6.2.3 Src signalling

Individual signalling pathways often overlap and 'cross-talk' with each other. Understanding the spatiotemporal and bidirectional intracellular signalling events is important in addressing the molecular mechanisms involved. We found that pSrc (Figure 26 and 27) was only detectable by Western blot analysis in a narrow window of time when cells were approaching confluence. Negative result for pSrc was consistently observed in both sparse culture (less than ~90%) and over confluent cells (more than 2 days), suggesting that the Src activation in our system is depended upon the cell density and degree of

culture confluence. To ensure general reproducibility of the overall results, the culture condition for all my experiments on Src signalling was standardised and carried out in freshly confluent culture. Cells were treated with calcium-free medium for 1 hour to disrupt the existing cell-cell adhesion and subsequently replaced with normal calcium containing medium (DMEM+10% FCS) for another 5 hours to allow the re-establishment of cell-cell contacts prior to co-immunoprecipitation. In this experimental setting, it is unlikely that replacing the calcium-free medium with normal calcium containing medium could contribute to the altered levels of Src activation as our measurement was based on the relative comparison between test and control samples. However, we cannot rule out the possibility that the baseline levels of tyrosine phosphorylation in my control cells (both A431-V and HaCaTs) were contributed by the growth factor from the normal calcium-containing medium. Alternative experimental approaches are required to validate whether the reduced levels of phospho-Src in E-cadherin immunoprecipitates was caused by the overall decrease of phospho-Src in lysates of Dsg3 RNAi (Figure 27). Nevertheless, our results do support the concept that the Dsg3 is involved in the regulation of Src signalling and the tyrosine phosphorylation of its downstream adherens junctional proteins.

Taken together, we believe that Dsg3 has a novel modulatory role in the regulation of E-cadherin-mediated adherens junctions by fine-tuning Src activation. The clinical relevant of this finding was further supported by immunostaining in *pemphigus* patient samples. Enhanced pSrc signals and disruption of E-cadherin are readily detected in the suprabasal layers above the blister as well as in the pre-lesional areas of oral mucosa in PV patients (Tsang et al, 2012b). This finding is consistent with our observation that the Src activation in our system is dependent upon the degree of culture confluence. Thus, we hypothesise that Src is only activated in conditions where cell-cell adhesion is weak/destabilised such as wounding or diseased skin such as *pemphigus*. It is likely that Src signalling is required during junction assembly or wound healing but shut down after establishment of

cell–cell junctions in confluent monolayer culture / intact normal epithelial tissue.

6.2.5 Future work

The Src family members such as c-Src, Yes and Fyn are predominantly expressed in keratinocytes and thus analysis of other Src family members or isoform(s) will provide further insight into the specific role(s) of Dsg3 in the regulation of Src family kinases. It is acknowledged that immunoprecipitation with phospho-tyrosine antibodies (Figure 28) would subject to caveats as this method does not distinguish between tyrosine-phosphorylated proteins and proteins associated with tyrosine-phosphorylated protein. Other experiment using reverse co-immunoprecipitation with specific catenin or cadherin can be used to confirm this result.

To confirm that the reduced levels of phospho-Src in E-cadherin immunoprecipitates are specific (Figure 27), other techniques such as kinase activity assay and phospho-specific Enzyme-Linked Immunosorbent Assay (ELISA) can be used. Kinase activity assay is used to directly detect or assess the activity of the specific kinases *in vitro.* It is performed by immunoprecipitating Src from lysate and incubates it with tyrosine kinase substrate in the presence of ATP. The kinase activity is measured by detecting the enzyme reaction by product, ATP. As for the indirect phospho-specific Enzyme-Linked Immunosorbent Assay, cell lysate was first added onto the plate coated with the capture antibody specific for Src. Subsequently, a secondary antibody, specifically for the phosphorylation site was added for the detection process. The intensity of the resulting signal from these methods could be measured using colorimetric or fluorometric detection systems. ELISAs are more quantitative than Western blotting and the use of two antibodies specific for the target protein increase the specificity and allow phospho-protein levels to be accurately assessed.

In agreement with the finding for Dsg2 (Brennan et al, 2011), other results based on sequence analysis identified a potential binding site at the residues 789-899 in the C-terminal of Dsg3 that could bind to caveolin-1 (internal communication). To examine whether caveolin-1 is indeed involved in the Dsg3 induced-Src activation, a GST pull down assay can be used to examine if caveolin-1 is directly interacted with the purified GST fusion protein containing the full-length or C-terminus of the Dsg3 protein immobilised on glutathione-agarose beads. To evaluate whether the Dsg3/caveolin-1 interaction occurs in this domain (aa 789-899), GST fusion proteins carrying various portions of the cytoplasmic domain of Dsg3 can be used to pull down with caveolin-1. This experiment will help to confirm that the interaction between Dsg3 and caveolin-1 is located within residues 789-899 of the C-terminal of Dsg3. To further substantiate the functional requirement of this domain *in vivo*, the same pull down experiment can be carried out with the truncated mutant of Dsg3 that lacks aa 789 – 899 and compare it with the full-length Dsg3 protein.

Since we assume that Dsg3 and Src bind to the same site of the caveolin-1 protein, it would be necessary to determine whether they can interact competitively with caveolin-1. To test this, pull down assay can be carried out in A431 cells using a purified GST fusion protein carrying the full-length caveolin-1 molecule immobilised on glutathione-agarose beads. If my hypothesis is correct, the GST-caveolin-1 would be able to pull-down Src in A431-V control cells as expected. Conversely, the enhanced levels of Dsg3 in A431-D3 cells would interfere with the interaction between Src and caveolin-1, such that the binding of Src to GST-caveolin-1 would be reduced accordingly. We would also expect to see the enhanced binding between Src and E-cadherin in A431-D3 cells.

6.2.6 Summary

Using both a gain- and loss-of-function analysis, I demonstrated that Dsg3-induced tyrosine phosphorylation of adherens junction proteins was Src-dependent in A431 cells. Overexpression of Dsg3 increased E-cadherin/Src signalling with enhanced levels of Src and pSrc co-purified with E-cadherin, while knockdown of Dsg3 inhibited this pathway with reversed effect. I also showed evidence that caveolin-1 is involved in this signalling pathway. It is likely that Dsg3 completes with Src for a common binding site of caveolin-1 and in turn causes the activation of Src in my system. Taken together, we believe that Dsg3 acts as an upstream regulator of Src signalling in the regulation of E-cadherin-mediated adherens junction formation.

CHAPTER 7

DSG3 IS INVOLVED IN THE REGULATION OF ACTIN CYTOSKELETON

7.1 Results

7.1.1 Dsg3 and actin colocalisation

It was demonstrated that overexpression of Dsg3 in A431 cells significantly enhances the membrane protrusions as compared with A431-V control cells or cells with relatively low levels of Dsg3 protein (Tsang et al, 2010). This observation was in line with the confocal analysis in Figure 31, which shows that Dsg3 co-localises with F-actin in HaCaT cells, particularly with the cortical actin at the cell borders (Tsang et al, 2012a). Based on these results, I speculated that Dsg3 might play a role in the regulation of actin organisation.

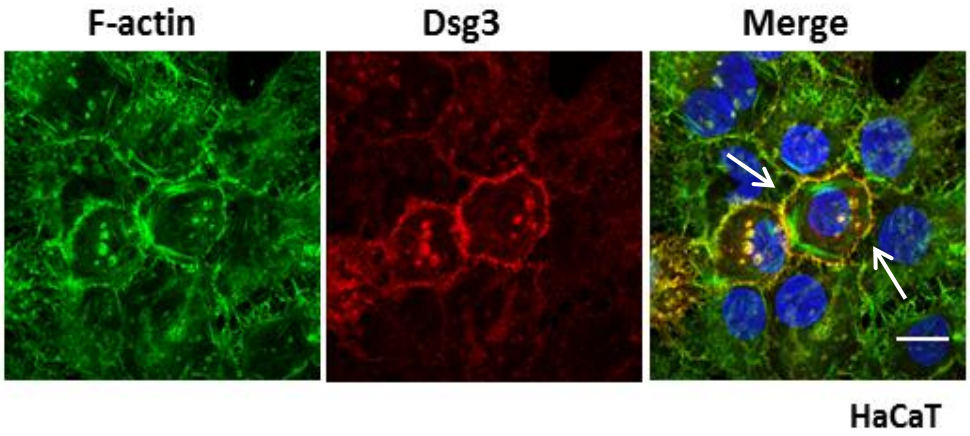

Figure 31: Colocalisation between Dsg3 and actin at the cell borders in HaCaT cells.

HaCaT cells were co-stained with mouse anti-Dsg3 antibody, 5H10 and the secondary conjugated antibody (Alexa Fluor 568) along with A488 conjugated phalloidin. Arrows indicate colocalisation between Dsg3 and F-actin at the cell borders. Two independent experiments were performed and similar reproducible results were obtained (confocal images courtesy of Wan H).

To address whether Dsg3 is involved in the regulation of actin organisation, immunofluorescence staining for Dsg3 and actin was carried out in cells with either overexpressing or knockdown of Dsg3 and the degree of colocalisation was quantifed and compared with their respective controls. In the gain of function approach, A431-V and -D3 cells were fixed with 3.8% formaldehyde and permeabilised with 0.1% Triton X-100. The cells were co-stained for mouse anti-Dsg3 antibody, 5H10 and the secondary conjugated antibody (Alexa Fluor 568) along with A488 conjugated phalloidin. Six arbitrary images were taken by fluorescence microscopy. The colocalisation index in Figure 32, which highlighted in white was quantified by ImageJ. As shown in Figure 32A and C, overexpression of Dsg3 enhanced the colocalisation of Dsg3 and actin by ~6-fold as compared with A431-V control cells ($p<0.001$). This finding is further strengthened by the loss of function approach in which siRNA-mediated knockdown of Dsg3 (RNAi-2) was carried out in HaCaT cells and co-stained with Dsg3 and F-actin as mentioned above. Figure 32C and D show that knockdown of Dsg3 caused the opposite effect with ~4-fold reduction in the colocalisation between Dsg3 and actin as compared with control siRNA-treated cells ($p<0.001$). The Western blots of total lysate show that Dsg3 was overexpressed in A431-D3 cells (Figure 32B), while efficient suppression of Dsg3 by RNAi-2 was observed in HaCaT cells (Figure 32D) with actin as the loading control. Taken together, these results suggest that the degree of colocalisation between Dsg3 and actin is highly dependent upon the Dsg3 protein levels.

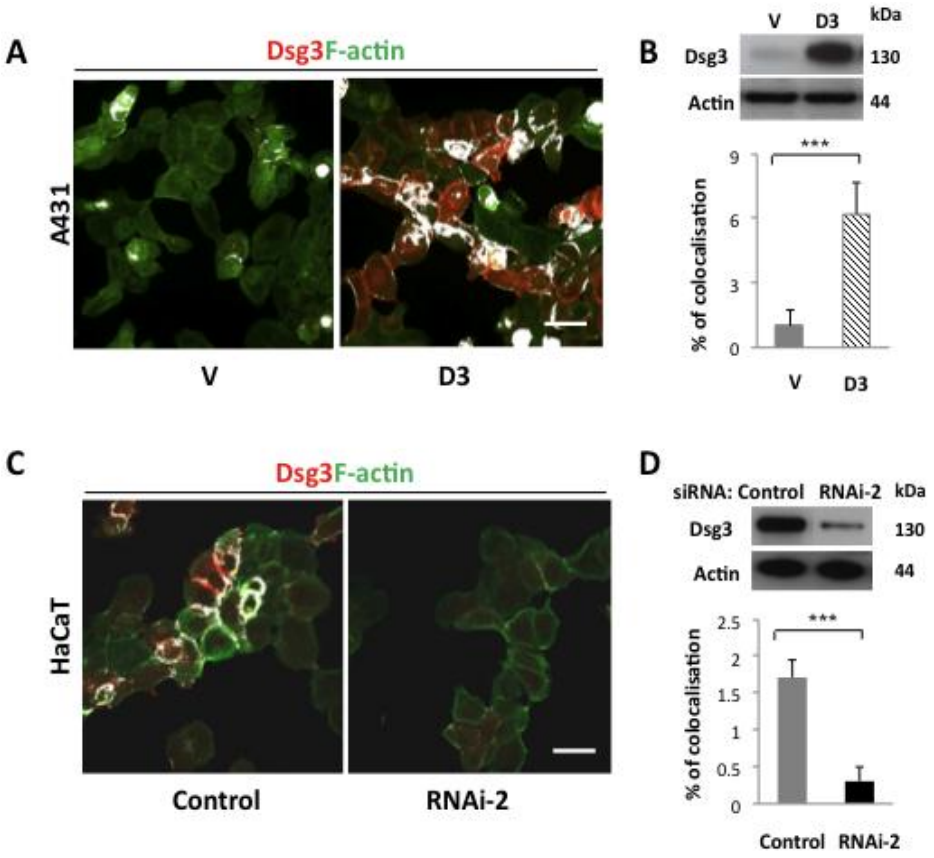

Figure 32: The colocalisation index between Dsg3 and F-actin in A431 and HaCaT cells.

A and C) The representative immunofluorescence images of cells with either overexpression of Dsg3 in A431 or knockdown of Dsg3 in HaCaT cells. Cells were co-stained for mouse anti-Dsg3 antibody, 5H10 and the secondary conjugated antibody (Alexa Fluor 568) (red) along with A488 conjugated phalloidin (green). The colocalisation between Dsg3 and F-actin was highlighted in white and measured by ImageJ. B and D) Western blot analysis of Dsg3 protein levels in A431 and HaCaT cells with actin as the loading controls. Two independent experiments were performed and similar reproducible results were obtained. The bar charts show the average colocalisation between Dsg3 and actin per cell. Error bars indicate mean ± SEM. Scale bars are 20µM.

7.1.2 Association between Dsg3 and actin

To determine whether Dsg3 formed a complex with actin, co-immunoprecipitation was performed using cell lysates prepared from both HaCaT cells and human breast skin samples. The epidermis was first separated from dermis using dispase and subsequently extracted with RIPA buffer containing 1% NP-40. In parallel, HaCaT cells were grown to freshly confluent and extracted using the same lysis buffer. The resulting protein lysates were subjected to co-immunoprecipation with mouse anti-Dsg3 antibody, 5H10 and Western blotted for actin, E-cadherin and Dsg3.

As shown in Figure 33, the Western blots of Dsg3 immunoprecipitates show that the Dsg3/actin association was detected in HaCaT cells as well as lysates from human epidermis. No binding of Dsg3 with actin was seen in the mouse pre-immune immunoprecipitate and was used as the negative control. For input, the Western blots of total lysates show that the protein levels of actin, E-cadherin and Dsg3 in both lysates. Taken together, these results indicate that Dsg3 associates with actin in normal keratinocyte HaCaTs as well as in the epidermis of human breast skin samples.

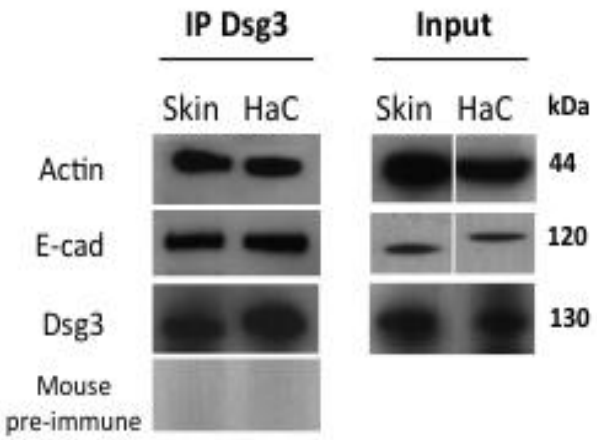

Figure 33: Association between Dsg3 and actin.

Western blots of Dsg3 immunoprecipitates and total lysates of HaCaT cells and the epidermis of human breast skin. Confluent HaCaT cells and epidermis of human breast skin were extracted with RIPA buffer containing 1% NP-40. Five hundred micrograms (µg) of the resulting protein lysates were subjected to co-immunoprecipation with mouse anti-Dsg3 antibody, 5H10 and Western blotted for actin, E-cadherin and Dsg3. Pre-immune mouse serum was used as the negative control. For input, 10µg of protein lysates were loaded in each lane and Western blotted for the indicated proteins. Two independent experiments were performed and similar reproducible results were obtained.

7.1.3 Overexpression of Dsg3 enhances cellular membrane protrusions and actin dynamics

In Figure 34A, the representative phase contrast images show that overexpression of Dsg3 elicited striking morphological changes, resulting in the formation of enhanced membrane protrusions in A431-D3 cells. Similarly, enhanced membrane protrusions were also observed in other Dsg3 overexpressing epithelial cells such as MDCK cells (internal communication). To compare the relative enhancement of membrane protrusions between A431-V and D3 cells, time-lapse video microscopy was used.

Firstly, a limiting dilution assay and clonal expansion were carried out (Refer to Material and Methods Chapter 3.2.2) to ensure a more homogeneous phenotype of A431-D3 cells prior to time-lapse video microscopy. Clones with relatively high levels of Dsg3 protein were selected from the A431-D3 mixed population. As demonstrated in Figure 34B, the Western blot shows that A431-C7 has the highest levels of Dsg3 protein as compared to A431-D3 cells with GAPDH as the loading control. We believe that A431-C7, the clone with the highest levels of Dsg3 protein, will give a more homogeneous phenotype and hence, was used in the time-lapse microscopy instead of A431-D3 cells. The video stills in Figure 34C shows that A431-V cells were less spread out and displayed much less pronounced membrane protrusions compared to that of A431-C7 cells.

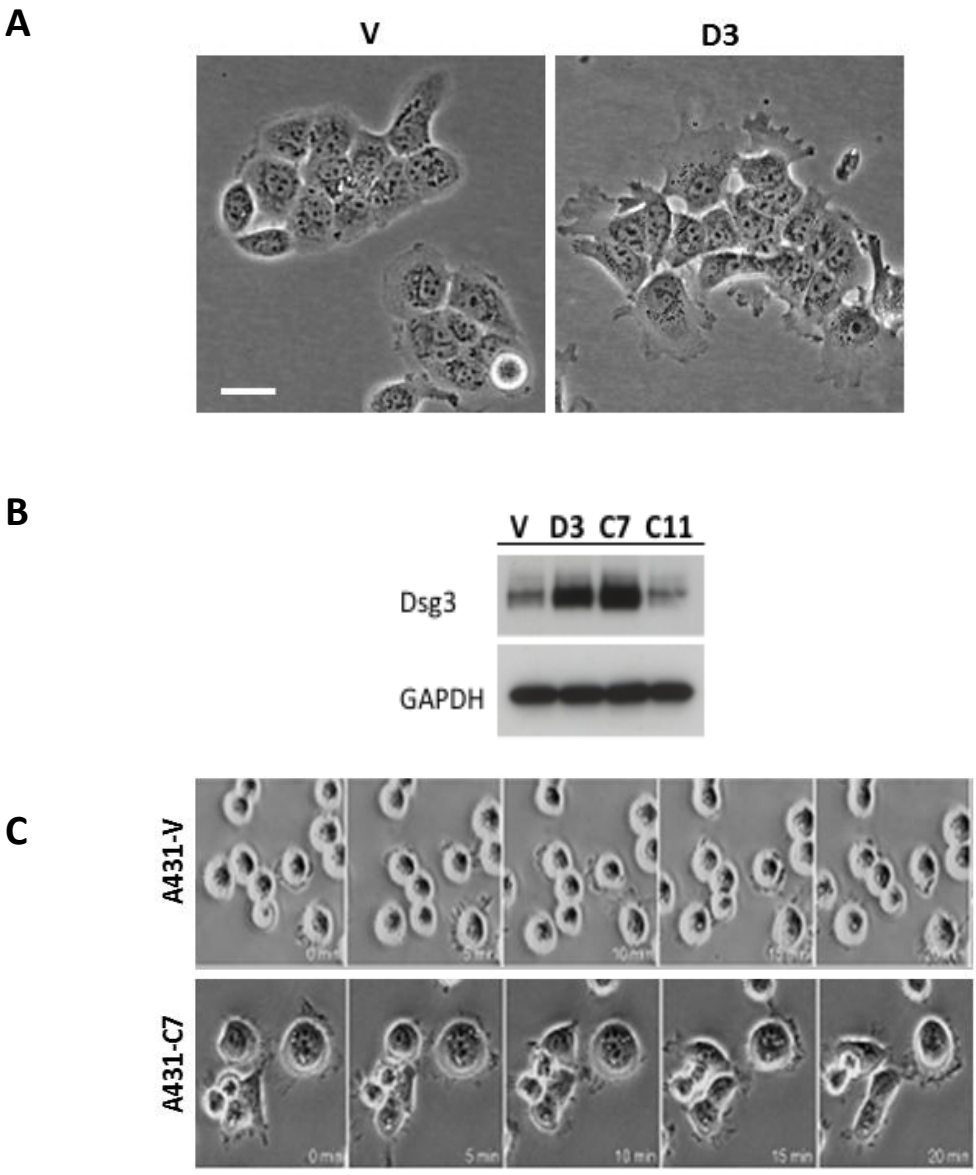

Figure 34: Overexpression of Dsg3 enhances membrane protrusions in A431-C7 cells.

A) The representative phase contrast images of A431-V and -D3 cells in the uncoated culture dish. B) Western blot analysis of Dsg3 protein levels in A431 cells with GAPDH as the loading control. C) The representative time-lapse video stills of A431-V and -C7 cells at 5 minutes interval (video courtesy of Wan H) (Tsang et al, 2012a). Cells were seeded in a dish 3 hours before time-lapse video microscopy.

Based on these observations, there appeared to be a direct positive relationship between the levels of Dsg3 protein and the formation of membrane protrusions, speculating that Dsg3 might exert a role in the regulation of actin organisation and dynamics. To address this question, the photoconvertible probe EosFP-actin, which switches from green (488 nm) to red emission (543 nm) upon photoconversion was used in the following experiment. By photoconverting a small region of actin, it is possible to analyse the actin turnover and trafficking of the photoconverted actin (Burnette et al, 2011). A431-V and -D3 cells were transiently transfected with the photoconvertible probe EosFP-actin and the effect of Dsg3 on the actin dynamics was analysed using a spinning disk confocal microscope.

At 48 hours post-transfection, cells were seeded onto the glass-bottom cell culture dishes in a low calcium medium (EpiLife) for 1 hour prior to photoconversion. Four to five different regions near the edge of cells expressing EosFP-actin were photoconverted and the dynamics for each region was followed by collecting an image every 10 sec for 10 minutes. The results were then combined to account for inherent variability in actin dynamics. As shown in Figure 35, quantitative analysis of the fluorescence intensity of actin in the photoconverted regions shows that A431-D3 cells exhibited a significantly faster turnover of actin as compared with A431-V control cells ($P < 0.001$, Figure 36A-C). In addition, the stress fibres were observed to be less stable (Figure 36A) and reduced immobile fraction of actin was noted in Dsg3 overexpressing cells as compared with A431-V cells ($p=0.05$, Figure 36D). Taken together, my results suggest that overexpression of Dsg3 causes the actin cytoskeleton to be more dynamic near the edges of cells.

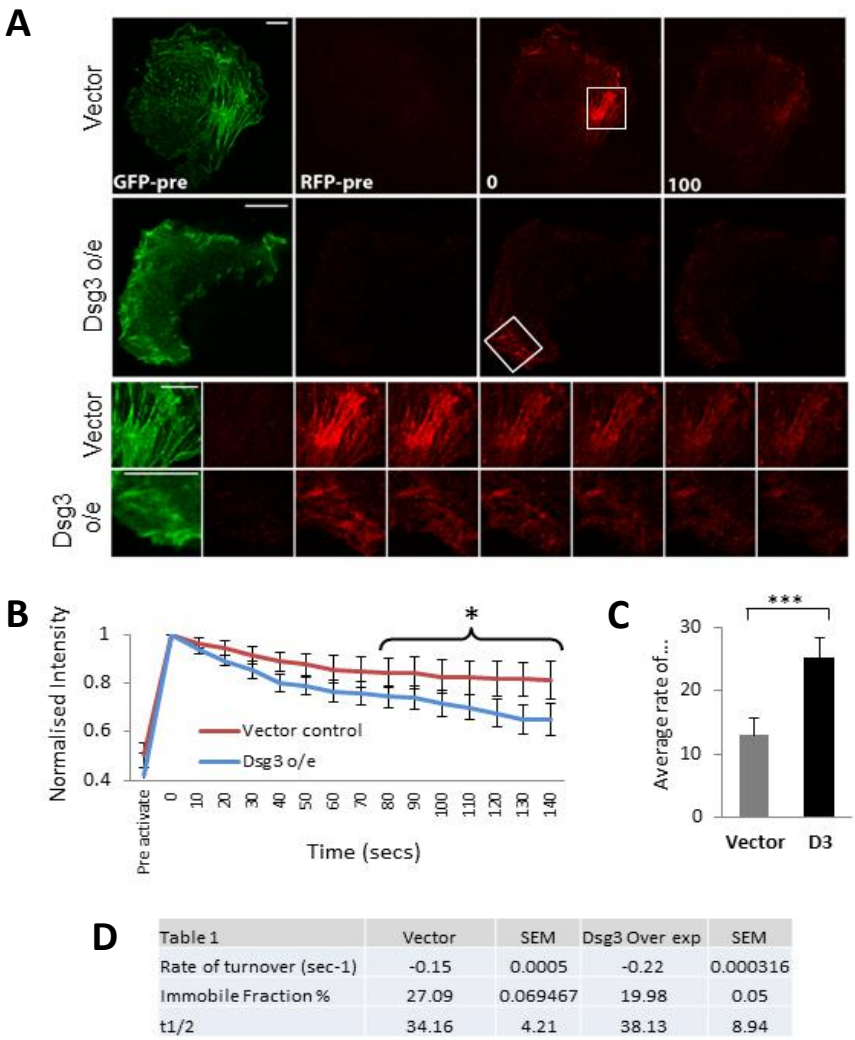

D

Table 1	Vector	SEM	Dsg3 Over exp	SEM
Rate of turnover (sec-1)	-0.15	0.0005	-0.22	0.000316
Immobile Fraction %	27.09	0.069467	19.98	0.05
t1/2	34.16	4.21	38.13	8.94

Figure 35: Overexpression of Dsg3 enhances actin turnover in A431 cells.

A) Confocal time-lapse series of A431 cells transfected with Eos-FP Actin. Images were acquired using 488 and 543nm laser lines showing the GFP and RFP species of actin. Images were acquired over a 3 minute duration, seconds after photo-conversion. Time-lapse frame rate was 1 image every 10 sec. Boxes show the region of interest (ROI) after being photoconverted. B) Graph shows quantification of actin dynamics in A431-V and -C7 cells following photoconversion of Eos-FP Actin from GFP to RFP over time. The intensity profiles for each ROI were normalised and the mean percentage recovery was measured. C) Graph shows quantification of the rate of actin turnover following photoconversion of a small region of Eos-FP actin. D) Summary table of results (courtesy of Wheeler A). Data were pooled of 20 ROI from 4 independent experiments (*P<0.05, ***P<0.001 using Students *t*-test). Scale bars, 5µM.

7.1.4 Dsg3 activates Rac1 and Cdc42 GTPases

It is known that overexpression or up-regulation of Rac1 and Cdc42 are associated with increased membrane protrusions and filopodia/microspike formation (Ridley, 2006), implying that Dsg3 may be involved in regulating these small GTPases. To determine whether overexpression of Dsg3 altered Rac or Cdc42 activity, a series of pull down experiments of the Rac1/Cdc42 activation assay were carried out (Refer to Materials and Methods Chapter 3.7.3.1). The CRIB domain of Pak-PBD fused with GST was used as the baits to selectively pull down the active GTP-bound form of Rac1 and Cdc42 from A431-V and-D3 cells and Western blotted for Cdc42 and Rac1.

In Figure 36A, the GST Pak-PBD pull down experiment shows that overexpression of Dsg3 significantly enhanced the active Rac1 and Cdc42 GTP levels as compared with A431-V control cells. No binding was observed in the GST alone and hence, rules out the possibility of non-specific binding. For input, the Western blots of total cell lysates show no difference in the total protein levels of Rac1 and Cdc42. In parallel, RhoA pull down was performed using the GST fused Rhotekin-PBD. Figure 36B shows that overexpression of Dsg3 also enhanced the active RhoA GTP levels, but to a lesser extent as compared to Rac1 and Cdc42. The Western blots of the total cell lysate show a small reduction of RhoA in A431-D3 cells. These findings suggest that Dsg3 might be involved in the regulation of Rho GTPase signalling pathways that control the actin-based junction formation, maintenance of cell shape and the epithelial morphogenesis.

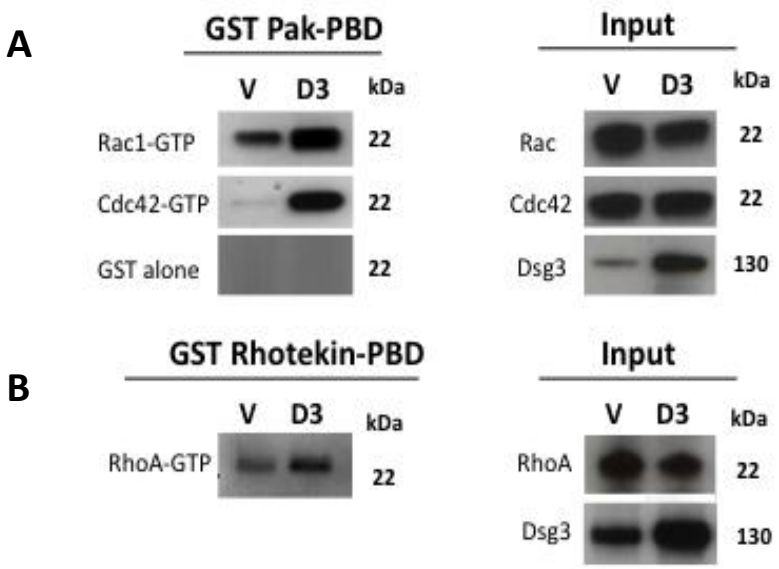

Figure 36: Overexpression of Dsg3 significantly enhances the active Rac1 and Cdc42 GTP levels.

Western blots of GST Pak- or Rhotekin-PBD pull down and total lysates of A431 cells. A431 cells were grown to freshly confluence, subjected to RIPA buffer extraction and 500 μg of the resulting protein lysates were used. A) The CRIB domain of Pak-PBD or B) Rhotekin-PBD fused with GST was used to pull down the active GTP-bound A) Rac1 and Cdc42 or B) RhoA from A431-V and -D3 cells. SDS sample buffer was used to elute the GTP-bound Rac1 and Cdc42/RhoA and their associated proteins. Twenty microliters (μl) of the protein lysates were loaded and Western blotted for Rac1, Cdc42 and RhoA. For input, 20μg of protein lysates were loaded in each lane and Western blotted for the indicated proteins. Three experiments (A) and two experiments (B) were performed and similar reproducible results were obtained.

To test whether Rac1 activation was required for the Dsg3-induced membrane activity, the A431 cells were treated with the Rac1 inhibitor, NSC23766, prior to spinning disk confocal microscopy. A431-V and -C7 cells were treated with or without 30μM Rac1 inhibitor for 6 hours before being transferred onto the glass-bottom culture dishes in a low calcium medium (EpiLife). Thirty minutes later, 1μM of carboxyfluorescein diacetate, succinimidyl ester (CFSE), which was used to label the cell membrane, was added into the medium prior to live cell imaging. Time-lapse series was collected every 10 sec for 3 minutes. Three to four different active regions per cell near the edge of cell were selected and data were pooled from 24 ROI in each cell type. The image data were analysed using kymograph in MetaMorph software.

Figure 37A shows the representative time-lapse video images of A431-V and -C7 cells prior to the addition of Rac1 inhibitor. The membrane protrusions were significantly enhanced in A431-C7 cells, whereas the plasma membrane of A431-V cells was relatively less active ($P< 0.01$). In addition, A431-C7 cells appeared to be larger and more spread out in proportion to the cell body size as compared with A431-V control cells. The addition of Rac1 inhibitor strongly affected the cell morphology of A431-D3 cells by reducing the average protrusion velocity to the baseline levels similar to that of A431-V cells treated with the Rac1 inhibitor (data not shown). It was also noted that the Rac1-inhibited cells were less spread out and smaller as compared with the untreated cells, suggesting that Rac1 activation is important in the Dsg3-induced protrusive membrane dynamics in A431 cells. The bar chart in Figure 37B shows the average protrusion velocity of A431-V and D3 cells with or without the drug treatment.

The observed Dsg3-dependent membrane protrusions are the morphological aspects of cell migration (Navarro et al, 2004) and hence, I sought to determine if the Dsg3-induced cell protrusions were associated with the enhancement of cell migration. To test this, A431 cells were treated with or without the Rac1 inhibitor NSC23766 (same as above) and the effect of Dsg3 on cell migration was filmed using a time-lapse microscopy for a duration of

18 hours. A time-lapse series was collected every 5 minutes and the cell speed was quantified by tracking an individual cell over the sequence of time-lapse digital images. However, only the first 3 hours of the time-lapse series were analysed since cells die after 3 hours of imaging.

As shown in Figure 38, no obvious change in the cell migration was observed in A431-V and -D3 cells within the 3 hours time frame. The bar chart shows the combined results of 80 cells from three independent experiments for each condition. Interestingly, it was noted that overexpression of Dsg3 enhanced cell motility initially in the presence of Rac1 inhibitor, NSC23766, but this phenomenon disappeared later due to cell death, which occurred after a 3 hour period of drug treatment. However, cell death was not observed in A431-V cells with NSC23766, which remained viable and grew normally. Further experimental investigations are needed in order to draw conclusions. These data suggest that the regulation of Dsg3 and Rac1 could play a role in apoptosis and cell survival.

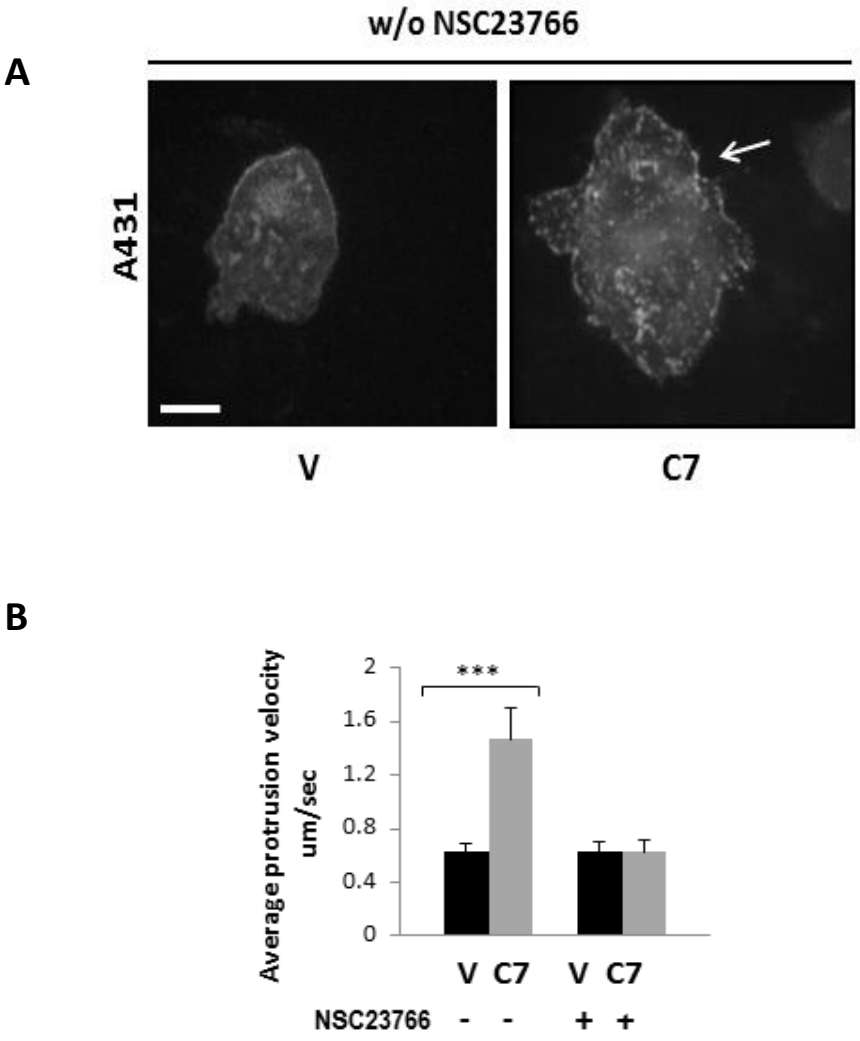

Figure 37: Overexpression of Dsg3 enhances the average protrusion velocity.

A431 cells were treated with or without the Rac1 inhibitor, NSC23766, at the concentration of 30µM and labeled with 1µM of carboxyfluorescein diacetate, succinimidyl ester (CFSE). Time-lapse series was collected every 10 sec for 3 minutes. A) The representative time-lapse video images of A431-V and -C7 cells without NSC23766. B) Bar chart shows the average protrusion velocity of A431-V and -C7 cells in Figure 37A. Velocity measurements were obtained from kymograph analysis of the cell membrane. The total number of cell edges analysed per condition is >24 (***p< 0.001).

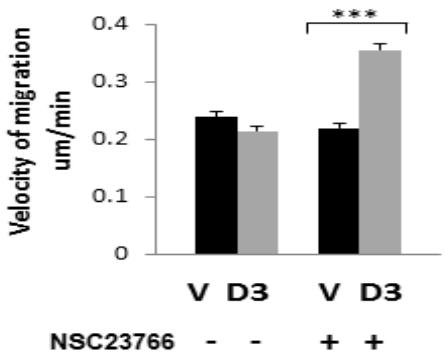

Figure 38: **Overexpression of Dsg3 enhanced cell motility initially in the presence of Rac1 inhibitor, NSC23766, but this phenomenon was disappeared later.**

Bar chart shows the average velocity of cell migration in A431-V and -D3 cells treated with or without Rac1 inhibitor. Time-lapse series of 18 hours duration were acquired at every 5 minutes intervals. Data were collected from the first 3 hours of migration due to cell death in A431-D3 cells treated with NSC23766 inhibitor. Data were pooled from three independent experiments (n=80, mean ± SEM, ***p< 0.001).

7.1.5 Rac1 activation is required for Dsg3/actin interaction and colocalisation

My result showed that Rac1 activity is enhanced in Dsg3 overexpressed A431 cells, raising the possibility that Rac1 might be involved in the interaction between Dsg3 and actin. To address this question, the effect of Rac1 mutants and Rac1 inhibitor on Dsg3/actin association and colocalisation were investigated. Co-immunoprecipiation with rabbit anti-actin antibody was performed in HaCaT cells pre-treated with either the dominantly negative N17Rac1 mutant or the Rac1 NSC23766 inhibitor. As demonstrated in Figure 39, transient expression of the dominantly negative N17Rac1 mutant, which suppresses the activity of cellular Rho GTPases, greatly reduced the association between Dsg3 and actin. In parallel, titrating the dose of the Rac1 inhibitor NSC23766 at the concentration of 30-50μM for 6 hours shows dose-dependent inhibition of Dsg3 and actin association. These results suggest that Rac1 activity is involved in the Dsg3-actin complex formation.

To validate this findings, A431 cloned cells expressing high (C7) or low (C11) levels of Dsg3 protein were pre-treated with either the Rac1 mutant or the Rac1 inhibitor prior to immunostaining for anti-Dsg3 antibody, 5H10 and the secondary conjugated antibody (Alexa Fluor 568) (red) along with A488 conjugated phalloidin (green). The percentage of colocalisation, which highlighted in white was quantified by ImageJ. In Figure 40, the representative immunofluorescence images show that the colocalisation between Dsg3 and F-actin was greatly reduced in cell expressing the N17Rac1 mutant or treated with the NSC23766 inhibitor ($n=6$, $p<0.001$), demonstrating that the colocalisation Dsg3 and actin is dependent on Rac activity. Taken together, both biochemical and immunostaining analysis suggest that Dsg3, Rac1 and actin are components of a novel signalling complex that might be associated with the actin-based motility and morphogensis.

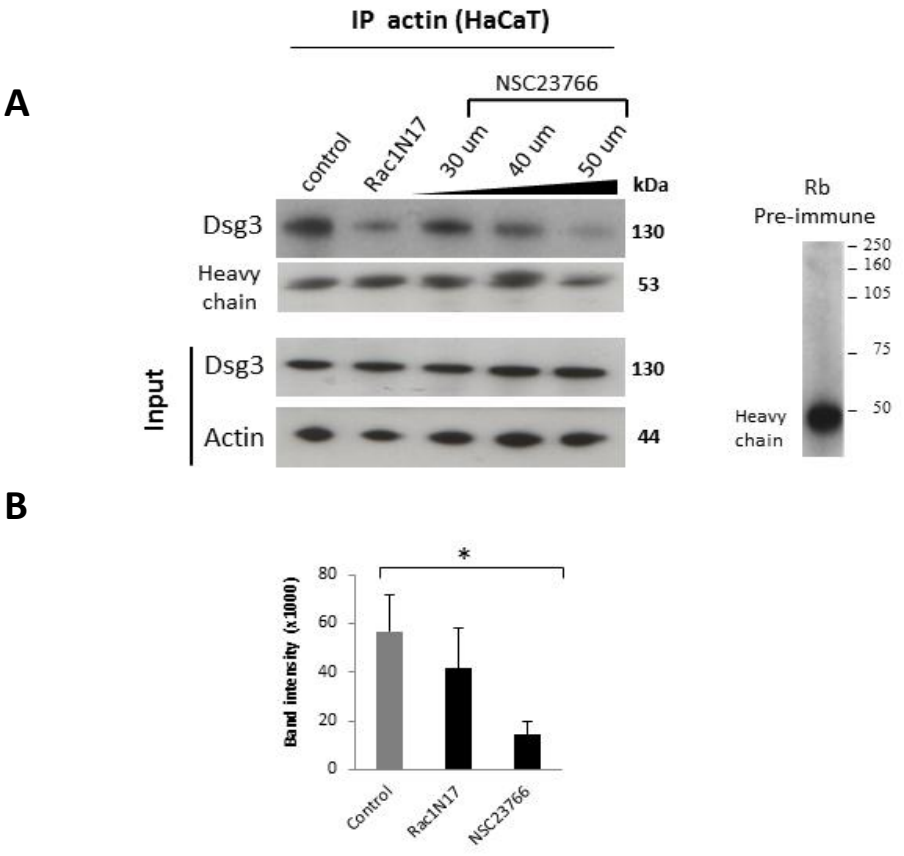

Figure 39: Rac1 activation is required for the association between Dsg3 and actin.

Western blots of actin immunoprecipiates and total lysates of HaCaT cells with or without treatment. HaCaT cells with either the expression of Rac1 dominant negative mutant (N17Rac1) or treated with the Rac1-specific inhibitor (NSC23766, 30-50µM, 6 hours) were extracted with RIPA buffer containing 1% NP-40. Five hundred micrograms (µg) of the resulting protein lysates were subjected to co-immunoprecipation with rabbit anti-actin antibody and Western blotted for Dsg3, actin and heavy chain. Pre-immune rabbit serum was used as the negative control. For input, 10µg of protein lysates were loaded in each lane and Western blotted for the indicated proteins. The representative Western blots were obtained from three independent experiments and similar reproducible results were obtained. B) The bar chart shows the average band densitometry of the association between Dsg3/actin obtained from three independent experiments (mean ± SEM, *P=0.03).

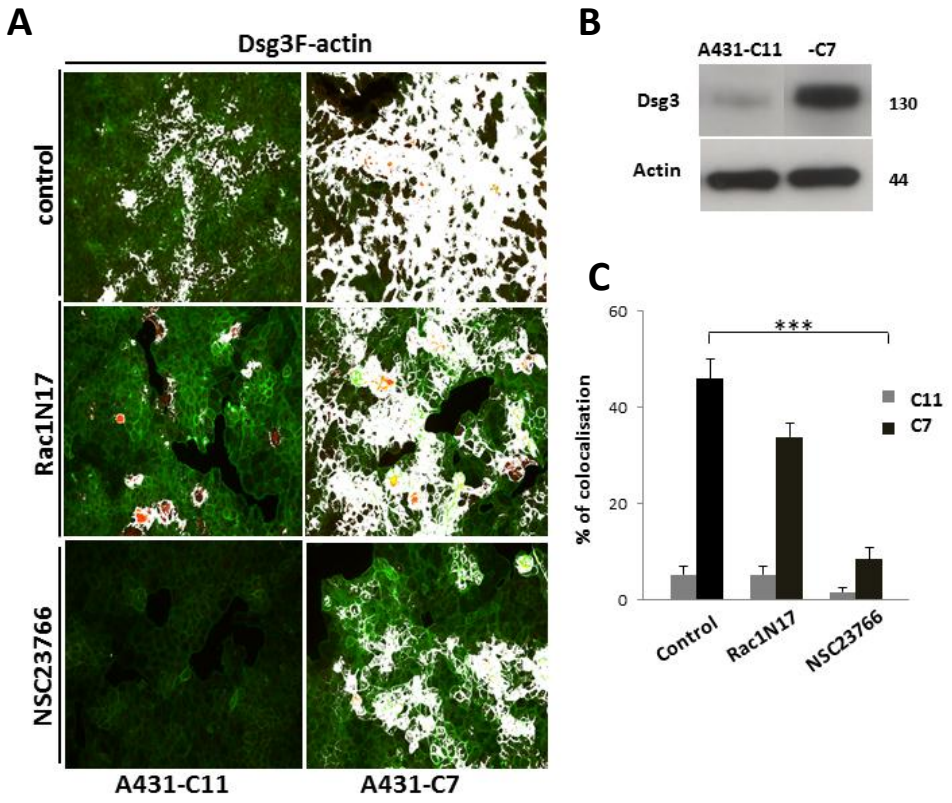

Figure 40: Rac1 activation is required for the colocalisation between Dsg3 and actin.

The representative immunofluorescence images of A431 cloned cells. A431-C11 and -C7 cells were pre-treated with either the N17Rac1 or NSC23766 (30µM) and co-stained with anti-Dsg3 antibody, 5H10 and the secondary conjugated antibody (Alexa Fluor 568) along with A488 conjugated phalloidin. Six arbitrary images in each coverslip were acquired. The colocalisation index, which highlighted in white was measured by ImageJ. B) Western blot of A431 cloned cells with actin as the loading control. Ten micrograms (µg) of protein lysates were loaded in each lane. C) The bar chart shows the average Dsg3/actin colocalisation obtained from two independent experiments (mean ± SEM, ***p<0.001).

7.2 Discussion

7.2.1 Role of Dsg3 in the regulation of actin cytoskeleton

We showed that the endogenous Dsg3 was partially colocalised with actin at cell periphery (Figure 31). Such colocalisation was affected by both overexpression and knockdown of Dsg3 (Figure 32), suggesting that the degree of colocalisation was dependent upon the levels of Dsg3 protein. It is acknowledged that the immunostaining in Figure 32 and Figure 39 were not carried out in freshly confluent cell culture like the Src signalling experiments in Chapter 6. However, we found that the interaction between Dsg3 and actin was consistently detected by both immunostaining and Western blot analysis. In addition, the levels of actin protein were not affected by calcium or cell confluence (Internal communication) and hence we believe that the effect of cell confluence would not be of any significance.

We further confirmed the Dsg3/actin association by co-immunoprecipitation, which showed that Dsg3 and actin could be immunoprecipitated as a complex in HaCaT cells as well as in human breast skin samples (Figure 33). The biological relevance of such interaction was supported by the observation that the junctional actin is severely affected in *pemphigus vulgaris,* where PV-IgG target Dsg3 and cause its depletion from the desmosomes. One may concern that the Dsg3/actin association could be a non-physiological event especially with the abundant proteins such as actin. However, this finding is further supported by other evidence obtained from the mass spectrometry studies, which showed that actin is indeed bound to the Dsg3 cytoplasmic tail (internal communication). Other experiment such as the GST pull down assays can be used to confirm the Dsg3 and actin interaction.

Next, Rac1 inhibition was carried out prior to immunostaining and co-immunoprecipitation to address whether Rac is important in the Dsg3/actin interaction. I showed that the Dsg3 and actin association was reduced by both Rac1 dominantly negative mutant, N17Rac1 and Rac1 specific inhibitor, NSC23766 in a dose-dependent manner (Figure 38). It is believe that the

reduced Dsg3/actin association was not related to the off-target effect of the Rac inhibition. It was established that NSC23766 is effective in inhibiting the Rac activation without interfering with Cdc42 or Rho and their respective GEFs (Gao et al, 2004). Additionally, its specificity has been validated by Rac silencing and Rac knock-out experiments in more than 90 scientific studies (Dwivedi et al, 2010). It is acknowleged that inhibition of Rac could remove cadherin complexes from junctions and have a negative impact on the actin cytoskeleton (Braga et al, 1997). However, the Western blot analysis of input showed that the protein levels of actin or Dsg3 were not affected by both treatments (Figure 38). Further investigation is needed to confirm this issue since it is known that the regulation of cadherin function by the small GTPases could be ascribed to cell type specificity.

A similar inhibitory effect with reduced colocalisation between Dsg3 and actin was observed following the Rac1 inhibition (Figure 39). The colocalisation index was quantified by ImageJ. We ruled out any false positive results contributed by bleed-through of fluorescence emission in the colocalisation analysis. The bleed-through artefact is unlikely to be an issue as each channel was acquired sequentially and no signal was detected when we tested the Alexa Fluor 488 fluorescence using the Alexa Fluor 568 detection channel and vice versa.

We further speculate that Dsg3 might exert a role in the regulation of the actin cytoskeleton via Rho GTPases. The PAK-GST pull down experiments revealed that overexpression of Dsg3 significantly enhanced the levels of GTP bound-Rac1 and -Cdc42 (Figure 36). This result was confirmed by the pull down of GST alone, a critical control, which rule out the possibility of non-specificity. The notion that Dsg3 regulates the actin dynamics is further corroborated by the fact that overexpression of Dsg3 considerably increased the rate of actin turnover. While the ability of active Rac1 and Cdc42 to produce enhanced membrane protrusions and ruffling has been well described previously (Ridley, 2006; Rudini & Dejana, 2008), the upstream signal regulators activating Rac1/Cdc42 during the process of cell-cell

adhesion is less studied. Other evidence suggests that both protein kinase C and the Rac exchange factor, Tiam-1 are acting upstream of Rac (Kovacs et al, 2002a). Our results indicate that Dsg3 is another potential candidate as the activator of Rac1/Cdc42 in cell adhesion, cell polarisation and dynamic morphogenesis. In the same set of experiments, a slight increase in the levels of RhoA GTP levels was detected in A431-D3 cells as compared to control cells. However, changes in the active RhoA levels between A431-V and D3 cells were not as significant as compared with Cdc42 and Rac1, and thus not investigated further in the present study.

A limiting dilution assay and clonal expansion were carried out to ensure a more homogeneous phenotype of A431-D3 cells. We believe that A431-C7, the clone with the highest levels of Dsg3 protein, will give a more homogeneous phenotype and hence, was used in the time-lapse microscopy instead of A431-D3 cells (Figure 34). It is acknowledged that the use of A431-C7 and -D3 cells interchangeably in different experiments are not ideal as this could affect the reliability of my results. The time-lapse video images of A431-V and -C7 cells showed that the membrane protrusions were significantly enhanced in A431-C7 cells as compared with A431-V control cells (Figure 37A). The addition of Rac1 inhibitor strongly affected the cell morphology of A431-D3 cells and reduced the average protrusion velocity to the baseline levels similar to that of A431-V cells treated with the Rac1 inhibitor. These findings suggest that Rac1 activation is likely required for the Dsg3-induced membrane activity. Unfortunately, this data was not shown due to corrupted files. The involvement of Cdc42 was not tested in the above experiments due to time limitation.

It is intriguing that overexpression of Dsg3 enhanced cell motility initially in the presence of Rac1 inhibitor, NSC23766, but this phenomenon disappeared later due to cell death that occurred after 3 hours of drug treatment (Figure 38). It is still unclear the molecular mechanism underlying this phenomenon, perhaps it is associated with cell apoptosis and survival and cell-cell/matrix adhesion mediated by Rac1. In this experiment, A431 cells were seeded

sparsely prior to the live cell microscopy and examined the individual cell migration by manual tracking of the cell over the sequence of time-lapse digital images. We anticipated that this analysis of A431-V and D3 cells would show differences in cell migration as the other method using the scratch wounding assay has shown enhanced cell migration in Dsg3 overexpressed A431 cells (Tsang et al, 2010).

The only difference between these two experiments was the cell density in which confluent culture was used in the scratch wounding assay, while sparse culture was used in the migration assay (Figure 38). We believe that cell death is unlikely caused by the cytotoxic effect of Rac1 inhibition as the concentrations of NSC23766 used in this study are similar to the concentrations used by others (Akunuru et al, 2012; Mitchell et al, 2008; Xu et al, 2009) and A431-V cells with NSC23766 remained viable throughout the duration of the experiment (18 hours). However, we cannot rule out the possibility that overexpression of Dsg3 in sparse culture might make cells more sensitive to the Rac inhibition-mediated apoptosis. This remains an interesting avenue of investigation in the future.

7.2.2 Future work

Further studies such as a GST pull-down assay can be use to confirm the existence of Dsg3 and actin interaction. The additional loss of function approach such as repeating the co-immunoprecipitation (Figure 33) in the Dsg3 knockdown cells or the use of reverse co-immunoprecipitation with actin and Western blot for Dsg3 will help to improve the reliablity of the results. Similarly, adjusting the washing stringency using a higher stringency buffer may help to reduce non-specific binding. It is noted that the Dsg3/actin colocalisation was not carried out in freshly confluent cell culture (Figure 32). It will be useful to evaluate the effect of cell density on the Dsg3/actin interaction and standardise the degree of cell confluence in each set of experiments. We demonstrated that Rac is important in the Dsg3/actin

association. To confirm the specificity of Rac1 inhibition (Figure 38 and 39), additional immunostaining experiments are needed to examine whether the inhibition of Rac could disrupt the localisation of E-cadherin in our cell system. Additionally, siRNA-mediated knockdown of Rac-1 prior to co-immunoprecipitation can be carried out and we would expect to get similar result with reduced Dsg3/actin association as observed in Figure 38.

We believe that A431-C7, the clone with the highest levels of Dsg3 protein, will give a more homogeneous phenotype in the time-lapse microscopy (Figure 34). Further characterisation on the protein levels of E-cadherin and Src will help to ensure that the A431-C7 sub-cloned cells remain similar (same basic phenotypes) to that of the parental A431-D3 cells. We hypothesised that the molecular mechanism underlying Dsg3-induced cell death in the presence of Rac1 inhibitor is associated with cell survival and cell-cell/matrix adhesion mediated by Rac1 (Figure 37). This experiment can be repeated with lower concentrations of the Rac1 inhibitor to rule out the possibility that cell death was induced by the cytotoxic effect of Rac1 inhibition. This will also help to determine if overexpression of Dsg3 in sparse culture would make cells more sensitive to Rac-mediated apoptosis. Alternatively, the scratch wounding assay can be used to examine cell migration in the presence or absent of Rac1 inhibitor.

7.2.3 Summary

Owing to the nature of protein abundant such as actin, I was unable to make a conclusion of the physiological interaction between Dsg3 and actin. However, my results suggested that Dsg3 colocalised and interacted with actin in a Rac1-dependent manner. In addition, overexpression of Dsg3 caused an overall increase in Rac1- and Cdc42-GTP activities, resulting in pronounced membrane protrusions and enhanced rate of actin turnover. The relationship between Dsg3 and Cdc42 or Rac1 activation is still only marginally analysed. We believe that this novel Dsg3-Rac1/Cdc42-actin pathway is essential for the

process of E-cadherin junctional assembly, cell polarisation and morphogenesis.

CHAPTER 8

FINAL DISCUSSION

8.1 Cross-talk between Dsg3 and E-cadherin as well as the actin cytoskeleton

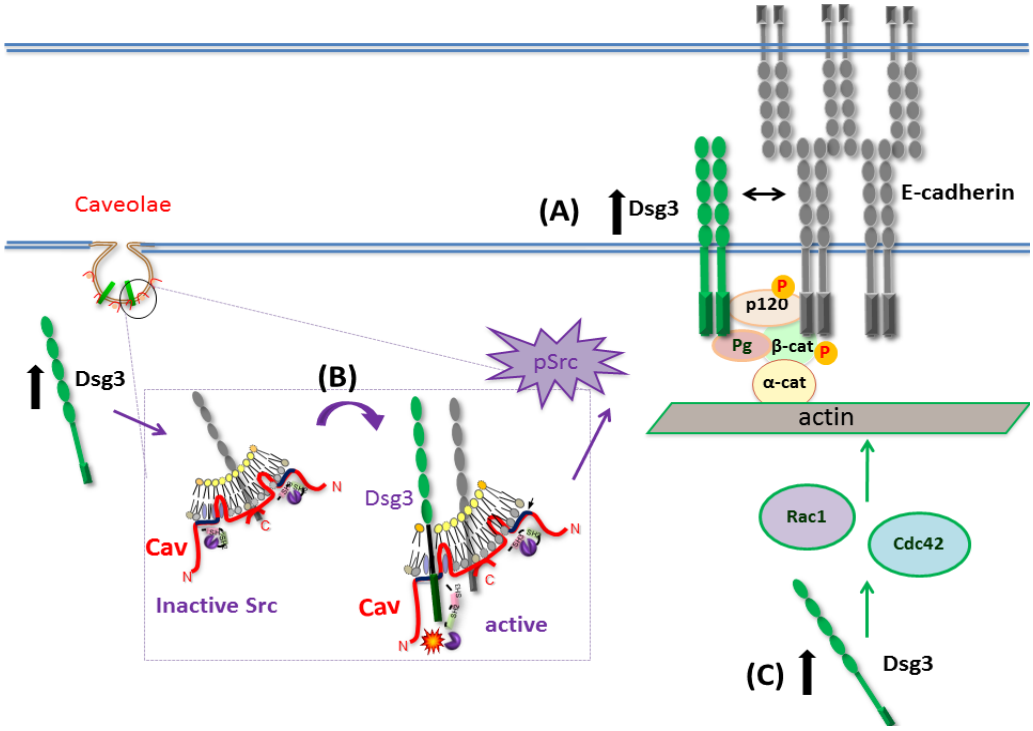

Figure 41: A schematic diagram of my working model.

A) The association between Dsg3 and E-cadherin enhances in a calcium-dependent manner and most likely involves both P120 and plakoglobin. B) Dsg3 might compete with Src for a potential binding site on the scaffold domain of caveolin-1 protein (Couet et al, 1997). Subsequently, Src is released from or loss its binding capacity with the caveolin-1 complex upon activation, allowing Src to associate preferentially with the E-cadherin/catenins complex and engages in E-cadherin-Src signalling. C) Dsg3 is also involved in the dynamic reorganisation of actin via Rho GTPases.

The aim of this study was to investigate the association between Dsg3 and E-cadherin or actin and determine whether these interactions have any functional influence on E-cadherin-mediated adherens junction formation, which in turn contributes to epithelial differentiation programs and tissue

morphogenesis. My study so far suggests that Dsg3 is capable of physically associating with E-cadherin or actin and functionally engages in the E-cadherin-mediated adherens junction formation and the reorganisation of actin cytoskeleton through mechanisms involving the activation of Src and Rho GTPases signalling pathways. The summary of my findings is shown in Figure 41.

Using both immunofluorescence and biochemical approaches, I demonstrated that Dsg3 and E-cadherin colocalised and associated with each other in keratinocytes of both cultured cell lines and human breast skin samples. I further demonstrated that this complex formation is dependent on the extracellular calcium and gradually enhanced in a time-dependent manner upon calcium induction of cell-cell contacts and junction formation in differentiating keratinocytes. Owing to the technical limitation of biochemical analysis, I cannot rule out the possibility that the Dsg3/E-cadherin association also existed in non-ionic detergent insoluble fraction that is associated with the intermediate filaments. However, we have evidence suggesting that the majority of the Dsg3/E-cadherin interaction was present outside of the intercellular junctions, i.e. in the Triton soluble fraction of epithelial cells.

The interactions between desmosomal and adherens junctional proteins have been reported in other tissues such as the intercalated discs of cardiac muscle (Borrmann et al, 2006), their biological significance remains unclear. To explore the physiological relevance of the Dsg3 and E-cadherin interaction in keratinocytes, a number of biochemical analysis were performed. We established our loss of function analysis in normal HaCaT keratinocytes, a spontaneously immortalised keratinocyte line-derived from human skin. My results indicated that knockdown of Dsg3 in HaCaT cells 1) caused reduction in the levels of the majority of desmosomal proteins; 2) resulted in retardation of E-cadherin recruitment to cell surface at early stages of calcium-induced cell-cell contacts and intercellular junction formation; and 3) had a negative impact on E-cadherin/Src signalling pathway with a consequence of reduction

in the phospho-tyrosine levels of the downstream adherens junctional proteins.

We observed that knockdown of Dsg3 in HaCaT cells caused substantial reduction in the levels of the majority of the desmosomal proteins (Figure 20). We believe that this effect could not be solely attributed by the reduction of the Dsg3 protein, but rather by the secondary events of Dsg3 depletion on the protein levels and/or distribution of plakoglobin and E-cadherin. It was suggested that plakoglobin and E-cadherin are required to direct the initiation and organisation of desmosome formation (Gosavi et al, 2011). Hence, it is likely that knockdown of Dsg3 affects the amount of plakoglobin and E-cadherin at the plasma membrane and this in turn prevents proper recruitment of desmosomal components into the junctions. This consequently changes the homeostasis of desmosomes and leads to elevated protein degradation and reduced levels of desmosomal proteins as observed by Western blot analysis (Figure 20). In this thesis, I did not address the effect of Dsg3 depletion on cell-cell adhesion strength. However, the results of the hanging drop and fragmentation assays obtained by other colleagues showed that weakening of cell-cell adhesion strength in epithelial cells with Dsg3 knockdown, suggesting that Dsg3 indeed plays a positive role in the maintenance of strong cell-cell adhesion (Mannan et al, 2011).

Although knockdown of Dsg3 did not affect the overall levels of E-cadherin protein (Figure 20), it caused delay or retardation of the E-cadherin recruitment at the cell-cell contacts during the process of calcium-induced junction assembly (Figure 23). We speculate that the molecular mechanism underlying the retardation of E-cadherin recruitment could be due to downregulation of Src signalling, which reduced the tyrosine phosphorylation of the adherens junctional proteins (Figure 28). As mentioned earlier in my introduction, Src-mediated tyrosine phosphorylation of the adherens junction proteins has a positive role in the regulation of cell-cell adhesion. For instance, inhibition of tyrosine kinase suppresses tyrosine phosphorylation of the

adherens junctional proteins and causes a significant reduction in adhesive strength of differentiating keratinocytes (Calautti et al, 1998). This is consistent with another study, which demonstrated that the decreased levels of tyrosine phosphorylation of E-cadherin cause its diffuse cytoplasmic distribution, resulting in a loss of functionality of the E-cadherin-catenin complex (Nawrocki et al, 1998). It is therefore attractive to postulate that knockdown of Dsg3 reduces the tyrosine phosphorylation of adherens junctional proteins and in turn affects the establishment of E-cadherin-mediated cell-cell contacts and junction formation in epithelial cells.

Alternatively, other proteins such as caveolin and p120 might play a role in the redistribution of E-cadherin in Dsg3 knockdown cells. Simultaneous expression of caveolin-1 and E-cadherin has been reported to be essential for the organisation and stability of adherens junctions. It was showed that knockdown of Cav-1 results in a fainter and discontinuous membrane staining of E-cadherin with a concomitant increase of its intracellular distribution (Miotti et al, 2005). In our study, we showed that overexpression of Dsg3 enhanced its colocalisation with caveolin-1 at the plasma membrane and proposed that such interaction is likely involved in the E-cadherin/Src signalling pathway (Figure 41B). Thus, it is likely that knockdown of Dsg3 could affect the Cav-1 distribution at the plasma membrane, and in turn impairs Src signalling and the E-cadherin-mediated junction formation.

It was shown that p120 is involved in stabilising the E-cadherin complexes when bound to the cell membrane (Anastasiadis & Reynolds, 2001). In the absence of E-cadherin, p120 is believed to accumulate in the cytoplasm and this characteristic is potentially relevant to the loss of E-cadherin in Dsg3-deficient cells. My results suggested that p120 might be involved in the complex formation between Dsg3 and E-cadherin (Figure 41A) and hence, we anticipate that p120 may accumulate in the cytoplasm in Dsg3-deficient cells and potentially affects E-cadherin recruitment to the cell surface. However, this possibility requires further experimental support as knockdown of Dsg3 did not affect the levels of P120 protein in HaCaT cells (Figure 18).

Aberrant levels of Dsg3 protein have been associated with tumourigenesis and metastasis (Chen et al, 2007; Teh et al, 2011), but its function during cancer progression has not been well investigated. We established our gain of function analysis in A431 cells and examined the effect of Dsg3 overexpression on the protein level of E-cadherin and its associated junction formation. It was tested that overexpression of Dsg3 in A431 cells, which express low levels of endogenous Dsg3 protein, was several folds higher than the A431-V control cells (Tsang et al, 2010). Our results showed that overexpression of Dsg3 in A431 reduced the levels of both adherens junctional and desmosomal proteins, suggesting that the cell-cell adhesion in Dsg3 overexpressed A431 cells is likely compromised. In addition, overexpression of Dsg3 also increased the tyrosine phosphorylation of adherens junctional proteins with enhanced levels of membrane protrusions, a similar phenotype to cells with aberrantly increased Src activation. These findings are consistent with others, which demonstrated that increased tyrosine phosphorylation of β-catenin, plakoglobin and p120 are correlated to the reduced cell-cell adhesion upon neoplastic transformation (Irby & Yeatman, 2000).

Based on these results, overexpression of Dsg3 appears to “hijack” the E-cadherin/Src signalling in A431 cells, and in turn has a negative impact on cadherin function, including cell-cell adhesion and junction stability. Thus, we speculate that overexpression of Dsg3 could have a negative regulatory influence on Src signalling, which in turn affects the assembly of E-cadherin in A431 cancer cell line. The Src-specific inhibitor PP2 has been reported to restore the E-cadherin/catenin adhesion system in human cancer cell lines (Nam et al, 2002). This is in agreement with my results, in which treating the A431-D3 cells with the Src-specific inhibitor PP2 was able to restore the reduced levels of E-cadherin protein as compared to control cells. It is therefore likely that Src inhibition is able to restore the negative impact of Src signalling in Dsg3 overexpressed A431 cells.

Taken together, my results agree with the notion proposed by McLachlan et al that a critical control of Src signalling is required for normal function of E-cadherin adhesion and stability i.e both up- and down-regulation of the Src signalling pathway could have a negative regulatory role on E-cadherin function (McLachlan et al, 2007) (Refer to Introduction Chapter 1). We believe that depletion of Dsg3 in normal HaCaT cells downregulates Src signalling and reduces the strength of tyrosine phosphorylation below the normal physiological levels and hence, contributes to its negative regulatory role. Overexpression of Dsg3 in tumour-derived A431 cells enhances this signalling pathway with abnormally high levels of tyrosine phosphorylation of adherens junction proteins and thus perturbing the cadherin-based adhesion.

In my A431 model, I also observed that overexpression of Dsg3 activated Rac1 and Cdc42 GTPases, resulting in pronounced membrane protrusions and enhanced rate of actin turnover. Other study demonstrated that the activation of Rac1 reduces the levels of E-cadherin at the cell surface, leading to internalisation of E-cadherin–catenin complexes and destabilisation of cell junctions in SCC12f keratinocytes. In agreement with this notion, we hypothesise that the enhanced levels of Rac1 GTPases (i.e activation) in response to Dsg3 overexpression might be correlated to the loss of E-cadhern protein and enhanced Src activation, all of which cooperatively contribute to destabilisation of cell junctions, enhanced membrane protrusions and cell migration (Tsang et al, 2012b). Taken together, we believe that the abnormally up-regulated Dsg3-Rac1/Cdc42 signalling is associated with reduced intercellular adhesion, an epithelial-mesenchymal transition-like phenotype in A431 cancer cells.

Numerous reports have demonstrated that Rac and other GTPases are required for the establishment of proper cadherin-mediated cell–cell adhesion and the reorganisation of actin cytoskeleton in normal keratinocytes. Using both immunofluorescence and biochemical approaches, I demonstrated that Dsg3 is capable of interacting with F-actin in HaCaT and human breast skin samples. This finding suggests a potential direct

participation of Dsg3 on actin remodeling at cell–cell contacts. However, I was unable to make a conclusion of the physiological interaction between Dsg3 and actin owing to the nature abundant of actin protein. Further studies such as the pull-down assay can be use to confirm the existence Dsg3 and actin interaction and identify the potential binding domain(s) involve. Additionally, I demonstrated that Rac is important in the Dsg3/actin interaction since reduction of this interaction was observed in cells treated with either Rac1 dominantly negative mutant, N17Rac1 or the Rac1 inhibitor, NSC23766. We speculate that Dsg3 might be involved in the local activation of GTPases at the plasma membrane that could contribute to actin accumulation and reorganisation necessary for cadherin adhesion in epithelial cells. Although it is known that these GTPases have both positively and negatively regulatory role on adherens junctions depending on cell context (Akhtar & Hotchin, 2001; Braga et al, 1997), we have yet to determine if the Dsg3-Rac1/Cdc42 signalling pathway participates in the assembly or the maintenance of cell-cell adhesion in normal keratinocytes.

Furthermore, the role of Cdc42 in A431 cancer cells and normal keratinocytes was not discussed in great details due to time limitation. Our initial results showed that the enhanced membrane protrusions were accompanied by changes in cell height (Tsang et al, 2012a). We believe that Dsg3 could exert its influence on cell polarity by modulating the downstream events of Cdc42 signalling pathway (Tsang et al, 2012a).

Taken together, both overexpression and knockdown of this gene have a negative impact on cell-cell adhesion and hence, we believe that a critical control of Dsg3 and its associated Src and Rho GTPases signalling are crucial for normal function and homeostasis of intercellular junctions. My study is in agreement with the work of Vasioukhin and colleagues, who suggested that desmosomal proteins are involved, at least in part, in stabilising the cytoskeletal anchorage of actin and cadherin–catenin complexes (Vasioukhin et al, 2001b). However, one main limitation was that our experiments were carried out in two different systems: keratinocyte cell and cancer cell systems.

A direct comparison between these systems is not ideal as each interpretation is strongly cell-type and context dependent. Thus, a single mechanism is not sufficient to explain the relationship between both a gain and loss of function of Dsg3.

8.2 Possible implication in the pathgenesis of *pemphigus* acantholysis

In the last few decades, the understanding in the pathogenesis of *pemphigus* has been significantly improved. However, there are also a number of crucial questions remained to be answered. A key question is whether the binding of autoantibodies to desmogleins contributes directly to epidermal blistering or whether the subsequent intracellular events are responsible for the loss of desmosome adhesion and blistering formation in the skin and oral mucosa. In addition, a growing body of evidence suggests that disruption of adherens junctions is involved in the pathogenesis of *pemphigus* acantholysis. It was demonstrated that E-cadherin is an additional immunological target for *pemphigus* autoantibodies, while other suggested that PV-IgG-induced inactivation of RhoA destabilises the adherens junctions and in turn affects the assembly of desmosomes (Evangelista et al, 2008; Sharma et al, 2007). It was also reported that the effect of PV-IgG on adherens junctions is not as severe as compared with desmosomes (de Bruin et al, 2007; Muller et al, 2008; Waschke et al, 2006), suggesting that E-cadherin is not the major contributor to blister formation. Thus, the role of E-cadherin in the pathogenesis of *pemphigus* remains an issue of debate.

Based on this study, we are inclined to believe that the direct disruption of desmosomal adhesion in *pemphigus vulgaris* is not the primary event responsible for the loss of cell-cell adhesion induced by PV-IgG, but rather by the inside-out signalling involving Src and GTPase signalling pathways. Indeed, confocal analysis of *pemphigus* patients specimens revealed that disruption of

E-cadherin junction and increased phospho-Src staining are readily detectable in the suprabasal layers above the blister as well as in the pre-lesional areas of oral mucosa in PV patients but not in those of normal control samples (Tsang et al, 2012b). This finding is also in line with other independent study based on the laser tweezer trapping of Dsg3-coated microbeads, which showed the initial loss of Dsg3 binding does not require Dsg3 depletion (Waschke et al, 2005).

We speculate that the Dsg3-induced activation of Src signalling and loss of E-cadherin in *pemphigus vulgaris* would make the region of the basal layer more vulnerable and rendering the site prone to separation. It is also believed that the down-regulation of other desmosomal proteins and the rearrangement of actin cytoskeleton in *pemphigus* are secondary events owing to the loss of E-cadherin and its associated junction. As such, it is inevitable that the activation of Rac1/Cdc42 could act synergistically in advancing the progression of *pemphigus* acantholysis. The new insights from this study not only advance our knowledge on the role of Dsg3 in epithelial cell biology but also enhance our understanding of the pathogenesis of skin diseases including *pemphigus*.

8.3 Future perspective

Epithelial junction formation is a complex process that involves the initiation of cell–cell contacts to the formation and maintanence of various intercellular junctions. In this study, I demonstrated the novel interactions between Dsg3 and E-cadherin or actin. We speculate that these associations may provide additional epidermal cohesions *in vivo* that are crucial for the maintenance and homeostasis of the adherens junctions. In addition, I showed that Dsg3 is an upstream regulator of Src and possibly Rho GTPases in the regulation of E-cadherin-mediated adherens junctions and the actin cytoskeleton. Future studies are necessary to support these novel concepts.

Characterisation of the nature interaction between Dsg3 and other junctional proteins: *In vitro* GST pull down assays with constructs carrying various portions of the cytoplasmic and/or N-terminus domain of Dsg3 can be used to pull down with E-cadherin or actin or plakoglobin or p120. This will allow us to distinguish a direct from an indirect interaction and map out the domain(s) involve.

The role of Dsg3 in the regulation of actin reorganisation: It would be interesting to determine if Dsg3 is involved in the regulation of actin accumulation and organisation through clustering of cadherin complexes. This question can be addressed by an established bead-binding assay using HaCaT cells with or without Dsg3 depletion. A suspension of latex beads coated with a specific antibody against E-cadherin can be used to cluster cadherin complexes and double labeled with phalloidin and anti–β-catenin, a marker for adherens junctions (Braga et al, 1997). This experiment will help to examine whether the F-actin and β-catenin recruitment to beads coated with anti-cadherin antibodies is indeed perturbed by Dsg3 depletion as compared to control cells.

The effects of Cdc42 and Rac1 on the Dsg3-induced membrane protrusions: Our results suggested that there is a direct positive relationship between the levels of Dsg3 protein and the formation of membrane protrusions. It is known that Cdc42 is the main driver for this type of membrane protrusions i.e filopodia (Krugmann et al, 2001) and hence, it will be interesting to carry out siRNA-mediated depletion of Cdc42 in HaCaT or A431 cells and assess the membrane activity by time-lapse video microscopy (same experiment as Figure 34). This experiment can be repeated using siRNA-mediated depletion of Rac1 to dissect the effects of Cdc42 and Rac1 on the Dsg3-induced membrane protrusions. To further confirm that Dsg3 is an upstream regulator of Rho GTPases, GST pull down assay can be used to determine whether knockdown of Dsg3 altered Rac or Cdc42 activity (same experiment as Figure 36).

Role of Caveolin/p120 in Dsg3-mediated Src activation: We proposed that modulation of Src signalling via caveolin-1 is one of the potential mechanisms underlying the loss of surface E-cadherin during the calcium-induced junction assembly. To validate this finding, it will be useful to examine whether knockdown of Dsg3 could concomitantly result in the loss of caveolin-1 and/or p120 catenin at the cell surface.

Establish both a gain and loss of Dsg3 function in one cell system: One of the main issues in this study is that two different cell systems were used and thus the results are difficult to reconcile with each other. In order to consolidate my results i.e the activation of Src signalling on E-cadherin junctions, it would be better to perform both overexpression and knockdown of Dsg3 in one cell system, which will help to clarify the conflicting findings in my study.

Triton soluble and insoluble fractions of Dsg3: Earlier, we suggested that the non-junctional Dsg3 pool is involved in the pathophysiology of pemphigus. Fractionation of Triton X-100 soluble and insoluble fractions can be repeated using other method such as the sedimentation of extracted proteins in sucrose gradients (Pasdar et al, 1991). Additional co-immunoprecipitation with PV IgG1 (Caldelari et al, 2001) using the soluble fraction of Dsg3 protein lysates would help to determine if the PV autoantibodies bind specifically to the non-junctional Dsg3.

The role of Dsg3 in *pemphingus* acantholysis: Finally, it will be useful to carry out *in vitro* studies on keratinocytes treated with or without PV-IgG and determine whether PV-IgG directly trigger Src activation and tyrosine phosphorylation of the E-cadherin/catenins proteins. This supplementary study will provide evidence of a direct link between PV-IgG and the activation of Dsg3-Src-E-cadherin pathway.

CHAPTER 9

REFERENCES

Aberle H, Butz S, Stappert J, Weissig H, Kemler R, Hoschuetzky H (1994) Assembly of the cadherin-catenin complex in vitro with recombinant proteins. *J Cell Sci* **107:** 3655-3663

Abram CL, Courtneidge SA (2000) Src family tyrosine kinases and growth factor signaling. *Exp Cell Res* **254:** 1-13

Akhtar N, Hotchin NA (2001) RAC1 regulates adherens junctions through endocytosis of E-cadherin. *Mol Biol Cell* **12:** 847-862

Akunuru S, James Zhai Q, Zheng Y (2012) Non-small cell lung cancer stem/progenitor cells are enriched in multiple distinct phenotypic subpopulations and exhibit plasticity. *Cell Death Dis* **3:** e352

Al-Amoudi A, Diez DC, Betts MJ, Frangakis AS (2007) The molecular architecture of cadherins in native epidermal desmosomes. *Nature* **450:** 832-837

Allen E, Yu QC, Fuchs E (1996) Mice expressing a mutant desmosomal cadherin exhibit abnormalities in desmosomes, proliferation, and epidermal differentiation. *J Cell Biol* **133:** 1367-1382

Amagai M (1999) Autoimmunity against desmosomal cadherins in pemphigus. *J Dermatol Sci* **20:** 92-102

Amagai M (2009) The molecular logic of pemphigus and impetigo: the desmoglein story. *Vet Dermatol* **20:** 308-312

Amagai M, Klaus-Kovtun V, Stanley JR (1991) Autoantibodies against a novel epithelial cadherin in pemphigus vulgaris, a disease of cell adhesion. *Cell* **67:** 869-877

Amagai M, Matsuyoshi N, Wang ZH, Andl C, Stanley JR (2000) Toxin in bullous impetigo and staphylococcal scalded-skin syndrome targets desmoglein 1. *Nat Med* **6:** 1275-1277

Anastasiadis PZ, Reynolds AB (2001) Regulation of Rho GTPases by p120-catenin. *Curr Opin Cell Biol* **13:** 604-610

Andl CD, Stanley JR (2001) Central role of the plakoglobin-binding domain for desmoglein 3 incorporation into desmosomes. *J Invest Dermatol* **117:** 1068-1074

Anhalt GJ, Labib RS, Voorhees JJ, Beals TF, Diaz LA (1982) Induction of pemphigus in neonatal mice by passive transfer of IgG from patients with the disease. *N Engl J Med* **306:** 1189-1196

Aoyama Y, Owada MK, Kitajima Y (1999) A pathogenic autoantibody, pemphigus vulgaris-IgG, induces phosphorylation of desmoglein 3, and its dissociation from plakoglobin in cultured keratinocytes. *Eur J Immunol* **29:** 2233-2240

Armstrong DK, McKenna KE, Purkis PE, Green KJ, Eady RA, Leigh IM, Hughes AE (1999) Haploinsufficiency of desmoplakin causes a striate subtype of palmoplantar keratoderma. *Hum Mol Genet* **8:** 143-148

Atsumi N, Ishii G, Kojima M, Sanada M, Fujii S, Ochiai A (2008) Podoplanin, a novel marker of tumor-initiating cells in human squamous cell carcinoma A431. *Biochem Biophys Res Commun* **373:** 36-41

Austinat M, Dunsch R, Wittekind C, Tannapfel A, Gebhardt R, Gaunitz F (2008) Correlation between beta-catenin mutations and expression of Wnt-signaling target genes in hepatocellular carcinoma. *Mol Cancer* **7:** 21

Avizienyte E, Wyke AW, Jones RJ, McLean GW, Westhoff MA, Brunton VG, Frame MC (2002) Src-induced de-regulation of E-cadherin in colon cancer cells requires integrin signalling. *Nat Cell Biol* **4:** 632-638

Awad MM, Dalal D, Tichnell C, James C, Tucker A, Abraham T, Spevak PJ, Calkins H, Judge DP (2006) Recessive arrhythmogenic right ventricular dysplasia due to novel cryptic splice mutation in PKP2. *Hum Mutat* **27:** 1157

Bass-Zubek AE, Godsel LM, Delmar M, Green KJ (2009) Plakophilins: multifunctional scaffolds for adhesion and signaling. *Curr Opin Cell Biol* **21:** 708-716

Baumgartner M, Radziwill G, Lorger M, Weiss A, Moelling K (2008) c-Src-mediated epithelial cell migration and invasion regulated by PDZ binding site. *Mol Cell Biol* **28:** 642-655

Bazzi H, Fantauzzo KA, Richardson GD, Jahoda CA, Christiano AM (2007) Transcriptional profiling of developing mouse epidermis reveals novel patterns of coordinated gene expression. *Dev Dyn* **236:** 961-970

Bear JE, Svitkina TM, Krause M, Schafer DA, Loureiro JJ, Strasser GA, Maly IV, Chaga OY, Cooper JA, Borisy GG, Gertler FB (2002) Antagonism between Ena/VASP proteins and actin filament capping regulates fibroblast motility. *Cell* **109:** 509-521

Behrens J, Vakaet L, Friis R, Winterhager E, Van Roy F, Mareel MM, Birchmeier W (1993) Loss of epithelial differentiation and gain of invasiveness correlates with tyrosine phosphorylation of the E-cadherin/beta-catenin complex in cells transformed with a temperature-sensitive v-SRC gene. *J Cell Biol* **120:** 757-766

Berkowitz P, Diaz LA, Hall RP, Rubenstein DS (2008) Induction of p38MAPK and HSP27 phosphorylation in pemphigus patient skin. *J Invest Dermatol* **128:** 738-740

Berkowitz P, Hu P, Liu Z, Diaz LA, Enghild JJ, Chua MP, Rubenstein DS (2005) Desmosome signaling. Inhibition of p38MAPK prevents pemphigus vulgaris IgG-induced cytoskeleton reorganization. *J Biol Chem* **280:** 23778-23784

Berkowitz P, Hu P, Warren S, Liu Z, Diaz LA, Rubenstein DS (2006) p38MAPK inhibition prevents disease in pemphigus vulgaris mice. *Proc Natl Acad Sci U S A* **103:** 12855-12860

Beutner EH, Lever WF, Witebsky E, Jordon R, Chertock B (1965) Autoantibodies in pemphigus vulgaris: response to an intercellular substance of epidermis. *JAMA* **192:** 682-688

Bierkamp C, McLaughlin KJ, Schwarz H, Huber O, Kemler R (1996) Embryonic heart and skin defects in mice lacking plakoglobin. *Dev Biol* **180:** 780-785

Blanchoin L, Michelot A (2012) Actin cytoskeleton: a team effort during actin assembly. *Curr Biol* **22:** R643-645

Bonne S, Gilbert B, Hatzfeld M, Chen X, Green KJ, van Roy F (2003) Defining desmosomal plakophilin-3 interactions. *J Cell Biol* **161:** 403-416

Bonne S, van Hengel J, Nollet F, Kools P, van Roy F (1999) Plakophilin-3, a novel armadillo-like protein present in nuclei and desmosomes of epithelial cells. *J Cell Sci* **112:** 2265-2276

Borisy GG, Svitkina TM (2000) Actin machinery: pushing the envelope. *Curr Opin Cell Biol* **12:** 104-112

Bornslaeger EA, Corcoran CM, Stappenbeck TS, Green KJ (1996) Breaking the connection: displacement of the desmosomal plaque protein desmoplakin from cell-cell interfaces disrupts anchorage of intermediate filament bundles and alters intercellular junction assembly. *J Cell Biol* **134:** 985-1001

Borrmann CM, Grund C, Kuhn C, Hofmann I, Pieperhoff S, Franke WW (2006) The area composita of adhering junctions connecting heart muscle cells of vertebrates. II. Colocalizations of desmosomal and fascia adhaerens molecules in the intercalated disk. *Eur J Cell Biol* **85:** 469-485

Boukamp P, Petrussevska RT, Breitkreutz D, Hornung J, Markham A, Fusenig NE (1988) Normal keratinization in a spontaneously immortalized aneuploid human keratinocyte cell line. *J Cell Biol* **106:** 761-771

Braga VM (2002) Cell–cell adhesion and signalling. *Curr Opin Cell Biol* **14:** 546-556

Braga VM, Machesky LM, Hall A, Hotchin NA (1997) The small GTPases Rho and Rac are required for the establishment of cadherin-dependent cell-cell contacts. *J Cell Biol* **137:** 1421-1431

Braga VM, Yap AS (2005) The challenges of abundance: epithelial junctions and small GTPase signalling. *Curr Opin Cell Biol* **17:** 466-474

Brennan D, Hu Y, Joubeh S, Choi YW, Whitaker-Menezes D, O'Brien T, Uitto J, Rodeck U, Mahoney MG (2007) Suprabasal Dsg2 expression in transgenic

mouse skin confers a hyperproliferative and apoptosis-resistant phenotype to keratinocytes. *J Cell Sci* **120:** 758-771

Brennan D, Mahoney MG (2009) Increased expression of Dsg2 in malignant skin carcinomas: A tissue-microarray based study. *Cell Adh Migr* **3:** 148-154

Brennan D, Peltonen S, Dowling A, Medhat W, Green KJ, Wahl JK, 3rd, Del Galdo F, Mahoney MG (2011) A role for caveolin-1 in desmoglein binding and desmosome dynamics. *Oncogene* **31:** 1636-48

Brieher WM, Yap AS (2012) Cadherin junctions and their cytoskeleton(s). *Curr Opin Cell Biol* **25:** 39-46

Brooke MA, Nitoiu D, Kelsell DP (2012) Cell-cell connectivity: desmosomes and disease. *J Pathol* **226:** 158-171

Brown MT, Cooper JA (1996) Regulation, substrates and functions of src. *Biochim Biophys Acta* **1287:** 121-149

Burnette DT, Sengupta P, Dai Y, Lippincott-Schwartz J, Kachar B (2011) Bleaching/blinking assisted localization microscopy for superresolution imaging using standard fluorescent molecules. *Proc Natl Acad Sci U S A* **108:** 21081-21086

Bystryn JC, Rudolph JL (2005) Pemphigus. *Lancet* **366:** 61-73

Calautti E, Cabodi S, Stein PL, Hatzfeld M, Kedersha N, Paolo Dotto G (1998) Tyrosine phosphorylation and src family kinases control keratinocyte cell-cell adhesion. *J Cell Biol* **141:** 1449-1465

Calautti E, Grossi M, Mammucari C, Aoyama Y, Pirro M, Ono Y, Li J, Dotto GP (2002) Fyn tyrosine kinase is a downstream mediator of Rho/PRK2 function in keratinocyte cell-cell adhesion. *J Cell Biol* **156:** 137-148

Calautti E, Missero C, Stein PL, Ezzell RM, Dotto GP (1995) fyn tyrosine kinase is involved in keratinocyte differentiation control. *Genes Dev* **9:** 2279-2291

Caldelari R, de Bruin A, Baumann D, Suter MM, Bierkamp C, Balmer V, Muller E (2001) A central role for the armadillo protein plakoglobin in the autoimmune disease pemphigus vulgaris. *J Cell Biol* **153:** 823-834

Chen J, Den Z, Koch PJ (2008) Loss of desmocollin 3 in mice leads to epidermal blistering. *J Cell Sci* **121:** 2844-2849

Chen YJ, Chang JT, Lee L, Wang HM, Liao CT, Chiu CC, Chen PJ, Cheng AJ (2007) DSG3 is overexpressed in head neck cancer and is a potential molecular target for inhibition of oncogenesis. *Oncogene* **26:** 467-476

Chernyavsky AI, Arredondo J, Kitajima Y, Sato-Nagai M, Grando SA (2007) Desmoglein versus non-desmoglein signaling in pemphigus acantholysis: characterization of novel signaling pathways downstream of pemphigus vulgaris antigens. *J Biol Chem* **282:** 13804-13812

Chidgey M, Brakebusch C, Gustafsson E, Cruchley A, Hail C, Kirk S, Merritt A, North A, Tselepis C, Hewitt J, Byrne C, Fassler R, Garrod D (2001) Mice lacking desmocollin 1 show epidermal fragility accompanied by barrier defects and abnormal differentiation. *J Cell Biol* **155:** 821-832

Chitaev NA, Troyanovsky SM (1997) Direct Ca2+-dependent heterophilic interaction between desmosomal cadherins, desmoglein and desmocollin, contributes to cell-cell adhesion. *J Cell Biol* **138:** 193-201

Choi HJ, Gross JC, Pokutta S, Weis WI (2009) Interactions of plakoglobin and beta-catenin with desmosomal cadherins: basis of selective exclusion of alpha- and beta-catenin from desmosomes. *J Biol Chem* **284:** 31776-31788

Cirillo N, Femiano F, Gombos F, Lanza A (2009) High-dose pemphigus antibodies against linear epitopes of desmoglein 3 (Dsg3) can induce acantholysis and depletion of Dsg3 from keratinocytes. *Immunol Lett* **122:** 208-213

Cirillo N, Lanza A, Prime SS (2010) Induction of hyper-adhesion attenuates autoimmune-induced keratinocyte cell-cell detachment and processing of adhesion molecules via mechanisms that involve PKC. *Exp Cell Res* **316:** 580-592

Cosentino-Gomes D, Rocco-Machado N, Meyer-Fernandes JR (2012) Cell Signaling through Protein Kinase C Oxidation and Activation. *Int J Mol Sci* **13:** 10697-10721

Couet J, Sargiacomo M, Lisanti MP (1997) Interaction of a receptor tyrosine kinase, EGF-R, with caveolins. Caveolin binding negatively regulates tyrosine and serine/threonine kinase activities. *J Biol Chem* **272:** 30429-30438

Culton DA, Qian Y, Li N, Rubenstein D, Aoki V, Filhio GH, Rivitti EA, Diaz LA (2008) Advances in pemphigus and its endemic pemphigus foliaceus (Fogo Selvagem) phenotype: a paradigm of human autoimmunity. *J Autoimmun* **31:** 311-324

Davis MA, Ireton RC, Reynolds AB (2003) A core function for p120-catenin in cadherin turnover. *J Cell Biol* **163:** 525-534

De Bruin A, Caldelari R, Williamson L, Suter MM, Hunziker T, Wyder M, Muller EJ (2007) Plakoglobin-dependent disruption of the desmosomal plaque in pemphigus vulgaris. *Exp Dermatol* **16:** 468-475

Delva E, Kowalczyk AP (2009) Regulation of cadherin trafficking. *Traffic* **10:** 259-267

Delva E, Tucker DK, Kowalczyk AP (2009) The desmosome. *Cold Spring Harb Perspect Biol* **1:** a002543

Demlehner MP, Schafer S, Grund C, Franke WW (1995) Continual assembly of half-desmosomal structures in the absence of cell contacts and their frustrated endocytosis: a coordinated Sisyphus cycle. *J Cell Biol* **131:** 745-760

Den Z, Cheng X, Merched-Sauvage M, Koch PJ (2006) Desmocollin 3 is required for pre-implantation development of the mouse embryo. *J Cell Sci* **119:** 482-489

Denning MF, Guy SG, Ellerbroek SM, Norvell SM, Kowalczyk AP, Green KJ (1998) The expression of desmoglein isoforms in cultured human keratinocytes is regulated by calcium, serum, and protein kinase C. *Exp Cell Res* **239:** 50-59

Desai RA, Gao L, Raghavan S, Liu WF, Chen CS (2009) Cell polarity triggered by cell-cell adhesion via E-cadherin. *J Cell Sci* **122:** 905-911

Dietrich KA, Schwarz R, Liska M, Grass S, Menke A, Meister M, Kierschke G, Langle C, Genze F, Giehl K (2009) Specific induction of migration and invasion of pancreatic carcinoma cells by RhoC, which differs from RhoA in its localisation and activity. *Biol Chem* **390:** 1063-1077

Drees F, Pokutta S, Yamada S, Nelson WJ, Weis WI (2005) Alpha-catenin is a molecular switch that binds E-cadherin-beta-catenin and regulates actin-filament assembly. *Cell* **123:** 903-915

Dwivedi S, Pandey D, Khandoga AL, Brandl R, Siess W (2010) Rac1-mediated signaling plays a central role in secretion-dependent platelet aggregation in human blood stimulated by atherosclerotic plaque. *J Transl Med* **8:** 128

Echarri A, Muriel O, Del Pozo MA (2007) Intracellular trafficking of raft/caveolae domains: insights from integrin signaling. *Semin Cell Dev Biol* **18:** 627-637

Eckert RL, Rorke EA (1989) Molecular biology of keratinocyte differentiation. *Environ Health Perspect* **80:** 109-116

Elias PM, Matsuyoshi N, Wu H, Lin C, Wang ZH, Brown BE, Stanley JR (2001) Desmoglein isoform distribution affects stratum corneum structure and function. *J Cell Biol* **153:** 243-249

Erasmus J, Aresta S, Nola S, Caron E, Braga VM (2010) Newly formed E-cadherin contacts do not activate Cdc42 or induce filopodia protrusion in human keratinocytes. *Biol Cell* **102:** 13-24

Eshkind L, Tian Q, Schmidt A, Franke WW, Windoffer R, Leube RE (2002) Loss of desmoglein 2 suggests essential functions for early embryonic development and proliferation of embryonal stem cells. *Eur J Cell Biol* **81:** 592-598

Evangelista F, Dasher DA, Diaz LA, Prisayanh PS, Li N (2008) E-cadherin is an additional immunological target for pemphigus autoantibodies. *J Invest Dermatol* **128:** 1710-1718

Farquhar MG, Palade GE (1963) Junctional complexes in various epithelia. *J Cell Biol* **17:** 375-412

Feliciani C, Toto P, Wang B, Sauder DN, Amerio P, Tulli A (2003) Urokinase plasminogen activator mRNA is induced by IL-1alpha and TNF-alpha in in vitro acantholysis. *Exp Dermatol* **12:** 466-471

Fey EG, Wan KM, Penman S (1984) Epithelial cytoskeletal framework and nuclear matrix-intermediate filament scaffold: three-dimensional organization and protein composition. *J Cell Biol* **98:** 1973-1984

Friesland A, Zhao Y, Chen YH, Wang L, Zhou H, Lu Q (2013) Small molecule targeting Cdc42-intersectin interaction disrupts Golgi organization and suppresses cell motility. *Proc Natl Acad Sci U S A* **110:** 1261-1266

Fuchs E, Byrne C (1994) The epidermis: rising to the surface. *Curr Opin Genet Dev* **4:** 725-736

Fujita Y (2002) Hakai, a c-Cbl-like protein, ubiquitinates and induces endocytosis of the E-cadherin complex. *Nature Cell Biol* **4:** 222-231

Fukata M, Kaibuchi K (2001) Rho-family GTPases in cadherin-mediated cell-cell adhesion. *Nat Rev Mol Cell Biol* **2:** 887-897

Fukata M, Nakagawa M, Itoh N, Kawajiri A, Yamaga M, Kuroda S, Kaibuchi K (2001) Involvement of IQGAP1, an effector of Rac1 and Cdc42 GTPases, in cell-cell dissociation during cell scattering. *Mol Cell Biol* **21:** 2165-2183

Fukata M, Nakagawa M, Kuroda S, Kaibuchi K (1999) Cell adhesion and Rho small GTPases. *J Cell Sci* **112:** 4491-4500

Furukawa F, Fujii K, Horiguchi Y, Matsuyoshi N, Fujita M, Toda K, Imamura S, Wakita H, Shirahama S, Takigawa M (1997) Roles of E- and P-cadherin in the human skin. *Microsc Res Tech* **38:** 343-352

Gallicano GI, Kouklis P, Bauer C, Yin M, Vasioukhin V, Degenstein L, Fuchs E (1998) Desmoplakin is required early in development for assembly of desmosomes and cytoskeletal linkage. *J Cell Biol* **143:** 2009-2022

Gao Y, Dickerson JB, Guo F, Zheng J, Zheng Y (2004) Rational design and characterization of a Rac GTPase-specific small molecule inhibitor. *Proc Natl Acad Sci U S A* **101:** 7618-7623

Garrod D (2010) Desmosomes in vivo. *Dermatol Res Pract* **2010:** 212439

Garrod D, Chidgey M (2008) Desmosome structure, composition and function. *Biochim Biophys Acta* **1778:** 572-587

Garrod D, Kimura TE (2008) Hyper-adhesion: a new concept in cell-cell adhesion. *Biochem Soc Trans* **36:** 195-201

Garrod D, Fisher C, Smith A, Nie Z (2008) Pervanadate stabilizes desmosomes. *Cell Adh Migr* **2:** 161-166

Garrod D, Merritt AJ, Nie Z (2002) Desmosomal cadherins. *Curr Opin Cell Biol* **14:** 537-545

Gaudry CA, Palka HL, Dusek RL, Huen AC, Khandekar MJ, Hudson LG, Green KJ (2001) Tyrosine-phosphorylated plakoglobin is associated with desmogleins but not desmoplakin after epidermal growth factor receptor activation. *J Biol Chem* **276:** 24871-24880

Gerull B, Heuser A, Wichter T, Paul M, Basson CT, McDermott DA, Lerman BB, Markowitz SM, Ellinor PT, MacRae CA, Peters S, Grossmann KS, Drenckhahn J, Michely B, Sasse-Klaassen S, Birchmeier W, Dietz R, Breithardt G, Schulze-Bahr E, Thierfelder L (2004) Mutations in the desmosomal protein plakophilin-2 are common in arrhythmogenic right ventricular cardiomyopathy. *Nat Genet* **36:** 1162-1164

Getsios S, Huen AC, Green KJ (2004) Working out the strength and flexibility of desmosomes. *Nat Rev Mol Cell Biol* **5:** 271-281

Getsios S, Simpson CL, Kojima S, Harmon R, Sheu LJ, Dusek RL, Cornwell M, Green KJ (2009) Desmoglein 1-dependent suppression of EGFR signaling promotes epidermal differentiation and morphogenesis. *J Cell Biol* **185:** 1243-1258

Gliem M, Heupel WM, Spindler V, Harms GS, Waschke J (2010) Actin reorganization contributes to loss of cell adhesion in pemphigus vulgaris. *Am J Physiol Cell Physiol* **299:** C606-613

Gloushankova NA (2008) Changes in regulation of cell-cell adhesion during tumor transformation. *Biochemistry (Mosc)* **73:** 742-750

Godsel LM, Dubash AD, Bass-Zubek AE, Amargo EV, Klessner JL, Hobbs RP, Chen X, Green KJ (2010) Plakophilin 2 couples actomyosin remodeling to desmosomal plaque assembly via RhoA. *Mol Biol Cell* **21:** 2844-2859

Godsel LM, Hsieh SN, Amargo EV, Bass AE, Pascoe-McGillicuddy LT, Huen AC, Thorne ME, Gaudry CA, Park JK, Myung K, Goldman RD, Chew TL, Green KJ (2005) Desmoplakin assembly dynamics in four dimensions: multiple phases differentially regulated by intermediate filaments and actin. *J Cell Biol* **171:** 1045-1059

Gosavi P, Kundu ST, Khapare N, Sehgal L, Karkhanis MS, Dalal SN (2011) E-cadherin and plakoglobin recruit plakophilin3 to the cell border to initiate desmosome assembly. *Cell Mol Life Sci* **68:** 1439-1454

Green KJ, Gaudry CA (2000) Are desmosomes more than tethers for intermediate filaments? *Nat Rev Mol Cell Biol* **1:** 208-216

Green KJ, Getsios S, Troyanovsky S, Godsel LM (2010) Intercellular junction assembly, dynamics, and homeostasis. *Cold Spring Harb Perspect Biol* **2:** a000125

Green KJ, Simpson CL (2007) Desmosomes: new perspectives on a classic. *J Invest Dermatol* **127:** 2499-2515

Grossmann KS, Grund C, Huelsken J, Behrend M, Erdmann B, Franke WW, Birchmeier W (2004) Requirement of plakophilin 2 for heart morphogenesis and cardiac junction formation. *J Cell Biol* **167:** 149-160

Gumbiner BM (1996) Cell adhesion: the molecular basis of tissue architecture and morphogenesis. *Cell* **84:** 345-357

Haftek M, Hansen MU, Kaiser HW, Kreysel HW, Schmitt D (1996) Interkeratinocyte adherens junctions: immunocytochemical visualization of

cell-cell junctional structures, distinct from desmosomes, in human epidermis. *J Invest Dermatol* **106:** 498-504

Hage B, Meinel K, Baum I, Giehl K, Menke A (2009) Rac1 activation inhibits E-cadherin-mediated adherens junctions via binding to IQGAP1 in pancreatic carcinoma cells. *Cell Commun Signal* **7:** 23

Hamaguchi M, Matsuyoshi N, Ohnishi Y, Gotoh B, Takeichi M, Nagai Y (1993) p60v-src causes tyrosine phosphorylation and inactivation of the N-cadherin-catenin cell adhesion system. *EMBO J* **12:** 307-314

Hanakawa Y, Amagai M, Shirakata Y, Sayama K, Hashimoto K (2000) Different effects of dominant negative mutants of desmocollin and desmoglein on the cell-cell adhesion of keratinocytes. *J Cell Sci* **113:** 1803-1811

Hansen MD, Ehrlich JS, Nelson WJ (2002) Molecular mechanism for orienting membrane and actin dynamics to nascent cell-cell contacts in epithelial cells. *J Biol Chem* **277:** 45371-45376

Hardman MJ, Liu K, Avilion AA, Merritt A, Brennan K, Garrod DR, Byrne C (2005) Desmosomal cadherin misexpression alters beta-catenin stability and epidermal differentiation. *Mol Cell Biol* **25:** 969-978

Harris TJC, Tepass U (2010) Adherens junctions: from molecules to morphogenesis. *Nat Rev Mol Cell Biol* **11:** 502-514

Hashimoto K, Shafran KM, Webber PS, Lazarus GS, Singer KH (1983) Anti-cell surface pemphigus autoantibody stimulates plasminogen activator activity of human epidermal cells. A mechanism for the loss of epidermal cohesion and blister formation. *J Exp Med* **157:** 259-272

Hatzfeld M (2007) Plakophilins: Multifunctional proteins or just regulators of desmosomal adhesion? *Biochim Biophys Acta* **1773:** 69-77

Hatzfeld M, Haffner C, Schulze K, Vinzens U (2000) The function of plakophilin 1 in desmosome assembly and actin filament organization. *J Cell Biol* **149:** 209-222

Hehlgans S, Eke I, Storch K, Haase M, Baretton GB, Cordes N (2009) Caveolin-1 mediated radioresistance of 3D grown pancreatic cancer cells. *Radiother Oncol* **92:** 362-370

Hennings H, Michael D, Cheng C, Steinert P, Holbrook K, Yuspa SH (1980) Calcium regulation of growth and differentiation of mouse epidermal cells in culture. *Cell* **19:** 245-254

Hernandez-Deviez DJ, Howes MT, Laval SH, Bushby K, Hancock JF, Parton RG (2008) Caveolin regulates endocytosis of the muscle repair protein, dysferlin. *J Biol Chem* **283:** 6476-6488

Heupel WM, Engerer P, Schmidt E, Waschke J (2009) Pemphigus vulgaris IgG cause loss of desmoglein-mediated adhesion and keratinocyte dissociation independent of epidermal growth factor receptor. *Am J Pathol* **174:** 475-485

Heupel WM, Zillikens D, Drenckhahn D, Waschke J (2008) Pemphigus vulgaris IgG directly inhibit desmoglein 3-mediated transinteraction. *J Immunol* **181:** 1825-1834

Hinck L, Nathke IS, Papkoff J, Nelson WJ (1994) Dynamics of cadherin/catenin complex formation: novel protein interactions and pathways of complex assembly. *J Cell Biol* **125:** 1327-1340

Hirai Y, Nose A, Kobayashi S, Takeichi M (1989) Expression and role of E- and P-cadherin adhesion molecules in embryonic histogenesis. II. Skin morphogenesis. *Development* **105:** 271-277

Hobbs RP, Green KJ (2012) Desmoplakin regulates desmosome hyperadhesion. *J Invest Dermatol* **132:** 482-485

Hodivala KJ, Watt FM (1994) Evidence that cadherins play a role in the downregulation of integrin expression that occurs during keratinocyte terminal differentiation. *J Cell Biol* **124:** 589-600

Huber O (2003) Structure and function of desmosomal proteins and their role in development and disease. *Cell Mol Life Sci* **60:** 1872-1890

Huen AC, Park JK, Godsel LM, Chen X, Bannon LJ, Amargo EV, Hudson TY, Mongiu AK, Leigh IM, Kelsell DP, Gumbiner BM, Green KJ (2002) Intermediate

filament-membrane attachments function synergistically with actin-dependent contacts to regulate intercellular adhesive strength. *J Cell Biol* **159:** 1005-1017

Irby RB, Yeatman TJ (2000) Role of Src expression and activation in human cancer. *Oncogene* **19:** 5636-5642

Ishii K, Lin C, Siegel DL, Stanley JR (2008) Isolation of pathogenic monoclonal anti-desmoglein 1 human antibodies by phage display of pemphigus foliaceus autoantibodies. *J Invest Dermatol* **128:** 939-948

Ishii K, Norvell SM, Bannon LJ, Amargo EV, Pascoe LT, Green KJ (2001) Assembly of desmosomal cadherins into desmosomes is isoform dependent. *J Invest Dermatol* **117:** 26-35

Jeanes A, Smutny M, Leerberg JM, Yap AS (2009) Phosphatidylinositol 3'-kinase signalling supports cell height in established epithelial monolayers. *J Mol Histol* **40:** 395-405

Johnson DI (1999) Cdc42: An essential Rho-type GTPase controlling eukaryotic cell polarity. *Microbiol Mol Biol Rev* **63:** 54-105

Kanno M, Aoyama Y, Isa Y, Yamamoto Y, Kitajima Y (2008a) P120 catenin is associated with desmogleins when desmosomes are assembled in high-Ca2+ medium but not when disassembled in low-Ca2+ medium in DJM-1 cells. *J Dermatol* **35:** 317-324

Kanno M, Isa Y, Aoyama Y, Yamamoto Y, Nagai M, Ozawa M, Kitajima Y (2008b) P120-catenin is a novel desmoglein 3 interacting partner: identification of the p120-catenin association site of desmoglein 3. *Exp Cell Res* **314:** 1683-1692

Kerr JB (1999) *Atlas of functional histology*, London: Mosby.

Kim SH, Li Z, Sacks DB (2000) E-cadherin-mediated cell-cell attachment activates Cdc42. *J Biol Chem* **275:** 36999-37005

Kimura TE, Merritt AJ, Garrod DR (2007) Calcium-independent desmosomes of keratinocytes are hyper-adhesive. *J Invest Dermatol* **127:** 775-781

Kljuic A, Bazzi H, Sundberg JP, Martinez-Mir A, O'Shaughnessy R, Mahoney MG, Levy M, Montagutelli X, Ahmad W, Aita VM, Gordon D, Uitto J, Whiting D, Ott J, Fischer S, Gilliam TC, Jahoda CA, Morris RJ, Panteleyev AA, Nguyen VT, Christiano AM (2003) Desmoglein 4 in hair follicle differentiation and epidermal adhesion: evidence from inherited hypotrichosis and acquired pemphigus vulgaris. *Cell* **113:** 249-260

Kobielak A, Fuchs E (2004) Alpha-catenin: at the junction of intercellular adhesion and actin dynamics. *Nat Rev Mol Cell Biol* **5:** 614-625

Koch PJ, Mahoney MG, Ishikawa H, Pulkkinen L, Uitto J, Shultz L, Murphy GF, Whitaker-Menezes D, Stanley JR (1997) Targeted disruption of the pemphigus vulgaris antigen (desmoglein 3) gene in mice causes loss of keratinocyte cell adhesion with a phenotype similar to pemphigus vulgaris. *J Cell Biol* **137:** 1091-1102

Kodama A, Takaishi K, Nakano K, Nishioka H, Takai Y (1999) Involvement of Cdc42 small G protein in cell-cell adhesion, migration and morphology of MDCK cells. *Oncogene* **18:** 3996-4006

Kottke MD, Delva E, Kowalczyk AP (2006) The desmosome: cell science lessons from human diseases. *J Cell Sci* **119:** 797-806

Kouklis PD, Hutton E, Fuchs E (1994) Making a connection: direct binding between keratin intermediate filaments and desmosomal proteins. *J Cell Biol* **127:** 1049-1060

Kovacs EM, Ali RG, McCormack AJ, Yap AS (2002a) E-cadherin homophilic ligation directly signals through Rac and phosphatidylinositol 3-kinase to regulate adhesive contacts. *J Biol Chem* **277:** 6708-6718

Kovacs EM, Goodwin M, Ali RG, Paterson AD, Yap AS (2002b) Cadherin-directed actin assembly: E-cadherin physically associates with the Arp2/3 complex to direct actin assembly in nascent adhesive contacts. *Curr Biol* **12:** 379-382

Kovacs EM, Yap AS (2008) Cell–cell contact: cooperating clusters of actin and cadherin. *Curr Biol* **18:** R667-R669

Kowalczyk AP, Bornslaeger EA, Borgwardt JE, Palka HL, Dhaliwal AS, Corcoran CM, Denning MF, Green KJ (1997) The amino-terminal domain of desmoplakin

binds to plakoglobin and clusters desmosomal cadherin-plakoglobin complexes. *J Cell Biol* **139:** 773-784

Kowalczyk AP, Stappenbeck TS, Parry DA, Palka HL, Virata ML, Bornslaeger EA, Nilles LA, Green KJ (1994) Structure and function of desmosomal transmembrane core and plaque molecules. *Biophys Chem* **50:** 97-112

Krugmann S, Jordens I, Gevaert K, Driessens M, Vandekerckhove J, Hall A (2001) Cdc42 induces filopodia by promoting the formation of an IRSp53:Mena complex. *Curr Biol* **11:** 1645-1655

Lahtinen AM, Lehtonen A, Kaartinen M, Toivonen L, Swan H, Widen E, Lehtonen E, Lehto VP, Kontula K (2008) Plakophilin-2 missense mutations in arrhythmogenic right ventricular cardiomyopathy. *Int J Cardiol* **126:** 92-100

Landegren U, Schallmeiner E, Nilsson M, Fredriksson S, Baner J, Gullberg M, Jarvius J, Gustafsdottir S, Dahl F, Soderberg O, Ericsson O, Stenberg J (2004) Molecular tools for a molecular medicine: analyzing genes, transcripts and proteins using padlock and proximity probes. *J Mol Recognit* **17:** 194-197

Lechler T, Fuchs E (2007) Desmoplakin: an unexpected regulator of microtubule organization in the epidermis. *J Cell Biol* **176:** 147-154

Lewis JE, Jensen PJ, Johnson KR, Wheelock MJ (1994) E-cadherin mediates adherens junction organization through protein kinase C. *J Cell Sci* **107:** 3615-3621

Lewis JE, Wahl JK, 3rd, Sass KM, Jensen PJ, Johnson KR, Wheelock MJ (1997) Cross-talk between adherens junctions and desmosomes depends on plakoglobin. *J Cell Biol* **136:** 919-934

Li S, Couet J, Lisanti MP (1996) Src tyrosine kinases, Galpha subunits, and H-Ras share a common membrane-anchored scaffolding protein, caveolin. Caveolin binding negatively regulates the auto-activation of Src tyrosine kinases. *J Biol Chem* **271:** 29182-29190

Lisanti MP, Tang Z, Scherer PE, Kubler E, Koleske AJ, Sargiacomo M (1995) Caveolae, transmembrane signalling and cellular transformation. *Mol Membr Biol* **12:** 121-124

Lo Muzio L, Pannone G, Staibano S, Mignogna MD, Rubini C, Farronato G, Ferrari F, Nocini PF, De Rosa G (2002) Strict correlation between uPAR and plakoglobin expression in pemphigus vulgaris. *J Cutan Pathol* **29:** 540-548

Mack NA, Whalley HJ, Castillo-Lluva S, Malliri A (2011) The diverse roles of Rac signaling in tumorigenesis. *Cell Cycle* **10:** 1571-1581

Mahoney MG, Hu Y, Brennan D, Bazzi H, Christiano AM, Wahl JK (2006) Delineation of diversified desmoglein distribution in stratified squamous epithelia: implications in diseases. *Exp Dermatol* **15:** 101-109

Mahoney MG, Wang ZH, Stanley JR (1999) Pemphigus vulgaris and pemphigus foliaceus antibodies are pathogenic in plasminogen activator knockout mice. *J Invest Dermatol* **113:** 22-25

Mannan T, Jing S, Foroushania SH, Fortune F, Wan H (2011) RNAi-mediated inhibition of the desmosomal cadherin (desmoglein 3) impairs epithelial cell proliferation. *Cell Prolif* **44:** 301-310

Mao X, Sano Y, Park JM, Payne AS (2011) p38 MAPK activation is downstream of the loss of intercellular adhesion in pemphigus vulgaris. *J Biol Chem* **286:** 1283-1291

Marchenko S, Chernyavsky AI, Arredondo J, Gindi V, Grando SA (2010) Antimitochondrial autoantibodies in pemphigus vulgaris: a missing link in disease pathophysiology. *J Biol Chem* **285:** 3695-3704

Marcozzi C, Burdett ID, Buxton RS, Magee AI (1998) Coexpression of both types of desmosomal cadherin and plakoglobin confers strong intercellular adhesion. *J Cell Sci* **111:** 495-509

Mascaro JM, Jr., Espana A, Liu Z, Ding X, Swartz SJ, Fairley JA, Diaz LA (1997) Mechanisms of acantholysis in pemphigus vulgaris: role of IgG valence. *Clin Immunol Immunopathol* **85:** 90-96

Mathur M, Goodwin L, Cowin P (1994) Interactions of the cytoplasmic domain of the desmosomal cadherin Dsg1 with plakoglobin. *J Biol Chem* **269:** 14075-14080

Matsuyoshi N, Hamaguchi M, Taniguchi S, Nagafuchi A, Tsukita S, Takeichi M (1992) Cadherin-mediated cell-cell adhesion is perturbed by v-src tyrosine phosphorylation in metastatic fibroblasts. *J Cell Biol* **118:** 703-714

Mattey DL, Garrod DR (1986) Splitting and internalization of the desmosomes of cultured kidney epithelial cells by reduction in calcium concentration. *J Cell Sci* **85:** 113-124

McGrath JA, McMillan JR, Shemanko CS, Runswick SK, Leigh IM, Lane EB, Garrod DR, Eady RA (1997) Mutations in the plakophilin 1 gene result in ectodermal dysplasia/skin fragility syndrome. *Nat Genet* **17:** 240-244

McKoy G, Protonotarios N, Crosby A, Tsatsopoulou A, Anastasakis A, Coonar A, Norman M, Baboonian C, Jeffery S, McKenna WJ (2000) Identification of a deletion in plakoglobin in arrhythmogenic right ventricular cardiomyopathy with palmoplantar keratoderma and woolly hair (Naxos disease). *Lancet* **355:** 2119-2124

McLachlan RW, Kraemer A, Helwani FM, Kovacs EM, Yap AS (2007) E-cadherin adhesion activates c-Src signaling at cell-cell contacts. *Mol Biol Cell* **18:** 3214-3223

McLachlan RW, Yap AS (2011) Protein tyrosine phosphatase activity is necessary for E-cadherin-activated Src signaling. *Cytoskeleton (Hoboken)* **68:** 32-43

Menke A, Giehl K (2012) Regulation of adherens junctions by Rho GTPases and p120-catenin. *Arch Biochem Biophys* **524:** 48-55

Merritt AJ, Berika MY, Zhai W, Kirk SE, Ji B, Hardman MJ, Garrod DR (2002) Suprabasal desmoglein 3 expression in the epidermis of transgenic mice results in hyperproliferation and abnormal differentiation. *Mol Cell Biol* **22:** 5846-5858

Mertens C, Hofmann I, Wang Z, Teichmann M, Sepehri Chong S, Schnolzer M, Franke WW (2001) Nuclear particles containing RNA polymerase III complexes associated with the junctional plaque protein plakophilin 2. *Proc Natl Acad Sci U S A* **98:** 7795-7800

Miotti S, Tomassetti A, Facetti I, Sanna E, Berno V, Canevari S (2005) Simultaneous expression of caveolin-1 and E-cadherin in ovarian carcinoma

cells stabilizes adherens junctions through inhibition of src-related kinases. *Am J Pathol* **167:** 1411-1427

Miravet S, Piedra J, Miro F, Itarte E, Garcia de Herreros A, Dunach M (2002) The transcriptional factor Tcf-4 contains different binding sites for beta-catenin and plakoglobin. *J Biol Chem* **277:** 1884-1891

Mitchell T, Lo A, Logan MR, Lacy P, Eitzen G (2008) Primary granule exocytosis in human neutrophils is regulated by Rac-dependent actin remodeling. *Am J Physiol Cell Physiol* **295:** C1354-1365

Morasso MI, Tomic-Canic M (2005) Epidermal stem cells: the cradle of epidermal determination, differentiation and wound healing. *Biol Cell* **97:** 173-183

Morioka S, Lazarus GS, Jensen PJ (1987) Involvement of urokinase-type plasminogen activator in acantholysis induced by pemphigus IgG. *J Invest Dermatol* **89:** 474-477

Muller E, Kernland K, Caldelari R, Wyder M, Balmer V, Hunziker T (2002) Unusual pemphigus phenotype in the presence of a Dsg1 and Dsg3 autoantibody profile. *J Invest Dermatol* **118:** 551-555

Muller E, Williamson L, Kolly C, Suter MM (2008) Outside-in signaling through integrins and cadherins: a central mechanism to control epidermal growth and differentiation? *J Invest Dermatol* **128:** 501-516

Nagathihalli NS, Merchant NB (2012) Src-mediated regulation of E-cadherin and EMT in pancreatic cancer. *Front Biosci* **17:** 2059-2069

Nam JS, Ino Y, Sakamoto M, Hirohashi S (2002) Src family kinase inhibitor PP2 restores the E-cadherin/catenin cell adhesion system in human cancer cells and reduces cancer metastasis. *Clin Cancer Res* **8:** 2430-2436

Narbutt J, Lukamowicz J, Bogaczewicz J, Sysa-Jedrzejowska A, Torzecka JD, Lesiak A (2008) Serum concentration of interleukin-6 is increased both in active and remission stages of pemphigus vulgaris. *Mediators Inflamm* **2008:** 875394

Navarro A, Anand-Apte B, Parat MO (2004) A role for caveolae in cell migration. *FASEB J* **18:** 1801-1811

Nawrocki B, Polette M, Van Hengel J, Tournier JM, Van Roy F, Birembault P (1998) Cytoplasmic redistribution of E-cadherin-catenin adhesion complex is associated with down-regulated tyrosine phosphorylation of E-cadherin in human bronchopulmonary carcinomas. *Am J Pathol* **153:** 1521-1530

Neuber S, Muhmer M, Wratten D, Koch PJ, Moll R, Schmidt A (2010) The desmosomal plaque proteins of the plakophilin family. *Dermatol Res Pract* **2010:** 101452

Nie Z, Merritt A, Rouhi-Parkouhi M, Tabernero L, Garrod D (2011) Membrane-impermeable cross-linking provides evidence for homophilic, isoform-specific binding of desmosomal cadherins in epithelial cells. *J Biol Chem* **286:** 2143-2154

Niessen CM (2007) Tight junctions/adherens junctions: basic structure and function. *J Invest Dermatol* **127:** 2525-2532

Noren NK, Liu BP, Burridge K, Kreft B (2000) p120 catenin regulates the actin cytoskeleton via Rho family GTPases. *J Cell Biol* **150:** 567-580

Noren NK, Niessen CM, Gumbiner BM, Burridge K (2001) Cadherin engagement regulates Rho family GTPases. *J Biol Chem* **276:** 33305-33308

O'Keefe EJ, Briggaman RA, Herman B (1987) Calcium-induced assembly of adherens junctions in keratinocytes. *J Cell Biol* **105:** 807-817

Obergfell A, Eto K, Mocsai A, Buensuceso C, Moores SL, Brugge JS, Lowell CA, Shattil SJ (2002) Coordinate interactions of Csk, Src, and Syk kinases with [alpha]IIb[beta]3 initiate integrin signaling to the cytoskeleton. *J Cell Biol* **157:** 265-275

Palacios AF, Tushir JS, Fujita Y, D'Souza-Schorey C (2005) Lysosomal targeting of E-cadherin: a unique mechanism for the down-regulation of cell-cell adhesion during epithelial to mesenchymal transitions. *Mol Cell Biol* **25:** 389-402

Palazzo AF, Joseph HL, Chen YJ, Dujardin DL, Alberts AS, Pfister KK, Vallee RB, Gundersen GG (2001) Cdc42, dynein, and dynactin regulate MTOC reorientation independent of Rho-regulated microtubule stabilization. *Curr Biol* **11:** 1536-1541

Parsons JT, Parsons SJ (1997) Src family protein tyrosine kinases: cooperating with growth factor and adhesion signaling pathways. *Curr Opin Cell Biol* **9:** 187-192

Pasdar M, Krzeminski KA, Nelson WJ (1991) Regulation of desmosome assembly in MDCK epithelial cells: coordination of membrane core and cytoplasmic plaque domain assembly at the plasma membrane. *J Cell Biol* **113:** 645-655

Patton WF, Dhanak MR, Jacobson BS (1989) Identification of Dictyostelium discoideum plasma membrane proteins by cell surface labeling and quantitative two-dimensional gel electrophoresis. *Anal Biochem* **179:** 37-49

Payne AS, Hanakawa Y, Amagai M, Stanley JR (2004) Desmosomes and disease: pemphigus and bullous impetigo. *Curr Opin Cell Biol* **16:** 536-543

Peifer M, Wieschaus E (1990) The segment polarity gene armadillo encodes a functionally modular protein that is the Drosophila homolog of human plakoglobin. *Cell* **63:** 1167-1176

Perez-Moreno M, Jamora C, Fuchs E (2003) Sticky business: orchestrating cellular signals at adherens junctions. *Cell* **112:** 535-548

Perez TD, Tamada M, Sheetz MP, Nelson WJ (2008) Immediate-early signaling induced by E-cadherin engagement and adhesion. *J Biol Chem* **283:** 5014-5022

Piedra J, Miravet S, Castano J, Palmer HG, Heisterkamp N, Garcia de Herreros A, Dunach M (2003) p120 Catenin-associated Fer and Fyn tyrosine kinases regulate beta-catenin Tyr-142 phosphorylation and beta-catenin-alpha-catenin Interaction. *Mol Cell Biol* **23:** 2287-2297

Pilichou K, Nava A, Basso C, Beffagna G, Bauce B, Lorenzon A, Frigo G, Vettori A, Valente M, Towbin J, Thiene G, Danieli GA, Rampazzo A (2006) Mutations in desmoglein-2 gene are associated with arrhythmogenic right ventricular cardiomyopathy. *Circulation* **113:** 1171-1179

Plott RT, Amagai M, Udey MC, Stanley JR (1994) Pemphigus vulgaris antigen lacks biochemical properties characteristic of classical cadherins. *J Invest Dermatol* **103:** 168-172

Pokutta S, Weis WI (2007) Structure and mechanism of cadherins and catenins in cell–cell contacts. *Annu Rev Cell Dev Biol* **23:** 237-261

Rampazzo A, Nava A, Malacrida S, Beffagna G, Bauce B, Rossi V, Zimbello R, Simionati B, Basso C, Thiene G, Towbin JA, Danieli GA (2002) Mutation in human desmoplakin domain binding to plakoglobin causes a dominant form of arrhythmogenic right ventricular cardiomyopathy. *Am J Hum Genet* **71:** 1200-1206

Renaudin A, Lehmann M, Girault J, McKerracher L (1999) Organization of point contacts in neuronal growth cones. *J Neurosci Res* **55:** 458-471

Reynolds AB (2007) p120-catenin: past and present. *Biochim Biophys Acta* **1773:** 2-7

Rickman L, Simrak D, Stevens HP, Hunt DM, King IA, Bryant SP, Eady RA, Leigh IM, Arnemann J, Magee AI, Kelsell DP, Buxton RS (1999) N-terminal deletion in a desmosomal cadherin causes the autosomal dominant skin disease striate palmoplantar keratoderma. *Hum Mol Genet* **8:** 971-976

Ridley AJ (2006) Rho GTPases and actin dynamics in membrane protrusions and vesicle trafficking. *Trends Cell Biol* **16:** 522-529

Ridley AJ (2012) Historical overview of Rho GTPases. *Methods Mol Biol* **827:** 3-12

Rivitti EA, Sanches JA, Miyauchi LM, Sampaio SA, Aoki V, Diaz LA (1994) Pemphigus foliaceus autoantibodies bind both epidermis and squamous mucosal epithelium, but tissue injury is detected only in the epidermis. The Cooperative Group on Fogo Selvagem Research. *J Am Acad Dermatol* **31:** 954-958

Roh JY, Stanley JR (1995) Intracellular domain of desmoglein 3 (pemphigus vulgaris antigen) confers adhesive function on the extracellular domain of E-cadherin without binding catenins. *J Cell Biol* **128:** 939-947

Rudini N, Dejana E (2008) Adherens junctions. *Curr Biol* **18:** R1080-1082

Ruiz P, Brinkmann V, Ledermann B, Behrend M, Grund C, Thalhammer C, Vogel F, Birchmeier C, Gunthert U, Franke WW, Birchmeier W (1996) Targeted mutation of plakoglobin in mice reveals essential functions of desmosomes in the embryonic heart. *J Cell Biol* **135:** 215-225

Runswick SK, O'Hare MJ, Jones L, Streuli CH, Garrod DR (2001) Desmosomal adhesion regulates epithelial morphogenesis and cell positioning. *Nat Cell Biol* **3:** 823-830

Sahai E, Marshall CJ (2002) ROCK and Dia have opposing effects on adherens junctions downstream of Rho. *Nat Cell Biol* **4:** 408-415

Saito H, Shimizu A, Tsunoda K, Amagai M, Ishiko A (2009) Subcellular localization of desmosomal components is different between desmoglein3 knockout mice and pemphigus vulgaris model mice. *J Dermatol Sci* **55:** 108-115

Sanchez-Carpintero I, Espana A, Pelacho B, Lopez Moratalla N, Rubenstein DS, Diaz LA, Lopez-Zabalza MJ (2004) In vivo blockade of pemphigus vulgaris acantholysis by inhibition of intracellular signal transduction cascades. *Br J Dermatol* **151:** 565-570

Savci-Heijink CD, Kosari F, Aubry MC, Caron BL, Sun Z, Yang P, Vasmatzis G (2009) The role of desmoglein-3 in the diagnosis of squamous cell carcinoma of the lung. *Am J Pathol* **174:** 1629-1637

Schaefer M, Jaeger CJ, Kramer MD (1996) Plasminogen activator system in pemphigus vulgaris. *Br J Dermatol* **135:** 726-732

Schenkel M, Sinclair AM, Johnstone D, Bewley JD, Mathur J (2008) Visualizing the actin cytoskeleton in living plant cells using a photo-convertible mEos::FABD-mTn fluorescent fusion protein. *Plant Methods* **4:** 21

Schiltz JR, Michel B (1976) Production of epidermal acantholysis in normal human skin in vitro by the IgG fraction from pemphigus serum. *J Invest Dermatol* **67:** 254-260

Seishima M, Esaki C, Osada K, Mori S, Hashimoto T, Kitajima Y (1995) Pemphigus IgG, but not bullous pemphigoid IgG, causes a transient increase in intracellular calcium and inositol 1,4,5-triphosphate in DJM-1 cells, a squamous cell carcinoma line. *J Invest Dermatol* **104:** 33-37

Sekiguchi M, Futei Y, Fujii Y, Iwasaki T, Nishikawa T, Amagai M (2001) Dominant autoimmune epitopes recognized by pemphigus antibodies map to the N-terminal adhesive region of desmogleins. *J Immunol* **167:** 5439-5448

Serrels A, Canel M, Brunton VG, Frame MC (2011) Src/FAK-mediated regulation of E-cadherin as a mechanism for controlling collective cell movement: insights from in vivo imaging. *Cell Adh Migr* **5:** 360-365

Sharma P, Mao X, Payne AS (2007) Beyond steric hindrance: the role of adhesion signaling pathways in the pathogenesis of pemphigus. *J Dermatol Sci* **48:** 1-14

Shen CH, Chen HY, Lin MS, Li FY, Chang CC, Kuo ML, Settleman J, Chen RH (2008) Breast tumor kinase phosphorylates p190RhoGAP to regulate rho and ras and promote breast carcinoma growth, migration, and invasion. *Cancer Res* **68:** 7779-7787

Shinmura K, Kohno T, Takahashi M, Sasaki A, Ochiai A, Guilford P, Hunter A, Reeve AE, Sugimura H, Yamaguchi N, Yokota J (1999) Familial gastric cancer: clinicopathological characteristics, RER phenotype and germline p53 and E-cadherin mutations. *Carcinogenesis* **20:** 1127-1131

Simpson CL, Patel DM, Green KJ (2011) Deconstructing the skin: cytoarchitectural determinants of epidermal morphogenesis. *Nat Rev Mol Cell Biol* **12:** 565-580

Skoudy A, Llosas MD, Garcia de Herreros A (1996) Intestinal HT-29 cells with dysfunction of E-cadherin show increased pp60src activity and tyrosine phosphorylation of p120-catenin. *Biochem J* **317:** 279-284

Smith EA, Fuchs E (1998) Defining the interactions between intermediate filaments and desmosomes. *J Cell Biol* **141:** 1229-1241

Spindler V, Drenckhahn D, Zillikens D, Waschke J (2007) Pemphigus IgG causes skin splitting in the presence of both desmoglein 1 and desmoglein 3. *Am J Pathol* **171:** 906-916

Spindler V, Waschke J (2011) Role of Rho GTPases in desmosomal adhesion and pemphigus pathogenesis. *Ann Anat* **193:** 177-180

Stanley JR, Amagai M (2006) Pemphigus, bullous impetigo, and the staphylococcal scalded-skin syndrome. *N Engl J Med* **355:** 1800-1810

Stappenbeck TS, Bornslaeger EA, Corcoran CM, Luu HH, Virata ML, Green KJ (1993) Functional analysis of desmoplakin domains: specification of the interaction with keratin versus vimentin intermediate filament networks. *J Cell Biol* **123:** 691-705

Takaishi K, Sasaki T, Kotani H, Nishioka H, Takai Y (1997) Regulation of cell-cell adhesion by rac and rho small G proteins in MDCK cells. *J Cell Biol* **139:** 1047-1059

Tang Z, Scherer PE, Okamoto T, Song K, Chu C, Kohtz DS, Nishimoto I, Lodish HF, Lisanti MP (1996) Molecular cloning of caveolin-3, a novel member of the caveolin gene family expressed predominantly in muscle. *J Biol Chem* **271:** 2255-2261

Teh MT, Parkinson EK, Thurlow JK, Liu F, Fortune F, Wan H (2011) A molecular study of desmosomes identifies a desmoglein isoform switch in head and neck squamous cell carcinoma. *J Oral Pathol Med* **40:** 67-76

Thomason HA, Scothern A, McHarg S, Garrod DR (2010) Desmosomes: adhesive strength and signalling in health and disease. *Biochem J* **429:** 419-433

Tinkle CL, Pasolli HA, Stokes N, Fuchs E (2008) New insights into cadherin function in epidermal sheet formation and maintenance of tissue integrity. *Proc Natl Acad Sci U S A* **105:** 15405-15410

Troyanovsky SM, Troyanovsky RB, Eshkind LG, Krutovskikh VA, Leube RE, Franke WW (1994) Identification of the plakoglobin-binding domain in desmoglein and its role in plaque assembly and intermediate filament anchorage. *J Cell Biol* **127:** 151-160

Tsang SM, Brown L, Gadmor H, Gammon L, Fortune F, Wheeler A, Wan H (2012a) Desmoglein 3 acting as an upstream regulator of Rho GTPases, Rac-

1/Cdc42 in the regulation of actin organisation and dynamics. *Exp Cell Res* **318:** 2269-2283

Tsang SM, Brown L, Lin K, Liu L, Piper K, O'Toole EA, Grose R, Hart IR, Garrod DR, Fortune F, Wan H (2012b) Non junctional human desmoglein 3 acts as an upstream regulator of Src in E-cadherin adhesion, a pathway possibly involved in the pathogenesis of pemphigus vulgaris. *J Pathol* 318: 2269-98

Tsang SM, Liu L, Teh MT, Wheeler A, Grose R, Hart IR, Garrod DR, Fortune F, Wan H (2010) Desmoglein 3, via an interaction with E-cadherin, is associated with activation of Src. *PLoS One* **5:** e14211

Tselepis C, Chidgey M, North A, Garrod D (1998) Desmosomal adhesion inhibits invasive behavior. *Proc Natl Acad Sci U S A* **95:** 8064-8069

Tsukamoto T, Nigam SK (1999) Cell-cell dissociation upon epithelial cell scattering requires a step mediated by the proteasome. *J Biol Chem* **274:** 24579-24584

Tsukita S, Nagafuchi A, Yonemura S (1992) Molecular linkage between cadherins and actin filaments in cell-cell adherens junctions. *Curr Opin Cell Biol* **4:** 834-839

Tsukita S, Oishi K, Akiyama T, Yamanashi Y, Yamamoto T (1991) Specific proto-oncogenic tyrosine kinases of src family are enriched in cell-to-cell adherens junctions where the level of tyrosine phosphorylation is elevated. *J Cell Biol* **113:** 867-879

Tu CL, Chang W, Xie Z, Bikle DD (2008) Inactivation of the calcium sensing receptor inhibits E-cadherin-mediated cell-cell adhesion and calcium-induced differentiation in human epidermal keratinocytes. *J Biol Chem* **283:** 3519-3528

Udey MC, Stanley JR (1999) Pemphigus--diseases of antidesmosomal autoimmunity. *JAMA* **282:** 572-576

Ueki S, Lacroix B, Citovsky V (2011) Protein membrane overlay assay: a protocol to test interaction between soluble and insoluble proteins in vitro. *J Vis Exp* **54:** 2961

Vasioukhin V, Bauer C, Degenstein L, Wise B, Fuchs E (2001a) Hyperproliferation and defects in epithelial polarity upon conditional ablation of alpha-catenin in skin. *Cell* **104:** 605-617

Vasioukhin V, Bowers E, Bauer C, Degenstein L, Fuchs E (2001b) Desmoplakin is essential in epidermal sheet formation. *Nat Cell Biol* **3:** 1076-1085

Wallis S, Lloyd S, Wise I, Ireland G, Fleming TP, Garrod D (2000) The alpha isoform of protein kinase C is involved in signaling the response of desmosomes to wounding in cultured epithelial cells. *Mol Biol Cell* **11:** 1077-1092

Wan H, Stone MG, Simpson C, Reynolds LE, Marshall JF, Hart IR, Hodivala-Dilke KM, Eady RA (2003) Desmosomal proteins, including desmoglein 3, serve as novel negative markers for epidermal stem cell-containing population of keratinocytes. *J Cell Sci* **116:** 4239-4248

Wan H, Yuan M, Simpson C, Allen K, Gavins FN, Ikram MS, Basu S, Baksh N, O'Toole EA, Hart IR (2007) Stem/progenitor cell-like properties of desmoglein 3dim cells in primary and immortalized keratinocyte lines. *Stem Cells* **25:** 1286-1297

Wang L, Liu T, Wang Y, Cao L, Nishioka M, Aguirre RL, Ishikawa A, Geng L, Okada N (2007) Altered expression of desmocollin 3, desmoglein 3, and beta-catenin in oral squamous cell carcinoma: correlation with lymph node metastasis and cell proliferation. *Virchows Arch* **451:** 959-966

Waschke J (2008) The desmosome and pemphigus. *Histochem Cell Biol* **130:** 21-54

Waschke J, Bruggeman P, Baumgartner W, Zillikens D, Drenckhahn D (2005) Pemphigus foliaceus IgG causes dissociation of desmoglein 1-containing junctions without blocking desmoglein 1 transinteraction. *J Clin Invest* **115:** 3157-3165

Waschke J, Spindler V, Bruggeman P, Zillikens D, Schmidt G, Drenckhahn D (2006) Inhibition of Rho A activity causes pemphigus skin blistering. *J Cell Biol* **175:** 721-727

Watt F, Mattey D, Garrod D (1984) Calcium-induced reorganization of desmosomal components in cultured human keratinocytes. *J Cell Biol* **99:** 2211-2215

Wei Y, Yang X, Liu Q, Wilkins JA, Chapman HA (1999) A role for caveolin and the urokinase receptor in integrin-mediated adhesion and signaling. *J Cell Biol* **144:** 1285-1294

Wheeler AP, Ridley AJ (2004) Why three Rho proteins? RhoA, RhoB, RhoC, and cell motility. *Exp Cell Res* **301:** 43-49

Wheelock MJ, Jensen PJ (1992) Regulation of keratinocyte intercellular junction organization and epidermal morphogenesis by E-cadherin. *J Cell Biol* **117:** 415-425

Wijnhoven BP, Dinjens WN, Pignatelli M (2000) E-cadherin-catenin cell-cell adhesion complex and human cancer. *Br J Surg* **87:** 992-1005

Williams TM, Lisanti MP (2005) Caveolin-1 in oncogenic transformation, cancer, and metastasis. *Am J Physiol Cell Physiol* **288:** C494-506

Williamson L, Raess NA, Caldelari R, Zakher A, de Bruin A, Posthaus H, Bolli R, Hunziker T, Suter MM, Muller EJ (2006) Pemphigus vulgaris identifies plakoglobin as key suppressor of c-Myc in the skin. *EMBO J* **25:** 3298-3309

Williamson L, Suter MM, Olivry T, Wyder M, Muller EJ (2007) Upregulation of c-Myc may contribute to the pathogenesis of canine pemphigus vulgaris. *Vet Dermatol* **18:** 12-17

Xu SW, Liu S, Eastwood M, Sonnylal S, Denton CP, Abraham DJ, Leask A (2009) Rac inhibition reverses the phenotype of fibrotic fibroblasts. *PLoS One* **4:** e7438

Xu W, Harrison SC, Eck MJ (1997) Three-dimensional structure of the tyrosine kinase c-Src. *Nature* **385:** 595-602

Yamada S, Pokutta S, Drees F, Weis WI, Nelson WJ (2005) Deconstructing the cadherin–catenin–actin complex. *Cell* **123:** 889-901

Yap AS, Crampton MS, Hardin J (2007) Making and breaking contacts: the cellular biology of cadherin regulation. *Curr Opin Cell Biol* **19:** 508-514

Yap AS, Kovacs EM (2003a) Direct cadherin-activated cell signaling: a view from the plasma membrane. *J Cell Biol* **160:** 11-16

Yap AS, Niessen CM, Gumbiner BM (1998) The juxtamembrane region of the cadherin cytoplasmic tail supports lateral clustering, adhesive strengthening, and interaction with p120ctn. *J Cell Biol* **141:** 779-789

Yashiro M, Nishioka N, Hirakawa K (2006) Decreased expression of the adhesion molecule desmoglein-2 is associated with diffuse-type gastric carcinoma. *Eur J Cancer* **42:** 2397-2403

Yeatman TJ (2004) A renaissance for SRC. *Nat Rev Cancer* **4:** 470-480

Yin T, Getsios S, Caldelari R, Godsel LM, Kowalczyk AP, Muller EJ, Green KJ (2005a) Mechanisms of plakoglobin-dependent adhesion: desmosome-specific functions in assembly and regulation by epidermal growth factor receptor. *J Biol Chem* **280:** 40355-40363

Yin T, Getsios S, Caldelari R, Kowalczyk AP, Muller EJ, Jones JC, Green KJ (2005b) Plakoglobin suppresses keratinocyte motility through both cell-cell adhesion-dependent and -independent mechanisms. *Proc Natl Acad Sci U S A* **102:** 5420-5425

Yin T, Green KJ (2004) Regulation of desmosome assembly and adhesion. *Semin Cell Dev Biol* **15:** 665-677

Yonemura S, Hirao-Minakuchi K, Nishimura Y (2004) Rho localization in cells and tissues. *Exp Cell Res* **295:** 300-314

Zhang J, Betson M, Erasmus J, Zeikos K, Bailly M, Cramer LP, Braga VM (2005) Actin at cell-cell junctions is composed of two dynamic and functional populations. *J Cell Sci* **118:** 5549-5562

APPENDIX-1

Figure 37: Overexpression of Dsg3 enhances the average protrusion velocity

	w/o drug		w drug	
	V	D3	V	D3
1	0.354	0.115	0.293	0.430
2	0.582	0.475	0.647	0.430
3	0.095	0.092	0.102	0.513
4	0.475	0.255	0.754	0.690
5	0.458	0.439	0.466	0.924
6	0.761	0.353	0.931	1.792
7	0.344	0.377	0.573	0.804
8	1.718	1.601	1.178	0.554
9	0.267	0.604	1.346	0.686
10	1.592	4.198	1.365	0.089
11	0.641	2.075	0.520	0.857
12	0.275	1.177	0.772	0.645
13	0.513	0.418	0.579	0.860
14	0.795	0.663	0.544	1.580
15	0.689	0.174	0.688	0.277
16	0.679	1.492	0.095	0.753
17	0.446	0.338	0.520	0.904
18	0.682	1.023	0.208	0.277
19	0.469	1.057	0.638	0.427
20	1.211	0.542	0.169	0.452
21	0.416	3.310	0.633	0.452
22	0.946	3.235	1.142	0.621
23	0.258	1.951	1.267	0.095

	w/o drug		w drug	
	V	D3	V	D3
Average	0.682	1.264	0.719	0.687
STDEV	0.405	1.136	0.384	0.404
ST Error	0.084	0.237	0.080	0.084
P Value	0.029		0.907	

Figure 38: Overexpression of Dsg3 enhanced cell motility initially in the presence of Rac1 inhibitor, NSC23766, but this phenomenon was disappeared later

w/o NSC23766				w NSC23766			
Name	Mean Velocity	Name	Mean Velocity	Name	Mean Velocity	Name	Mean Velocity
v p2-1wo	0.197	D p2-1wo	0.189	v p2-1w	0.160	D p2-1w	0.312
v p2-1wo	0.222	D p2-1wo	0.380	v p2-1w	0.206	D p2-1w	0.346
v p2-1wo	0.291	D p2-1wo	0.212	v p2-1w	0.257	D p2-1w	0.356
v p2-1wo	0.172	D p2-1wo	0.225	v p2-1w	0.189	D p2-1w	0.377
v p2-1wo	0.155	D p2-1wo	0.247	v p2-1w	0.261	D p2-1w	0.395
v p2-1wo	0.175	D p2-1wo	0.215	v p2-1w	0.171	D p2-1w	0.219
v p2-1wo	0.210	D p2-1wo	0.375	v p2-1w	0.276	D p2-1w	0.316
v p2-1wo	0.213	D p2-1wo	0.151	v p2-1w	0.270	D p2-1w	0.362
v p2-1wo	0.150	D p2-1wo	0.135	v p2-1w	0.296	D p2-1w	0.257
v p2-1wo	0.193	D p2-1wo	0.283	v p2-1w	0.203	D p2-1w	0.392
v p2-1wo	0.236	D p2-1wo	0.245	v p2-1w	0.234	D p2-1w	0.367
v p2-1wo	0.289	D p2-1wo	0.248	v p2-1w	0.246	D p2-1w	0.378
v p2-2wo	0.320	D p2-1wo	0.243	v p2-1w	0.262	D p2-1w	0.311
v p2-2wo	0.231	D p2-1wo	0.133	v p2-1w	0.268	D p2-2w	0.342
v p2-2wo	0.427	D p2-1wo	0.157	v p2-2w	0.288	D p2-2w	0.315
v p2-2wo	0.149	D p2-2wo	0.161	v p2-2w	0.228	D p2-2w	0.397
v p2-2wo	0.187	D p2-2wo	0.127	v p2-2w	0.228	D p2-2w	0.309
v p2-2wo	0.312	D p2-2wo	0.280	v p2-2w	0.329	D p2-2w	0.327
v p2-2wo	0.410	D p2-2wo	0.256	v p2-2w	0.206	D p2-2w	0.354
v p2-2wo	0.352	D p2-2wo	0.149	v p2-2w	0.340	D p2-2w	0.263
v p2-2wo	0.248	D p2-2wo	0.174	v p2-2w	0.257	D p2-2w	0.370
v p2-2wo	0.171	D p2-2wo	0.282	v p2-2w	0.283	D p2-2w	0.344
v p2-2wo	0.345	D p2-2wo	0.212	v p2-2w	0.273	D p2-2w	0.364
v p2-2wo	0.300	D p2-2wo	0.134	v p2-2w	0.389	D p2-2w	0.321
v p2-2wo	0.173	D p2-2wo	0.136	v p2-2w	0.269	D p2-2w	0.364
v p2-2wo	0.162	D p2-2wo	0.192	v p2-2w	0.288	D p2-2w	0.340
v p3-1wo	0.227	D p2-2wo	0.471	v p2-2w	0.260	D p2-2w	0.306
v p3-1wo	0.109	D p2-2wo	0.203	v p2-2w	0.260	D p2-2w	0.437
v p3-1wo	0.199	D p2-2wo	0.194	v p3-1w	0.337	D p2-2w	0.327
v p3-1wo	0.328	D p2-2wo	0.263	v p3-1w	0.128	D p3-1w	0.289
v p3-1wo	0.150	D p2-2wo	0.180	v p3-1w	0.280	D p3-1w	0.405
v p3-1wo	0.192	D p2-2wo	0.215	v p3-1w	0.152	D p3-1w	0.162
v p3-1wo	0.362	D p2-2wo	0.196	v p3-1w	0.352	D p3-1w	0.263
v p3-1wo	0.110	D p3-1wo	0.344	v p3-1w	0.213	D p3-1w	0.338
v p3-1wo	0.346	D p3-1wo	0.256	v p3-1w	0.212	D p3-1w	0.307
v p3-1wo	0.169	D p3-1wo	0.441	v p3-1w	0.143	D p3-1w	0.319

v p3-1wo	0.332	D p3-1wo	0.267	v p3-1w	0.161	D p3-1w	0.319
v p3-1wo	0.333	D p3-1wo	0.175	v p3-1w	0.331	D p3-1w	0.250
v p3-1wo	0.135	D p3-1wo	0.105	v p3-2w	0.271	D p3-1w	0.335
v p3-2wo	0.189	D p3-1wo	0.285	v p3-2w	0.284	D p3-1w	0.298
v p3-2wo	0.200	D p3-1wo	0.363	v p3-2w	0.245	D p3-1w	0.162
v p3-2wo	0.230	D p3-1wo	0.161	v p3-2w	0.202	D p3-1w	0.243
v p3-2wo	0.223	D p3-1wo	0.289	v p3-2w	0.309	D p3-1w	0.313
v p3-2wo	0.238	D p3-1wo	0.352	v p3-2w	0.258	D p3-1w	0.206
v p3-2wo	0.228	D p3-1wo	0.186	v p3-2w	0.285	D p3-2w	0.320
v p3-2wo	0.157	D p3-1wo	0.145	v p3-2w	0.243	D p3-2w	0.348
v p3-2wo	0.225	D p3-1wo	0.410	v p3-2w	0.335	D p3-2w	0.376
v p3-2wo	0.128	D p3-2wo	0.167	v p4-1w	0.220	D p3-2w	0.384
v p3-2wo	0.178	D p3-2wo	0.181	v p4-1w	0.153	D p3-2w	0.310
v p3-2wo	0.222	D p3-2wo	0.134	v p4-1w	0.234	D p3-2w	0.378
v p3-2wo	0.191	D p3-2wo	0.128	v p4-1w	0.341	D p3-2w	0.284
v p4-1wo	0.179	D p3-2wo	0.206	v p4-1w	0.241	D p3-2w	0.287
v p4-1wo	0.226	D p3-2wo	0.251	v p4-1w	0.255	D p3-2w	0.092
v p4-1wo	0.271	D p3-2wo	0.113	v p4-1w	0.311	D p3-2w	0.074
v p4-1wo	0.276	D p3-2wo	0.250	v p4-1w	0.195	D p3-2w	0.120
v p4-1wo	0.212	D p3-2wo	0.195	v p4-1w	0.279	D p4-1w	0.350
v p4-1wo	0.363	D p3-2wo	0.218	v p4-2w	0.173	D p4-1w	0.379
v p4-1wo	0.237	D p3-2wo	0.134	v p4-2w	0.342	D p4-1w	0.298
v p4-1wo	0.394	D p3-2wo	0.221	v p4-2w	0.241	D p4-1w	0.343
v p4-1wo	0.283	D p3-2wo	0.184	v p4-2w	0.236	D p4-1w	0.315
v p4-1wo	0.342	D p3-2wo	0.280	v p4-2w	0.218	D p4-1w	0.383
v p4-1wo	0.141	D p3-2wo	0.116	v p4-2w	0.187	D p4-1w	0.398
v p4-1wo	0.151	D p4-1wo	0.301	v p4-2w	0.238	D p4-1w	0.344
v p4-1wo	0.246	D p4-1wo	0.181	v p4-2w	0.204	D p4-1w	0.256
v p4-2wo	0.251	D p4-1wo	0.172	v p4-2w	0.268	D p4-1w	0.255
v p4-2wo	0.231	D p4-1wo	0.202	v p2-1w	0.196	D p4-1w	0.360
v p4-2wo	0.258	D p4-1wo	0.111	v p2-1w	0.226	D p4-1w	0.275
v p4-2wo	0.401	D p4-1wo	0.172	v p2-1w	0.249	D p4-1w	0.288
v p4-2wo	0.283	D p4-1wo	0.112	v p2-1w	0.269	D p4-1w	0.324
v p4-2wo	0.146	D p4-1wo	0.236	v p2-1w	0.200	D p4-2w	0.340
v p4-2wo	0.181	D p4-1wo	0.112	v p2-1w	0.335	D p4-2w	0.270
v p4-2wo	0.306	D p4-1wo	0.216	v p2-1w	0.195	D p4-2w	0.433
v p4-2wo	0.228	D p4-1wo	0.140	v p2-1w	0.231	D p4-2w	0.308
v p4-2wo	0.230	D p4-1wo	0.268	v p2-1w	0.234	D p4-2w	0.404
v p4-2wo	0.201	D p4-2wo	0.432	v p2-1w	0.266	D p4-2w	0.341
v p4-2wo	0.438	D p4-2wo	0.243	v p2-1w	0.282	D p4-2w	0.301
v p4-2wo	0.190	D p4-2wo	0.221	v p2-2w	0.158	D p4-2w	0.392
v p4-2wo	0.254	D p4-2wo	0.126	v p2-2w	0.259	D p4-2w	0.281
v p4-2wo	0.260	D p4-2wo	0.129	v p2-2w	0.284	D p4-2w	0.350
v p4-2wo	0.142	D p4-2wo	0.168	v p2-2w	0.203	D p4-2w	0.361

v p4-2wo	0.290	D p4-2wo	0.120	v p2-2w	0.212	D p4-2w	0.319
v p4-2wo	0.384	D p4-2wo	0.205	v p2-2w	0.275	D p4-2w	0.317
v p4-2wo	0.231	D p4-2wo	0.299	v p2-2w	0.289	D p4-2w	0.315
Average	0.240		0.217		0.249		0.318

		Mean Velocity	STDEV	ST Error	P value
w/o drug	V	0.240	0.079	0.009	0.06592336
	D3	0.217	0.083	0.009	
w drug	V	0.249	0.054	0.006	2.0287E-11
	D3	0.318	0.068	0.008	